DISSERTATION

MECHANISMS OF IFN-γ AND CEFTAZIDIME INTERACTION FOR SYNERGISTIC KILLING OF *BURKHOLDERIA*

Submitted by

Kara Mosovsky

Department of Microbiology, Immunology, and Pathology

In partial fulfillment of the requirements

For the Degree of Doctor of Philosophy

Colorado State University

Fort Collins, Colorado

Spring 2014

Doctoral Committee:

Advisor: Steven Dow

Alan Schenkel
Herbert Schweizer
Robert Callan

ABSTRACT

MECHANISMS OF IFN-γ AND CEFTAZIDIME INTERACTION

FOR SYNERGISTIC KILLING OF *BURKHOLDERIA*

Burkholderia pseudomallei is a Gram negative, facultative intracellular pathogen which infects both phagocytes and non-phagocytes and causes severe acute infections in humans and animals. Due to its inherent resistance to many classes of antibiotics, new therapies are needed which can supplement or substitute for conventional treatments in order to combat this emerging infectious disease. We have previously shown that interferon-gamma (IFN-γ) can interact with the conventionally administered antibiotic, ceftazidime, to synergistically control intracellular bacteria burden of *Burkholderia* infected macrophages. The goal of the studies presented here was to determine the mechanism by which IFN-γ and ceftazidime exert their synergistic effect.

After investigating several potential mediators of immuno-antimicrobial synergy, we showed that IFN-γ stimulation of macrophages led to increased generation of reactive oxygen species (ROS), which led us to hypothesize that IFN-γ induced ROS may interact with ceftazidime to control intracellular bacterial burden. We next found that ROS scavenging antioxidants such as N-acetylcysteine (NAC) and reduced glutathione (GSH) were capable of reversing the IFN-γ and ceftazidime synergistic effect, while the ROS-inducing drug buthionine sulfoximine (BSO) could not only potentiate the synergy, but could completely substitute for IFN-γ to synergize with ceftazidime and control intracellular bacterial burden. These results were consistent with a ROS interaction with ceftazidime. We further showed that IFN-γ prevented vacuolar escape and actin polymerization, a finding which was recapitulated with

BSO. Taken together, these results suggested that generation of IFN-γ induced ROS responses synergized with ceftazidime to enhance control of intracellular bacterial burden. IFN-γ induced ROS was also responsible for preventing vacuolar escape and therefore may have limited intracellular replication and spread of infection.

In the second half of our study we identified and then investigated the separate and compartmentalized contributions of IFN-γ and ceftazidime to the overall synergistic effect. We determined that ceftazidime alone controlled extracellular killing in our macrophage infection model while IFN-γ alone controlled the killing of *Burkholderia* in the intracellular compartment. We confirmed a role for IFN-γ induced ROS responses to kill intracellular bacteria and control intracellular replication, though we also conclude that other IFN-γ-dependent and ROS-independent pathways are at play. Overall we suggest a new model to describe the dynamics of the classically used macrophage infection model. We suggest that both intracellular and extracellular control of bacteria is required for the overall synergistic effect we see with combination of IFN-γ and ceftazidime. Together our studies have implications for the use of IFN-γ, or other ROS-inducing drugs, as non-specific antibiotic potentiating agents for enhanced clearance of bacterial pathogens.

ACKNOWLEDGEMENTS

A sincere thank you goes to my adviser Dr. Steven Dow. Steve, you taught me that curiosity and perseverance are two of the finest qualities in a scientist. The way you conduct your lab, with such trust in its individuals, gave me a great sense of personal responsibility for and ownership of my project, which in turn inspired and motivated me to investigate our research questions. Through your own patience and flexibility, but also by demanding excellence, you showed me examples of how best to mentor my own undergraduate and graduate helpers. You also created a low-stress environment, which as a graduate student I can say is certainly impressive! I always felt like I was your colleague and we were working together on a team, rather than me working *for* you. You created this environment by valuing my thoughts and opinions on projects and encouraging me to "stick to my guns" if I thought differently than you, and I'm very thankful for this. I will never forget your eternal optimism about negative or hard-to-interpret results because it helped me remember that science is made up of all the little parts and that negative data has value too. This was also the first research lab I was part of that encouraged occasional hiking or white-water rafting trips with the lab. These trips were not only bonding experiences but reminded us to strike a healthy balance between work and play. I have truly loved being a part of the Dow Lab. Thank you for taking a chance on me.

Thank you to all of my friends and colleagues in the Dow Lab especially Andrew Goodyear, Ediane Silva, Marjorie Sutherland, and Valerie Johnson. Our daily interactions kept me sane through the ups and downs of research and brought so much love and laughter into the workplace. You guys certainly made it an enjoyable 4 years inside and out of lab!

Another big thank you goes to my committee members. I know that your time is valuable and you are always busy with numerous obligations, however, I truly appreciate the

three of you serving on my committee and giving me such valuable advice and suggestions for experiments along the way. You have shown me first hand that sharing expertise allows us, as scientists, to see a problem with new understanding--which is extremely valuable for innovative research.

Thank you to all of my friends and family who supported my career goals and gave me encouragement along the way. You provided me with the best balance of work and play and those of you that worked alongside me on your own degree, I always felt like, for better or for worse, we were in it together!

The last and biggest thank you goes to my husband Paul, for we are nothing without our support systems at home. Thank you, Paul, for being my career therapist, my foot-massage therapist, my life coach, my entertainment, and at times my personal chef and house keeper throughout the busiest and most trying times of my graduate career. Your hugs were a reliable source of instant stress-relief. I truly appreciate you for respecting and encouraging my career goals and being so flexible these last four years! Thank you for being patient, dear.

TABLE OF CONTENTS

LIST OF FIGURES

CHAPTER 1: LITERATURE REVIEW

BURKHOLDERIA AND MELIOIDOSIS

Epidemiology of melioidosis

B. pseudomallei is an aerobic, Gram negative bacillus, isolated from soil and water in the environment (1, 2). It causes the emerging infectious disease called melioidosis, which is highly endemic in northern Australia and Thailand, less endemic in areas throughout southeast Asia, and appears sporadically in Central and South America as well as Africa (3-5) (see Figure 1.1). In northeast Thailand, melioidosis is the third leading cause of death due to infectious disease, after human immunodeficiency virus and tuberculosis (5).

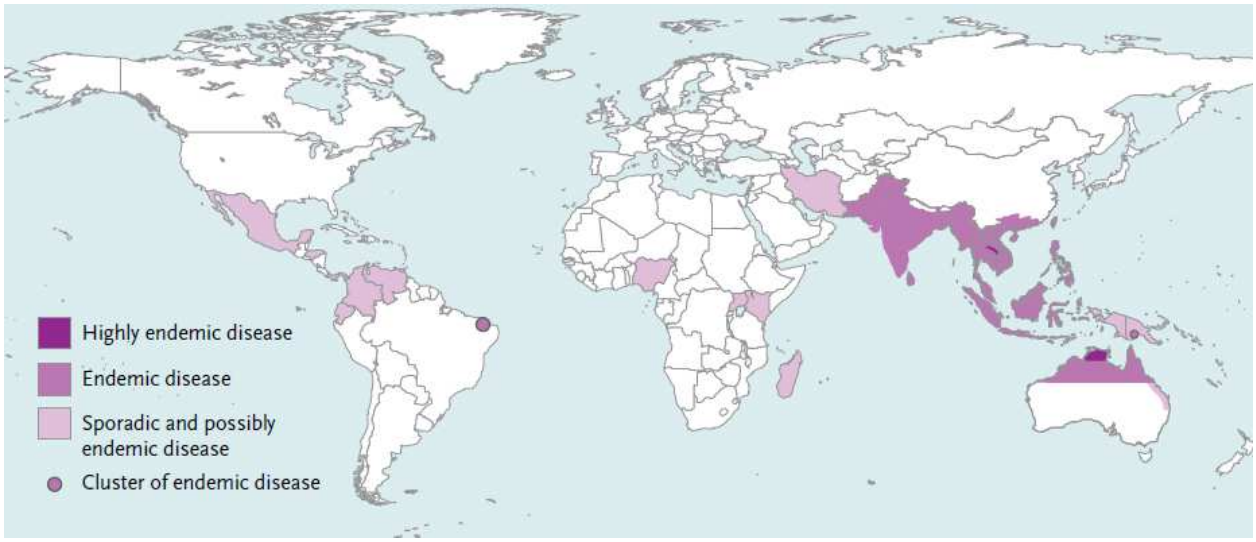

Figure 1.1: Distribution of melioidosis around the world Melioidosis is highly endemic in Thailand and northern Australia. Other areas of endemic disease include southeast Asia with sporadic disease in parts of Africa as well as Central and South America (4).

Incidence rates greatly depend on geographical location. For example, Northeast Thailand has reported incidence of 4.4-21/100,000 (5, 6) while Northern Australia has reported

incidence of 19.6-102.4/100,000 (7-9), with similar incidence rates in Taiwan (10) and Malaysia (11). The incidence in Thailand seems to be increasing, as one study showed evidence of increased incidence rates from 8/100,000 in the year 2000 to 21.3/100,000 in the year 2006 (5). The variability of seasons also greatly impacts incidence rates. For example, highest incidence rates occur after monsoonal rains (2-4, 6, 7, 10, 12, 13). In the abnormally rainy 2009-2010 season in northern Australia, incidence rose to a rate of 50.2/100,000 with incidence in indigenous populations as high as 102.4/100,000 (8). Up until that season, the average incidence rate over the past 20 years had been 19.6/100,000 (8).

At the present time, inhalation, ingestion, and percutaneous inoculation are considered the three major routes of acquisition, though the proportional relevance of each is still speculative (2, 13, 14). In cases where inoculation was reasonably recalled as percutaneous contact with muddy soil or water, clinical lesions were usually not discovered at the inoculation site, but in fact disseminated far from it (7). These types of percutaneous infection followed by dissemination seems to be the most common route of inoculation, especially for rice farmers who have high exposure to muddy water and soil (2, 3). Cases like these make it challenging to definitively identify the exact route of inoculation. However, a 12-year study by Currie and colleagues suggests that inoculation through the inhalation route may be increased during the rainy season due to monsoonal wind and rain (12).

Several risk factors are associated with contraction of melioidosis. These include diabetes mellitus, chronic renal disease, chronic pulmonary disease, heavy alcohol use, and other immune-compromised individuals (3, 4, 6-9, 12). Increased susceptibility of type 2 diabetes mice to *B. pseudomallei* infection has been linked to decreased macrophage function, particularly the ability to contain and kill intracellular *Burkholderia* (15). Age does not seem to be a major

risk-factor since *B. pseudomallei* can infect persons of all ages, however the average infected individual is usually between 40-60 years old (2, 4-7, 10, 11).

Clinical manifestations, diagnosis, and treatments for melioidosis

The incubation period for melioidosis is typically 1-21 days (7) though latent infections have surfaced decades after geographic exposure (16, 17). Melioidosis can present as acute, sub-acute, or chronic infection. The most common presentation of melioidosis is respiratory pneumonia with other clinical manifestations including sepsis, abscess formation in skin or soft tissue, suppurative parotitis, peritonitis, arthritis, genito-urinary infection, encephalomyelitis, and others (3, 7, 13, 18, 19).

Melioidosis can sometimes be confused with tuberculosis in areas where *B. pseudomallei* is not endemic (20, 21). Unfortunately a wrong diagnosis can be fatal since acute melioidosis can cause death within a few days. Therefore correct and rapid diagnosis of melioidosis is extremely important. *B. pseudomallei* is not considered normal microbial flora and there is no evidence of asymptomatic carriers, therefore a culture-positive specimen from an individual leads to a definitive clinical diagnosis of melioidosis (13, 22). Diagnosis through culture, however, has its limitations because infected individuals may still culture negative for *B. pseudomallei* (13, 23). Polymerase chain reaction (PCR) is frequently used to confirm the identity of positive-cultures, though this method is imperfect as well, due to probe targets that cross-react with other non-virulent *Burkholderia* species (13). Although the *B. pseudomallei* antigen in blood samples usually falls below the limit of detection of most immunofluorescent assays, Chantraitita and colleagues have shown that standard culture of blood samples prior to immunofluorescence greatly increases sensitivity and specificity of their detection system (23).

A reagent consisting of monoclonal antibody against *B. pseudomallei* exopolysaccharide and fluorescent secondary antibody was added to blood cultures on a slide and viewed by microscopy to detect fluorescence. Their methods remarkably diagnosed melioidosis with a 97.4% sensitivity and 100% specificity (23).

B. pseudomallei is intrinsically resistant to penicillin, ampicillin, macrolides, aminoglycosides, rifamycins, polymyxin, and first and second generation cephalosporins (2, 4, 21). Chromosomally encoded, putative, resistance genes in *B. pseudomallei* account for all resistance to antibiotics and among others, encode for several β-lactamases and ten multidrug efflux pumps (24). Aside from inherent antibiotic resistance, *B. pseudomallei* has also been shown to be resistant to innate immunity host-defenses and antimicrobial peptides (AMPs) (25, 26). Tandhavanant and colleagues found that *B. pseudomallei* was resistant to 200 µg/ml of lysozyme and 3 mg/ml of lactoferrin (25). In one study, *B. pseudomallei* was shown to be resistant to both human neutrophil peptide-1 and human beta-defensin-2, an antimicrobial peptide of epithelial cells, at concentrations of 100 µg/ml (25). On the other hand, *B. pseudomallei* was shown to be susceptible to the antimicrobial peptide LL-37 at concentrations of 6.25 µM (25).

Due to the inherent antibiotic resistance of *B. pseudomallei*, the first line antibiotic of choice to treat melioidosis is typically ceftazidime. The current suggested antibiotic course for treatment of melioidosis includes a two-week minimum intravenous administration of ceftazidime or meropenem, followed by oral eradication therapy with trimethoprim and sulfamethoxazole for an additional three months (2, 3, 24). However, even with antibiotic therapy, overall mortality rates have been reported between 20%-50%, dependent on geographical and seasonal variability (5, 7, 10, 11, 27). Furthermore, greater than 10% of

patients can face recurrent infection, with around 75% of recurrent infections due to relapse versus reinfection (19, 27, 28). Poor adherence to the antibiotic regimen is a major risk factor for relapse (19, 27).

Similarities and differences between *B. pseudomallei* and *B. thailandensis*

B. thailandensis E264 is an environmental isolate from Thailand which was once classified as a strain of *B. pseudomallei* due to their similarities, but was eventually reclassified based on several key differences identified between the species (29-31). *B. pseudomallei* and *B. thailandensis* have a similar ability to replicate and survive intracellularly, and the mammalian cell response to both bacteria appears to be similar in regards to induction of cytokine response, costimulatory molecule expression, and differentiation bias towards a Th1 cell population (32). Furthermore, *B. thailandensis* and *B. pseudomallei* are morphologically and antigenically similar, and although they only differ in genetic sequence by 15 nucleotides, *B. pseudomallei* is considered highly virulent while *B. thailandensis* is considered to be less virulent (2, 30, 31). In fact, *B. thailandensis* is considered to be at least 10^5 times less virulent than *B. pseudomallei* (29, 30). For example, while clinical isolate *B. pseudomallei* 1026b has been shown to kill Syrian golden hamsters with less than 12 colony forming units (CFU), the 50% lethal dose (LD_{50}) of *B. thailandensis* E264 was 1.8×10^6 CFU (29). In mice, the LD_{50} inoculum for *B. pseudomallei* was found to be 182 CFU in BALB/c mice versus around 10^9 CFU/mouse for *B. thailandensis* (30).

Differences in virulence between *B. thailandensis* and *B. pseudomallei* may depend on any number of small differences between the two organisms. For instance, *B. thailandensis* secretions show proteolytic and siderophore activity, similar to *B. pseudomallei* 1026b, but also

shows lipase and lecithinase activities and are able to assimilate L-arabinose (29, 30). *B. thailandensis* also lacks the *B. pseudomallei* T3SS-1, though the exact role of T3SS-1 in virulence is still unknown (2, 33).

Another key difference between these two *Burkholderia* species may be their abilities to inflict damage on eukaryotic cells. Early studies show that supernatants of *B. thailandensis* E264, which contained secretion products as well as bacterial antigens, were more cytotoxic to HeLa cells over a 48 hr period than supernatants from *B. pseudomallei* 1026b (29). *B. pseudomallei*, however, appear to inflict more damage than *B. thailandensis* when bacteria exert their virulence from within infected macrophages. Kespichayawattana found condensed and fragmented nuclei in 43% of macrophages after just 6 hours of infection with virulent *B. pseudomallei*, but just 23% of cells infected with less virulent, arabinose-assimilating *Burkholderia* (34).

B. pseudomallei and *B. thailandensis* may also differ in structure and components of their lipopolysaccharide (LPS) and capsular polysaccharide (CPS) (35, 36). The lipid A moiety of *B. pseudomallei* but not *B. thailandensis* is modified with 4-amino-4-deoxy-arabinose (35). This modification may be a mechanism of immune system evasion through resistance to cationic antimicrobial peptides (35). *B. pseudomallei* and *B. thailandensis* also differ in CPS. Four putative CPS biosynthesis and export operons have been identified in *B. pseudomallei*. The type I capsular polysaccharide, mannoheptose, associated with *B. pseudomallei* but not *B. thailandensis*, has been shown to inhibit C3b complement deposition and inhibit phagocytosis by polymorphonuclear leukocytes (37). On the other hand, the type III CPS operon, identified in *B. pseudomallei* as well as *B. thailandensis*, was shown to be unnecessary for virulence in a Syrian

hamster model of melioidosis, but was suggested to contribute to the organisms' abilities to live in the environment (36).

Due to its high infectivity, high associated mortality rates, and high level of inherent resistance to antibiotics, *B. pseudomallei* is classified as a potential bio-threat agent by the Centers for Disease Control and Prevention (CDC), containing most *B. pseudomallei* research to biosafety level 3 (BSL-3) facilities (2). *B. thailandensis*, on the other hand, is considered a BSL-2 organism and is frequently used as a model organism for in vitro pathogenesis studies of melioidosis (38).

Intracellular lifestyle of *Burkholderia*

Burkholderia is a facultative intracellular organism which can infect and survive within professional and non-professional phagocytes as well as non-phagocytes (2, 26, 34, 39). In fact, intracellular replication rates of *B. pseudomallei* can be similar to growth in liquid broth (34). The progressive steps associated with *Burkholderia* intracellular lifestyle are well known (Figure 1.2). Within minutes *Burkholderia* subverts host microfilaments to facilitate its internalization into membrane-bound vacuoles or phagosomes (40-44). Within 2 hours, *Burkholderia* typically lyses the vacuole membrane to escape into the cytoplasm where it replicates, though some replication can begin in the vacuole (26, 40, 41, 45, 46). In the cytoplasm *Burkholderia* polymerizes host cell actin and protrudes from membranes to spread from cell to cell (47, 48). Induction of host cell fusion and formation of multinucleated giant cells (MNGCs) is also thought to be a major mechanism of cell-to-cell spread (43).

MNGC formation is a rapid pathology that can develop in infected macrophages within 6-8 hours time (49, 50). Furthermore, MNGC formation is a clinically relevant histopathology

that occurs in human melioidosis as well (51). These MNGC were shown to contain large numbers of intracellular *B. pseudomallei* in the lung, kidney, and spleen (51). Direct cell-to-cell spread through actin polymerization and membrane protrusions, or induction of cell fusion, leads to formation of MNGCs with a correlation between intracellular bacterial burden and the rate of MNGC formation (34, 43).

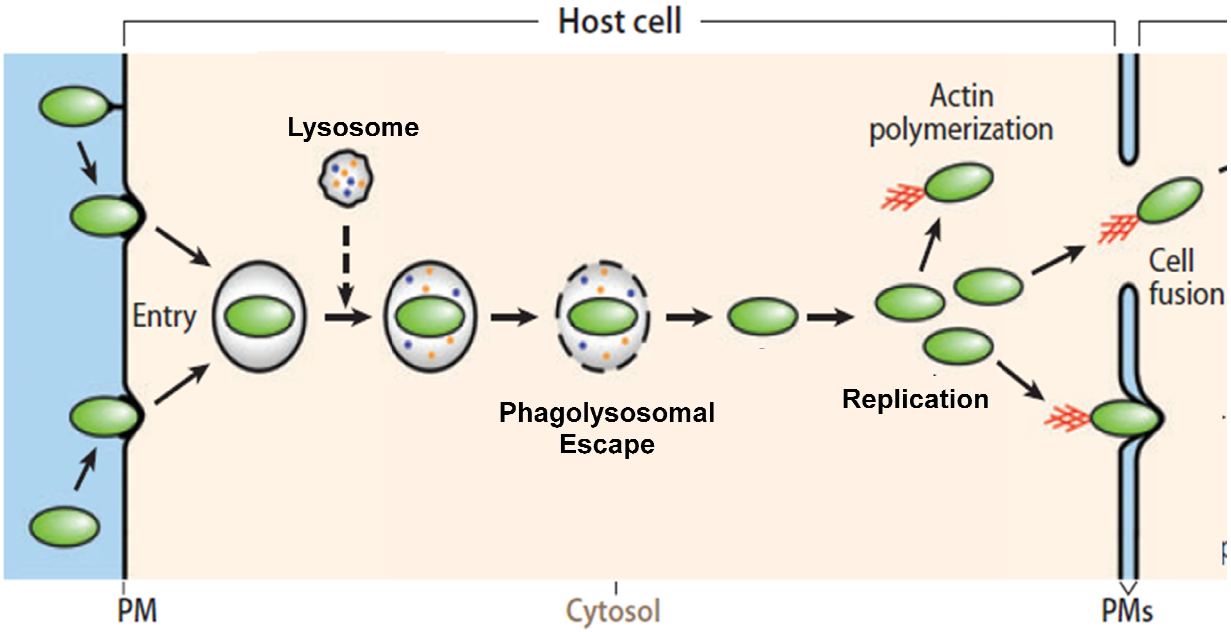

Figure 1.2: Intracellular lifestyle of *Burkholderia*. Upon contact with host cell, *Burkholderia* is taken up into phagosomes. It escapes into the cytoplasm by lysing the phagolysosomal membrane. Once in the cytoplasm, *Burkholderia* can replicate, polymerize actin, and induce cell fusion leading to the formation of MNGC formation. Figure modified from (38).

BimA is a bacterial protein, located at the pole of *Burkholderia* where actin nucleation takes place (52). BimA subverts host cell actin for use by *B. pseudomallei* and is necessary for actin polymerization and actin-based motility (52). French et. al. found that Bim-A mediated actin polymerization and membrane protrusions were not essential for spread of *B. thailandensis* from cell-to-cell, and suggested that induction of host cell fusion was the primary mechanism of intercellular spread for this species (43). Regardless of the mechanism, *Burkholderia* cell-to-cell

spread is aimed at minimizing exposure to extracellular environments which may contain antibiotics and antibodies (2, 34, 48).

Several virulence factors are known to be required for the intracellular survival of *Burkholderia*. *B. pseudomallei* contains three, type three secretion systems (T3SS) and in particular, T3SS gene cluster 3 (T3SS-3) is known to play an important role in virulence (2, 53). Known as the *Burkholderia* secretion apparatus (bsa), T3SS-3 is activated after initial contact with macrophages (54). Furthermore, it is known to modulate intracellular survival and is essential for escape of endocytic vacuoles (43, 53). A study by Stevens and colleagues suggests that *B. pseudomallei* is capable of escaping the vacuole before phagosome-lysosome fusion events take place owing to observations of rare colocalization between wild-type *B. pseudomallei* and lysosome-associated membrane glycoprotein 1 (LAMP-1), a lysosomal marker which is enriched in phagolysosomes (53). On the other hand *B. pseudomallei* which contained mutations to the *bsa* locus were almost exclusively colocalized with LAMP-1 and were contained within membrane-bound vesicles, signifying a failure to escape the vacuole and demonstrating the importance of T3SS-3 for vacuole escape (53). Burtnick et. al. further evaluated the vacuolar escape of *bsa* mutants and found that they *were* capable of vacuolar escape, although escape was significantly delayed by 6 to 12 hours (55). She also found that triple T3SS mutants also exhibited this delayed vacuolar escape phenotype, suggesting that T3SSs may enable rapid escape but are not essential for *Burkholderia* degradation of vacuole membranes and escape into the cytoplasm (55). The T3SS-3 of *B. pseudomallei* likely displays virulence due to secretion of effector proteins through the secretion system apparatus into host cytoplasm. Suparak and colleagues further investigated a T3SS-3 effector protein. They found

that BipB, a translocator protein of the T3SS-3, played a role in MNGC formation and apoptosis of host cells (49).

B. pseudomallei also encodes six, type six secretion systems (T6SS) (56). T6SS-1 is another putative virulence factor that may play important roles in the intracellular lifestyle of *Burkholderia*. T6SS-1 gene cluster transcription is dependent on internalization by host cells and similar to T3SS-3 is important for intracellular growth, and MNGC formation (54, 57, 58). Burtnick et. al. showed that *Hcp1* mutants lacking hemolysin co-regulated protein (Hcp1), a critical component of the T6SS apparatus as well as a secreted immunogenic protein, showed decreased growth rates in RAW 264.7 macrophages as well as decreased cytotoxicity and an inability to form MNGCs (57). *Hcp1* mutants were also less virulent in a Syrian hamster challenge model, again suggesting a role for T6SS-1 in the virulence of *B. pseudomallei* (57). Burtnick et. al. similarly showed that T6SS-1 was a virulence factor in *B. mallei*, a closely related species of *B. pseudomallei*. They showed that T6SS-1 was required for actin tail polymerization and MNGC formation (59). Burtnick and Brett found that T6SS-1 gene expression, as measured by Hcp1 production, was negatively regulated by the divalent cations iron and zinc for both *B. mallei* and *B. pseudomallei*, but not *B. thailandensis* (60). This finding is consistent with increased T6SS-1 expression in host environments such as phagosomes or phagolysosomes which often contain limited nutrients (60). T6SS-5 has also been implemented in MNGC formation and virulence due to VgrG-5, a T6SS-5 effector protein (50).

Eventually, intracellular *B. pseudomallei* replicates to such numbers inside cells that it ruptures the macrophage, releasing bacteria back into the extracellular space to re-infect healthy cells (40). The entire progression of intracellular infection can be so rapid that certain clinical isolates of *B. pseudomallei* can invade, escape vacuoles, replicate and rupture macrophages all

within 120 minutes (40). Other studies have confirmed rapid cell destruction from *B. pseudomallei* infection and found that *B. pseudomallei* could cause severe cytotoxicity to cultures of in vitro macrophages---up to 20-60% cell destruction by 24 hours post-infection (45, 61, 62).

Aside from cell damage through cytotoxicity or rupture, *B. pseudomallei* has been shown to induce apoptotic-like appearance in macrophages such as condensed and fragmented nuclei, positive phosphatidylserine staining, and DNA breakage (34). In one study, condensed and fragmented nuclei were seen in 43% of macrophages after just 6 hours of infection with *B. pseudomallei* (34).

However, since the time of that publication, scientists have significantly advanced their awareness of programmed cell death beyond the simple apoptosis-necrosis paradigm and have characterized the nuances of the several different types of programmed cell death. Apoptosis is characterized as a caspase-3 and caspase-7 dependent, anti-inflammatory mode of cell death with orderly dismantling and compartmentalization of cellular contents (42, 63-65). On the other hand, pyroptosis is defined as a caspase-1 dependent, proinflammatory programmed cell death that results in pore formation in the plasma membrane and release of intracellular contents (42, 63-65).

Armed with new awareness of the different kinds of programmed cell death, others have more recently described *Burkholderia*-induced macrophage cell death as pyroptosis due to the proinflammatory nature of the programmed cell death, rather than apoptosis which is typically anti-inflammatory (42, 63). For example, Sun and colleagues found that *B. pseudomallei* induced caspase-1 dependent cell death in macrophages, causing a release of proinflammatory cytokines IL-1β and IL-18 into extracellular milieu (42). T3SS-3 was found to be necessary for

the rapid killing of macrophages which suggested that T3SS-3 effector proteins may be responsible for induction of cell death (42). Sun also postulated that rapid killing of macrophages by *B. pseudomallei* was ironically a mechanism to evade death itself--a sort of kill or be killed situation (42). Studies by Miao et. al. confirmed a role for caspase-1 dependent pyroptosis in *B. thailandensis* infection but unlike Sun, proposed pyroptosis as a *host* defense mechanism to eliminate intracellular *Burkholderia* rather than a *bacterial* defense to avoid killing by macrophages (63). Breitbach et. al. also suggested that caspase-1 dependent macrophage death is a *host* survival adaptation to limit the intracellular niche for bacterial replication (66). They found that caspase-1 was actually essential for the resistance of C57BL/6 mice to *B. pseudomallei* infection since caspase 1 $^{-/-}$ mice showed rapid mortality and increased bacterial burden compared to wild type mice (66).

HOST RESPONSE TO *BURKHOLDERIA*

Immune response to *Burkholderia* infection

There are several lines of evidence which suggest that *B. pseudomallei*, in many ways, fails to activate a strong immune response in macrophages. *B. pseudomallei* stimulation of macrophages fails to induce inducible nitric oxide synthase (iNOS), a key enzyme and antimicrobial mediator of macrophages that produces nitric oxide ($NO^{\bullet}$), a reactive nitrogen species (RNS) (67, 68). Utaisincharoen also observed a 10x weaker activation of RAW 264.7 macrophage cells as well as slower kinetics of expression of iNOS and tumor necrosis factor alpha (TNF-α) due to stimulation with *B. pseudomallei* compared with *Escherichia coli* or *Salmonella typhi* (69).

The properties of *B. pseudomallei* LPS and CPS may account for its failure to sufficiently activate the antimicrobial properties of macrophages (35, 37). Matsuura and colleagues found that the LPS of *B. pseudomallei* was 100x less pyrogenic, 30x less toxic, and a 10x weaker stimulant of macrophage activation than *Salmonella abortus typhi* (70). They proposed that the longer-chain fatty acids of the lipid A structure of *B. pseudomallei* may account for these differences (70). A different study showed that the O-antigenic polysaccharide moiety of *B. pseudomallei* was accountable for a lack of activation due to interference with Toll-like receptor (TLR) signaling and specifically the MyD88-independent pathway, which is responsible for iNOS expression (68). Although several types of LPS have been identified in *B. pseudomallei*, each with distinct antigens, no association has been found between LPS serotype and clinical presentation or outcome of disease (71). Further studies will be required to determine the specific role of LPS types in the pathogenesis of melioidosis (71). In summary, the immune response to *B. pseudomallei* may be less robust than other Gram negative pathogens in some aspects, however a properly functioning immune system is still the host's best hope for resistance to *B. pseudomallei* and several cell types and cytokines in particular, have been shown to be protective.

Macrophages are one such cell type that are essential for control of acute *B. pseudomallei* infection, as intravenous delivery of liposomal clodronate, a macrophage depleting drug, resulted in greatly increased mortality rates in both C57BL/6 and BALB/c mice (72). In another study, by Haque et. al., macrophages were found to play an important role in acute phase infection presumably through production of IL-12 and IL-18 cytokines which are important inducers of IFN-γ, and are themselves essential for resistance (73).

Neutrophils are another cell type which play an essential role in control of *B. pseudomallei* infection (74-77). Neutrophils were rapidly recruited to the site of infection and were the predominant cell type associated with *B. pseudomallei* in mouse lung tissue at 36 hours post-aerosol infection (76). Easton et. al. also found that activated neutrophils were critical for resistance to *B. pseudomallei* infection, even though their role was most important starting a few days after challenge (74). Woodman et. al studied the role of complement and serum opsonization on uptake and killing of *Burkholderia* in neutrophils. They first found that both *B. pseudomallei* and *B. thailandensis* were extremely resistant to complement-mediated killing alone (75). However, complement-opsonized bacteria were required for the NADPH oxidase-mediated respiratory burst from neutrophils and subsequent intracellular killing of *Burkholderia*, suggesting an important role for complement after all (75).

B cells are known to have a minor and non-essential role in resistance to acute melioidosis. Haque et. al. showed that μMT mice, which lack B cells, had equal mortality rates to *B. pseudomallei* infection compared to wild-type mice, suggesting that B cells are not required for protection against *B. pseudomallei* (73). However, some studies have suggested that B cell antibody response *may* offer some protection against melioidosis (78, 79). Additionally, sero-positivity increases with age for children in northeast Thailand, and as many as 75% of children have been exposed to *B. pseudomallei* by the age of 4 (22). As it turns out this sero-positivity may not have much of a protective effect. Immune system memory to *Burkholderia* from a previous exposure may be inadequate to protect individuals against re-infection since one study showed that 25% of recurrent melioidosis cases were thought to be re-infection rather than relapse (28).

T cells are another cell type that play an important role in melioidosis and seem to have a biphasic role in controlling resistance to *Burkholderia* (73). Early in melioidosis T cells produce the critically important cytokine IFN-γ. More information regarding the specific role of T cells as major producers of IFN-γ can be found in the section on the role of IFN-γ in *B. pseudomallei* infection (below). In the later stages of infection, T cells are important for adaptive immunity. A study be Haque et. al. showed that *B. pseudomallei* primes antigen-specific $CD4^+$ and $CD8^+$ T cells however only mice depleted of $CD4^+$ T cells, before and throughout a *B. pseudomallei* challenge model had greater mortality rates than control mice (73). Mice depleted of $CD8^+$ T cells did not have significantly different mortality rates compared to control mice, although the mean survival time was lower (73). Taken together, these results suggest that T cells, but particularly $CD4^+$ T cells play an important role in adaptive immunity during melioidosis.

Mouse models of melioidosis

In regards to in vivo models of *B. pseudomallei* infection, C57BL/6 mice are considered approximately 100 fold more resistant to the particularly susceptible BALB/c strain, which can be killed with as few as 4 CFU (41, 80-82). Regardless of their differences, both strains are valuable tools to study pathogenesis of melioidosis. BALB/c mice are a better model for acute melioidosis because they mimic several aspects of human disease such as elevated IFN-γ and rapidly increasing bacteremia for several days before death (81). Additionally, a correlation between increased IFN-γ and increased bacterial burden and severity of disease has been identified in both BALB/c mice as well as patients with melioidosis (82, 83). On the other hand, C57BL/6 mice may serve as a model for chronic disease since they are able to survive for weeks after infection but still carry heavy bacteria loads in liver and spleen (81). Furthermore, studying

C57BL/6 mice can provide insight into their resistance mechanisms and may help identify new drug targets or therapies to treat melioidosis. For example, we know that a rapid and effective innate response contributes to C57BL/6 resistance since C57BL/6 mice can rapidly clear an infection that would kill BALB/c mice (41, 81).

The role of IFN-γ in bacterial pathogenesis

IFN-γ is a cytokine secreted mainly by T cells and natural killer (NK) cells, which serves as one of the two essential activation signals for macrophages (84-86). Macrophages activated by IFN-γ increase their antibacterial properties in several ways (84, 87). They increase expression of NADPH phagocyte oxidase subunits, they restrict nutrients such as iron and tryptophan from the phagosome while enriching for copper, and they are primed for NO production (84, 85, 87). Furthermore, IFN-γ and IFN-γ + LPS stimulated macrophages showed continuous phagosome-lysosome fusion events for up to 5-10 hours after stimulation, which led to great concentrations of lysosomal constituents in the phagolysosome (88).

Through activation of macrophages, IFN-γ has been shown to increase microbicidal activity against many intracellular pathogens, though the roles of IFN-γ are diverse (89). During *S. typhimurium* infection of macrophages, IFN-γ reduces iron uptake, increases iron efflux, and increases expression of the siderophore and antimicrobial peptide lipocalin 2 (90). In these ways, the macrophage limits the availability of iron, an essential nutrient for bacterial growth. In *Mycobacterium tuberculosis*, IFN-γ is thought to have both beneficial and detrimental effects to macrophages depending on the level of intracellular infection. IFN-γ inhibits *M. tuberculosis* replication during low-infection loads, but accelerates cell death by necrosis in heavily infected macrophages (91). In *Listeria monocytogenes* infected macrophages, IFN-γ stimulation has been

shown to increase the intracellular killing capacity of macrophages (92). IFN-γ has also been shown to restrict intracellular replication of *L. monocytogenes* (92). This effect was confirmed by Ouadrhiri and colleagues who showed that IFN-γ induced ROS and RNS were together responsible for restricting intracellular *L. monocytogenes* replication (93).

Several studies have also shown a role for IFN-γ prevention of vacuolar escape in a number of intracellular pathogens (92, 94, 95). For instance, Myers et. al. showed that ROS, and to a smaller degree RNS, were required for the preventing *L. monocytogenes* from escaping vacuoles (95). This study also showed that ROS and RNS inhibitors could partially reverse this effect, which is consistent with a ROS-mediated mechanism (95). Similarly, Lindgren and colleagues found that IFN-γ activation of peritoneal exudate cells partially prevented *Francisella tularensis* from escaping phagosomes (94). Furthermore they proposed that the bacteria which did escape were too damaged to replicate in the cytoplasm (94). These results show an important role for IFN-γ to interfere with intracellular pathogen lifestyles in mammalian host cells, a mechanism that may increase killing of intracellular bacteria as well as prevent spread and further replication.

The role of IFN-γ in *B. pseudomallei* infection

In a previous section we described several experiments that showed a failure of *B. pseudomallei*, by itself, to stimulate a strong immune response from macrophages. However, several studies have shown a role for interferons to increase activation of *B. pseudomallei*-stimulated macrophages. For example, even though *B. pseudomallei* was unable to elicit iNOS expression in macrophages or control intracellular bacterial burden by itself, simultaneous stimulation of macrophages with exogenous IFN-β and *B. pseudomallei* led to greatly increased

levels of iNOS and increased killing of intracellular bacteria through $NO^{\bullet}$ production (67). Similarly, although the LPS from *B. pseudomallei* interfered with MyD88-independent pathways and prevented iNOS production, pre-activation of macrophages with IFN-γ and then subsequent infection increased expression of MyD88-independent pathways and increased expression of iNOS in macrophages (68). Several other studies have shown an increased ability of macrophages to kill intracellular *Burkholderia* due to IFN-γ stimulation (32, 44, 66).

Both BALB/c and C57BL/6 strains of mice produce high levels of IFN-γ in response to *B. pseudomallei* infection, with BALB/c mice producing slightly higher levels both locally and systemically, but with slightly delayed expression, compared to C57BL/6 mice (82, 96, 97). High IFN-γ levels in BALB/c correlate to increased bacteria burden in tissue, suggesting that hyperproduction of IFN-γ in BALB/c mice may actually be more detrimental than protective (82). Regardless, it is undisputed that IFN-γ, at some level, is necessary to control infection. In fact, several studies have shown an absolutely obligatory role of IFN-γ for resistance to *B. pseudomallei* infection (72-74, 80). For instance, IFN-γ was found to be essential for Taylor Outbred mouse resistance to *B. pseudomallei* as neutralizing antibody against IFN-γ lowered the lethal dose by 100,000 fold and caused great increases in bacterial burden in liver and spleen (80). Additionally, IFN-γ neutralization in C57BL/6 mice led to greatly increased mortality rates while BALB/c mice retained significant protection, suggesting a different requirement for IFN-γ between these two breeds of mice (72). Furthermore, while there was no role for iNOS in the C57BL/6 mouse resistance to *B. pseudomallei*, an important role was identified for nicotinamide adenine dinucleotide phosphate (NADPH) phagocyte oxidase and specifically macrophage NADPH oxidase to control infection (72).

Other immune cells are the main sources of the necessary IFN-γ response. Studies show that NK cells as well as $CD3^+$ T cells are the major producers of IFN-γ due to *B. pseudomallei* infection (74, 96). Antigen-unspecific bystander T cells, particularly $CD8^+$ T cells, can also be activated to produce IFN-γ upon stimulation by cytokines IL-12 and IL-18 (73, 98).

One of the main antimicrobial mechanisms of IFN-γ activated macrophages is the degradation of internalized bacteria in the phagolysosome. Activated macrophages increase production of NADPH phagocyte oxidase subunits and subsequently increase intracellular ROS production (85, 86, 99, 100). As phagosomes mature they fuse with lysosomes, exposing the phagocytosed bacteria to antimicrobial peptides (AMPs), lysozyme, and proteases (101). While lysosomes are always acidic (pH ~4.8), phagosomes increase in acidity with increased lysosomal fusion events (102). Phagosome-lysosome fusion can occur within 20 minutes of *Burkholderia* uptake, which closely correlates to the minimum time required by *B. pseudomallei* to escape into the cytoplasm (39, 40, 45). Those bacteria which take longer to escape are under attack by the toxic environment of the phagolysosome. Puthucheary et. al. have shown the phagolysosome to have microbicidal activity against *B. pseudomallei* by showing that the number of bacteria inside phagolysosomes decreases with increased lysosome fusion (40).

Finally, IFN-γ has also been shown to interfere with normal *Burkholderia* pathogenesis. Both pre-treatment of macrophages with IFN-γ prior to infection or co-administration of IFN-γ with infection led to almost complete prevention of cell fusion and multinucleated giant cell formation (MNGC) by eight hours post-infection (103, 104).

REACTIVE OXYGEN SPECIES AND ANTIOXIDANTS

Generation and detrimental effects of reactive oxygen species

The term "reactive oxygen species" refers to a group of highly reactive, short lived, partially reduced, oxygen-derived molecules which are capable of causing damage through reactions with nucleic acids, lipids, and proteins (87, 105, 106). Some ROS such as superoxide anion ($O_2^{\bullet -}$) or hydroxyl radical ($OH^{\bullet}$) are also free radicals due to their unpaired electron, while others such as hydrogen peroxide (H_2O_2) are simply unstable and highly reactive.

ROS are formed at low levels in all cell types as a byproduct of cellular respiration, although phagocytes are capable of generating higher levels of ROS as an antimicrobial response through the nicotinamide adenine dinucleotide phosphate (NADPH) phagocyte oxidase (100, 101, 105, 107-109). NADPH phagocyte oxidase is a large complex composed of five essential subunits. The cytosolic proteins $p47^{phox}$, $p67^{phox}$, and Rac assemble with $gp91^{phox}$ and $p22^{phox}$ in the membrane (100, 108). NADPH phagocyte oxidase assembles primarily on phagosome and plasma membranes and is expressed in macrophages, neutrophils, and eosinophils (100, 108). Once assembled, NADPH phagocyte oxidase functions as an electron transporter to pump electrons into the compartment, reduce oxygen, and generate superoxide anion (100, 101, 108). It is estimated that the NADPH oxidase generates large amounts of superoxide, which could equate to concentrations of 2 μM in acidified phagosome compartments (101).

Since ROS are produced in all cells to varying extents, it is crucial for cells to degrade ROS or contain them in specialized compartments in order to avoid their toxic effects. Eukaryotes possess mechanisms to deal with ROS in essentially all compartments and organelles (105). In just about every cell, superoxide anion is formed when oxygen accidentally gains an electron from the electron transport chain in mitochondria. Superoxide dismutase (SOD) is an

enzyme which rapidly catalyzes the conversion of superoxide to hydrogen peroxide (H_2O_2), another form of ROS (105, 110, 111). Of the known ROS, only H_2O_2 is thought to be stable enough to cross membranes, however the rates of H_2O_2 turnover inside cells is so rapid that the concentrations between intracellular and extracellular environments never equilibrate and can differ by a factor of ten (101, 105). Catalases and peroxidases are responsible for degradation of H_2O_2 into water and oxygen.

Besides the directly toxic effects of superoxide to biomolecules, superoxide can also create more ROS. It can react with iron-sulfur clusters, important enzymatic cofactors and redox sensors in the cell, releasing free iron that then reacts with hydrogen peroxide through Fenton chemistry to form deadly hydroxyl radicals ($OH^{\bullet}$) (105, 112, 113). Hydroxyl radicals react almost instantly with biomolecules at the site of their creation and are considered an extremely toxic form of ROS (105).

Antioxidants and ROS scavengers

Glutathione (GSH), or γ-glutamylcysteinylglycine, is the most abundant thiol and cellular antioxidant present in cells (114, 115). GSH is formed in two steps. The first reaction, which is also the rate limiting reaction, is catalyzed by glutamate cysteine ligase, also known as γ-glutamylcysteine synthetase, which joins glutamate to cysteine (115-117). The second step, catalyzed by glutathione synthetase, joins glycine to γ-glutamylcysteine to form GSH (115, 117). GSH synthesis takes place in the cytoplasm where these enzymes are localized (118). NAC is a precursor to GSH synthesis.

Intracellular GSH exists primarily in the reduced thiol form and has consistently high distribution within the cytoplasm, mitochondria, and nucleus of almost all eukaryotic cells (119,

120). Intracellular concentrations of GSH are typically between 1-10 mM in most cell types (115). GSH directly reacts with and eliminates ROS such as hypochlorous acid (HOCl) and is also utilized by the family of glutathione peroxidases (GPx) to reduce H_2O_2 to water (115, 120). GSSG, the oxidized, disulfide form of GSH is also produced from GPx reactions, but glutathione reductases quickly return glutathione to its reduced form using NADPH reducing equivalents (114, 115). Figure 1.3 shows select pathways of ROS production and degradation that will come into play in chapters 2-6.

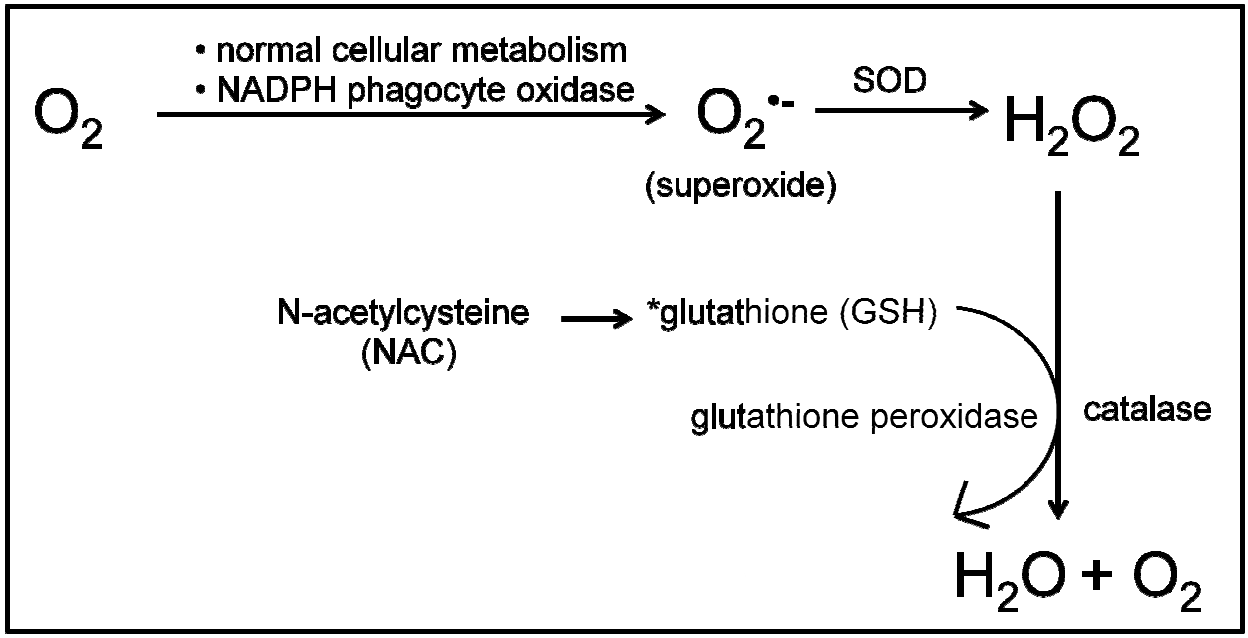

Figure 1.3: Select pathways of ROS production and degradation. All cells make some level of ROS through normal cellular metabolism, but macrophages use NADPH phagocyte oxidase to make large quantities of ROS such as superoxide ($O_2^{\bullet-}$) anion. The enzyme superoxide dismutase (SOD) can convert superoxide into hydrogen peroxide (H_2O_2), another form of ROS. Both catalase and glutathione peroxidase can degrade hydrogen peroxide into non-toxic compounds. Glutathione peroxidase needs to use GSH to do this. NAC is a precursor to GSH production.

GSH also has antioxidant roles as a secreted peptide, especially in the fluid lining in the lungs (115). GSH is extremely resistant to protease degradation as only one enzyme, γ-glutamyl transpeptidase, has been identified which is capable of GSH hydrolysis (121).

GSH is known to play an antioxidant role during oxidative stress. Increased intracellular oxidative stress is associated with decreased intracellular glutathione, with the largest decreases of GSH occurring in the cytoplasm and nucleus (119, 122-124). Mitochondrial GSH can also be depleted, though a low level of GSH is maintained in this organelle to counter the constant low level of ROS produced in mitochondria by cellular respiration (119). NAC also serves as an antioxidant and ROS scavenger, and can decrease the respiratory burst exhibited by polymorphonuclear cells (125).

GSH biosynthesis is most commonly and effectively inhibited by the compound buthionine sulfoximine (BSO), a specific inhibitor of glutamate cysteine ligase (116, 126). BSO depletes intracellular GSH by inhibiting new synthesis, but the length of time required to achieve its effects depends on the turnover rate of glutathione in a particular cell type as well as the permeability of the cells to BSO (126). For example, treatment of cultured red blood cells with BSO (4 mM) for two hours resulted in 0.2 mM intracellular concentrations of BSO and greater than 90% inhibition of GSH biosynthesis, however detection of depleted GSH was not measurable until six hours post-treatment due to the slow turnover rate of GSH in red blood cells (126). To contrast, in murine lymphoma cells, BSO (0.2 mM) took 12-15 hours to deplete GSH by greater than 90% while the same reduction in GSH content took 7.5 hours in mouse peritoneal macrophages (126). Stevenson et. al. used 150 μM BSO for 20 hours to deplete hepatocyte GSH by 69% (123).

BSO is also safe and effective for GSH depletion in vivo (126). Griffith dosed mice up to 32 mmol/kg without any signs of adverse effects. Although BSO isn't metabolized quickly in mice, it *is* excreted in urine, so a dose of 8 mmol/kg every four hours is suggested to keep the concentration of BSO at an inhibitory level in most tissues (126).

Diethyl maleate (DEM) is another GSH depleting agent though it functions through a non-specific mechanism to directly deplete GSH rather than prevent de novo synthesis (127). DEM is not typically a first choice drug to deplete GSH because it has effects outside of the depletion of GSH which can complicate interpretation of experimental results (127). Furthermore since DEM works by direct depletion, cells sense the decreased presence of GSH and actually increase synthesis of GSH during treatment with DEM (127).

ROS generation and degradation in bacteria

Bacteria not only produce high levels of ROS themselves, but they also face toxic levels of ROS from eukaryotic hosts. Most intracellular bacteria have evolved mechanisms of resistance to ROS. Target modification is rarely seen as a mechanism of resistance to ROS since the detrimental effects of ROS have atomic and chemical specificities to their targets unlike antibiotics with macromolecular specificity (109). Instead, evasion of host ROS production, degradation of ROS, or simply repair from ROS damage are the most frequently observed mechanisms of resistance to ROS (109).

For the most part, pathways of ROS generation are similar between both eukaryotic and prokaryotic cells (105). Bacteria produce significant levels of ROS through normal cellular processes, similar to eukaryotes. *E. coli* has been shown to produce 15 µM H_2O_2 per second and about 5 µM superoxide anion per second (105). Also similar to eukaryotes, bacteria have similar

ROS degradation pathways involving SOD, catalases, and peroxidases (105). If these antioxidant and ROS scavenging strategies fail, as little as 1 μM intracellular H_2O_2 can cause deadly levels of DNA damage (105). As an example of the critical importance of cellular defenses against ROS, *E. coli* produce SOD in quantities approximately 4 orders of magnitude greater than needed (105).

Proteobacteria produce glutathione to eliminate ROS, similarly to eukaryotes (121). Bacteria contain high concentrations of intracellular GSH ranging from 0.1-10 mM (121). Increasing availability of cysteine may be able to increase GSH production in bacteria and increase protection against oxidative stress (100, 107, 121, 128). Bacteria may also be able to utilize exogenous sources of GSH. A major mechanism of exogenous GSH utilization in bacteria is thought to occur through degradation by γ-glutamyl transpeptidase followed by cysteine or glycine salvage (121, 129, 130). Uptake of whole reduced glutathione may also take place (131, 132).

Several studies have proven the ability of antioxidants, including NAC and GSH, to protect bacteria against killing by antibiotics (133-136). Through mutant deletion of *gshB,* which encodes for a key enzyme in glutathione synthesis, Dhamdhere and colleagues showed that exogenously added GSH was able to protect bacteria from both bactericidal and bacteriostatic antibiotics, suggesting the mechanism of GSH protection may be localized to the outer structures of bacteria (134). Interestingly, endogenously produced GSH was actually detrimental to the protection (134). Furthermore, a recent study showed that 10 mM GSH did not protect *Staphylococcus aureus* against ciprofloxacin, gentamicin, or chloramphenicol (137), suggesting that antioxidant protection against antibiotics may be specific to Gram-negative bacteria.

ROS generation and degradation in *B. pseudomallei*

Specifically, *Burkholderia* possess several mechanisms by which they can defend against oxidative stress. These include degradation through catalases and SOD enzymes, through scavenging molecules such as glutathione, sequestration of iron, and through transcriptional regulation of oxidative stress response proteins (OxyR and SoxRS). *B. pseudomallei* expresses a dual, catalase-peroxidase enzyme (katG) which is important for resistance to killing by several pro-oxidant drugs (138). *KatG* is transcriptionally regulated by OxyR under conditions of oxidative stress (138).

A study by Chieng et. al. investigated transcriptional changes to *B. pseudomallei* during 6 hours of macrophage infection (45). They surprisingly found that most oxidative-stress related genes, including *katG*, *oxyR*, and the general stress response alternative sigma factor, *rpoS*, were either down-regulated or remained similar to levels in bacteria that were grown in cell culture media alone (45). This result suggests that *B. pseudomallei* is well-adapted to evade the oxidative environment of the phagolysosome, presumably by rapidly escaping into the cytoplasm (45).

B. pseudomallei also expresses at least one superoxide dismutase (SOD) enzyme which can convert superoxide anion ($O_2^{\bullet-}$) to hydrogen peroxide. Vanaporn and colleagues identified a copper and zinc dependent sodC enzyme from *B. pseudomallei* (139). An *sodC* deletion mutant of *B. pseudomallei* exhibited increased sensitivity to killing by superoxide, decreased survival inside macrophages, and led to lower mortality rates in BALB/c compared with the wild-type control (139). These results show the importance of *sodC* to *B. pseudomallei* intracellular survival and virulence.

Role of ROS as the mechanism of antibiotic killing

There has been considerable controversy over the last decade as to whether or not bactericidal antibiotics kill bacteria through a common ROS-mediated pathway, regardless of antibiotic target. On the one hand, there have been numerous studies supporting a common mechanism of bactericidal antibiotics through ROS induction. These studies suggest that antibiotics stimulate hyperactivation of the electron transport chain in bacteria which decreases the levels of NADH, increases the levels of superoxide anion, release of iron from iron-sulfur clusters, and generation of hydroxyl radicals through the Fenton reaction which eventually cause death due to irreparable damage to DNA (107, 140-143).

Aminoglycosides are one of the bactericidal classes of antibiotics thought to function through the common oxidative pathway for antibiotic killing. Briefly, aminoglycoside interaction with the ribosome led to mistranslation of proteins, which were then misfolded in the periplasmic space, activating bacterial envelope stress responses which then interfere with various metabolic pathways including the TCA cycle and electron transport chain (144).

Foti and colleagues studied the mechanism by which antibiotic ROS leads to irreparable DNA damage. They found that guanine nucleotides were particularly susceptible to oxidation, forming 7,8-dihydro-8-oxyguanine (8-oxo-guanine) (141). This molecule was potentially mutagenic because it could pair with either adenine or cytosine. If mismatches arose close to one another in the DNA, double stranded breaks could occur during glycosalase excision and repair (105, 141). Shatalin et. al. confirmed that antibiotics caused double-stranded breaks in DNA, an effect which could be reversed by protection against oxidative stress (145).

Studies by Grant et. al showed that increased oxygen availability could increase hydroxyl radical formation in and killing of persister cells, a dormant and naturally resistant subpopulation

of bacteria (146). Indeed, others agree that oxygen concentration is proportional to levels of ROS production (147). Other evidence for oxidative killing by antibiotics came from studies by Wang and Zhao which showed that mutant *E. coli* deficient in either *sodA*, *sodB*, or *katG*, showed increased susceptibilities to fluoroquinolones (148). Furthermore, the ROS scavenger thiourea was able to reduce the killing effectiveness of fluoroquinolones which is consistent with an oxidative pathway for antibiotic killing (148).

Goswami et. al. showed that both 10 mM ascorbic acid as well as 10 mM GSH partially protected *E. coli* from the killing effects of fluoroquinolones (135). Furthermore, mutants deficient in catalase and peroxidase activities were significantly protected from ciprofloxacin killing, suggesting a role for oxidative stress in the mechanism of ciprofloxacin (135). However, a separate study showed that GSH could protect *E. coli* against bacteriostatic drugs as well, which are not known to induce ROS-mediated death, suggesting a role for GSH protection beyond its antioxidant function (134).

More recent investigations into the notion of ROS mediated antibiotic killing show that ROS is *not* involved in antibiotic-mediated killing. In a beautifully elegant experiment, Keren et. al. showed that the bacteria cells which had higher intracellular ROS levels due to bactericidal antibiotics, were not more likely to be killed (149). Their study showed that hydroxyphenyl fluorescein (HPF) which many studies have used to measure intracellular ROS, was not an indicator of impending bacterial death (149). Furthermore, thiourea, a commonly used ROS-scavenger was only effective at protecting bacteria from low concentrations of antibiotics, but not higher, clinically relevant concentrations (149). One criticism of this result is that the researchers did not increase the concentration of thiourea along-side increased antibiotic concentration. It would be expected that as bacteria killing is increased with increasing

antibiotic concentration, a higher concentration of ROS-scavengers would be needed to provide the same level of protection. Finally, they showed that *E. coli* grown and treated with antibiotics in completely anaerobic conditions were killed equally or better than bacteria grown and treated in aerobic conditions, an effect which is in direct contradiction to a ROS-mediated pathway for antibiotic-mediated death (149).

Another recent study by Imlay and colleagues confirmed that antibiotics, specifically ampicillin and norfloxacin were capable of the same efficiency of killing in anaerobic versus aerobic conditions, an effect which undermines a ROS-mediated pathway for antibiotic killing (150). They went on to show that an *E. coli* mutant, lacking catalase and peroxidase activity, was more sensitive to fluoroquinolones but not aminoglycosides or β-lactams. The mutant's decreased sensitivity to fluoroquinolones was thought to be due to the effects of fluoroquinolones on DNA metabolism (150). They also showed that oxygen consumption, and therefore respiration, didn't substantially increase in antibiotic treated *E. coli*, but in fact *declined* with kanamycin treatment. Furthermore, they showed that β-lactams and fluoroquinolones failed to induce OxyR-controlled genes which were rapidly upregulated due to H_2O_2 alone, and confirmed a lack of antibiotic induced H_2O_2 by direct measure in the supernatants, using catalase/peroxidase mutants (150). Finally, Ezraty and Barras also showed that *E. coli* mutants lacking both *sodA* and *sodB* or lacking *oxyR* were similarly sensitive to ampicillin or gentamicin compared to wild type bacteria (151).

The recent studies described above utilized both elegant and creative approaches to show that antibiotic-mediated cell death occurs independently of ROS. However as ROS proponent James Collins points out, ROS has never been suggested to be the sole way in which antibiotics exert their killing effects (152). In addition, these studies focused on one organism, *E. coli*. It is

possible that other organisms respond differently to antibiotics. Furthermore, these studies did not address the use of other antioxidants, besides thiourea, to reverse killing effects of antibiotics. Therefore, there may still be a small role for ROS-mediated effects in antibiotic killing.

Summary of literature review

The studies and results discussed in this chapter serve as background for the remaining chapters. The current literature suggests a key role for IFN-γ stimulated responses in host defense against intracellular pathogens, especially through activation of macrophages to enhance their killing capabilities. There is also a known role for ROS responses in host defense against bacterial pathogens. Understanding connections between these pathways and their interactions with antibiotics may offer insights into improving antibacterial therapies and treatments.

REFERENCES

1. **Dance DA.** 1991. Melioidosis: the tip of the iceberg? Clin Microbiol Rev **4:**52-60.

2. **Wiersinga WJ, van der Poll T, White NJ, Day NP, Peacock SJ.** 2006. Melioidosis: insights into the pathogenicity of *Burkholderia pseudomallei*. Nat Rev Microbiol **4:**272-282.

3. **Jabbar Z, Currie BJ.** 2013. Melioidosis and the kidney. Nephrology (Carlton) **18:**169-175.

4. **Wiersinga WJ, Currie BJ, Peacock SJ.** 2012. Melioidosis. N Engl J Med **367:**1035-1044.

5. **Limmathurotsakul D, Wongratanacheewin S, Teerawattanasook N, Wongsuvan G, Chaisuksant S, Chetchotisakd P, Chaowagul W, Day NP, Peacock SJ.** 2010. Increasing incidence of human melioidosis in Northeast Thailand. Am J Trop Med Hyg **82:**1113-1117.

6. **Suputtamongkol Y, Hall AJ, Dance DA, Chaowagul W, Rajchanuvong A, Smith MD, White NJ.** 1994. The epidemiology of melioidosis in Ubon Ratchatani, northeast Thailand. Int J Epidemiol **23:**1082-1090.

7. **Currie BJ, Fisher DA, Howard DM, Burrow JN, Selvanayagam S, Snelling PL, Anstey NM, Mayo MJ.** 2000. The epidemiology of melioidosis in Australia and Papua New Guinea. Acta Trop **74:**121-127.

8. **Parameswaran U, Baird RW, Ward LM, Currie BJ.** 2012. Melioidosis at Royal Darwin Hospital in the big 2009-2010 wet season: comparison with the preceding 20 years. Med J Aust **196:**345-348.

9. **Currie BJ, Jacups SP, Cheng AC, Fisher DA, Anstey NM, Huffam SE, Krause VL.** 2004. Melioidosis epidemiology and risk factors from a prospective whole-population study in northern Australia. Trop Med Int Health **9:**1167-1174.

10. **Mu JJ, Cheng PY, Chen YS, Chen PS, Chen YL.** 2014. The occurrence of melioidosis is related to different climatic conditions in distinct topographical areas of Taiwan. Epidemiol Infect **142:**415-423.

11. **Hassan MR, Pani SP, Peng NP, Voralu K, Vijayalakshmi N, Mehanderkar R, Aziz NA, Michael E.** 2010. Incidence, risk factors and clinical epidemiology of melioidosis: a complex socio-ecological emerging infectious disease in the Alor Setar region of Kedah, Malaysia. BMC Infect Dis **10:**302.

12. **Currie BJ, Jacups SP.** 2003. Intensity of rainfall and severity of melioidosis, Australia. Emerg Infect Dis **9:**1538-1542.

13. **Cheng AC, Currie BJ, Dance DA, Funnell SG, Limmathurotsakul D, Simpson AJ, Peacock SJ.** 2013. Clinical definitions of melioidosis. Am J Trop Med Hyg **88:**411-413.

14. **Glass MB, Gee JE, Steigerwalt AG, Cavuoti D, Barton T, Hardy RD, Godoy D, Spratt BG, Clark TA, Wilkins PP.** 2006. Pneumonia and septicemia caused by *Burkholderia thailandensis* in the United States. J Clin Microbiol **44:**4601-4604.

15. **Hodgson KA, Morris JL, Feterl ML, Govan BL, Ketheesan N.** 2011. Altered macrophage function is associated with severe *Burkholderia pseudomallei* infection in a murine model of type 2 diabetes. Microbes Infect **13:**1177-1184.

16. **Ngauy V, Lemeshev Y, Sadkowski L, Crawford G.** 2005. Cutaneous melioidosis in a man who was taken as a prisoner of war by the Japanese during World War II. J Clin Microbiol **43:**970-972.

17. **Mays EE, Ricketts EA.** 1975. Melioidosis: recrudescence associated with bronchogenic carcinoma twenty-six years following initial geographic exposure. Chest **68:**261-263.

18. **Fisher DA, Harris PN.** 2013. Melioidosis: refining management of a tropical time bomb. Lancet.

19. **Currie BJ, Fisher DA, Anstey NM, Jacups SP.** 2000. Melioidosis: acute and chronic disease, relapse and re-activation. Trans R Soc Trop Med Hyg **94:**301-304.

20. **Brent AJ, Matthews PC, Dance DA, Pitt TL, Handy R.** 2007. Misdiagnosing melioidosis. Emerg Infect Dis **13:**349-351.

21. **Wuthiekanun V, Peacock SJ.** 2006. Management of melioidosis. Expert Rev Anti Infect Ther **4:**445-455.

22. **Kanaphun P, Thirawattanasuk N, Suputtamongkol Y, Naigowit P, Dance DA, Smith MD, White NJ.** 1993. Serology and carriage of *Pseudomonas pseudomallei*: a prospective study in 1000 hospitalized children in northeast Thailand. J Infect Dis **167:**230-233.

23. **Chantratita N, Tandhavanant S, Wongsuvan G, Wuthiekanun V, Teerawattanasook N, Day NP, Limmathurotsakul D, Peacock SJ.** 2013. Rapid detection of *Burkholderia pseudomallei* in blood cultures using a monoclonal antibody-based immunofluorescent assay. Am J Trop Med Hyg **89:**971-972.

24. **Schweizer HP.** 2012. Mechanisms of antibiotic resistance in *Burkholderia pseudomallei*: implications for treatment of melioidosis. Future Microbiol **7:**1389-1399.

25. **Tandhavanant S, Thanwisai A, Limmathurotsakul D, Korbsrisate S, Day NP, Peacock SJ, Chantratita N.** 2010. Effect of colony morphology variation of *Burkholderia pseudomallei* on intracellular survival and resistance to antimicrobial environments in human macrophages in vitro. BMC Microbiol **10:**303.

26. **Jones AL, Beveridge TJ, Woods DE.** 1996. Intracellular survival of *Burkholderia pseudomallei*. Infect Immun **64:**782-790.

27. **Chaowagul W, Suputtamongkol Y, Dance DA, Rajchanuvong A, Pattara-arechachai J, White NJ.** 1993. Relapse in melioidosis: incidence and risk factors. J Infect Dis **168:**1181-1185.

28. **Maharjan B, Chantratita N, Vesaratchavest M, Cheng A, Wuthiekanun V, Chierakul W, Chaowagul W, Day NP, Peacock SJ.** 2005. Recurrent melioidosis in patients in northeast Thailand is frequently due to reinfection rather than relapse. J Clin Microbiol **43:**6032-6034.

29. **Brett PJ, Deshazer D, Woods DE.** 1997. Characterization of *Burkholderia pseudomallei* and *Burkholderia pseudomallei*-like strains. Epidemiol Infect **118:**137-148.

30. **Smith MD, Angus BJ, Wuthiekanun V, White NJ.** 1997. Arabinose assimilation defines a nonvirulent biotype of *Burkholderia pseudomallei*. Infect Immun **65:**4319-4321.

31. **Brett PJ, DeShazer D, Woods DE.** 1998. *Burkholderia thailandensis* sp. nov., a *Burkholderia pseudomallei*-like species. Int J Syst Bacteriol **48 Pt 1:**317-320.

32. **Charoensap J, Utaisincharoen P, Engering A, Sirisinha S.** 2009. Differential intracellular fate of *Burkholderia pseudomallei* 844 and *Burkholderia thailandensis* UE5 in human monocyte-derived dendritic cells and macrophages. BMC Immunol **10:**20.

33. **Rainbow L, Hart CA, Winstanley C.** 2002. Distribution of type III secretion gene clusters in *Burkholderia pseudomallei, B. thailandensis* and *B. mallei*. J Med Microbiol **51:**374-384.

34. **Kespichayawattana W, Rattanachetkul S, Wanun T, Utaisincharoen P, Sirisinha S.** 2000. *Burkholderia pseudomallei* induces cell fusion and actin-associated membrane protrusion: a possible mechanism for cell-to-cell spreading. Infect Immun **68:**5377-5384.

35. **Novem V, Shui G, Wang D, Bendt AK, Sim SH, Liu Y, Thong TW, Sivalingam SP, Ooi EE, Wenk MR, Tan G.** 2009. Structural and biological diversity of lipopolysaccharides from *Burkholderia pseudomallei* and *Burkholderia thailandensis*. Clin Vaccine Immunol **16:**1420-1428.

36. **Reckseidler-Zenteno SL, Viteri DF, Moore R, Wong E, Tuanyok A, Woods DE.** 2010. Characterization of the type III capsular polysaccharide produced by *Burkholderia pseudomallei*. J Med Microbiol **59:**1403-1414.

37. **Reckseidler-Zenteno SL, DeVinney R, Woods DE.** 2005. The capsular polysaccharide of *Burkholderia pseudomallei* contributes to survival in serum by reducing complement factor C3b deposition. Infect Immun **73:**1106-1115.

38. **Galyov EE, Brett PJ, DeShazer D.** 2010. Molecular insights into *Burkholderia pseudomallei* and *Burkholderia mallei* pathogenesis. Annu Rev Microbiol **64:**495-517.

39. **Stevens MP, Galyov EE.** 2004. Exploitation of host cells by *Burkholderia pseudomallei*. Int J Med Microbiol **293:**549-555.

40. **Puthucheary SD, Nathan SA.** 2006. Comparison by electron microscopy of intracellular events and survival of *Burkholderia pseudomallei* in monocytes from normal subjects and patients with melioidosis. Singapore Med J **47:**697-703.

41. **Hoppe I, Brenneke B, Rohde M, Kreft A, Haussler S, Reganzerowski A, Steinmetz I.** 1999. Characterization of a murine model of melioidosis: comparison of different strains of mice. Infect Immun **67:**2891-2900.

42. **Sun GW, Lu J, Pervaiz S, Cao WP, Gan YH.** 2005. Caspase-1 dependent macrophage death induced by *Burkholderia pseudomallei*. Cell Microbiol **7:**1447-1458.

43. **French CT, Toesca IJ, Wu TH, Teslaa T, Beaty SM, Wong W, Liu M, Schroder I, Chiou PY, Teitell MA, Miller JF.** 2011. Dissection of the *Burkholderia* intracellular life cycle using a photothermal nanoblade. Proc Natl Acad Sci U S A **108:**12095-12100.

44. **Bast A, Schmidt IH, Brauner P, Brix B, Breitbach K, Steinmetz I.** 2011. Defense Mechanisms of Hepatocytes Against *Burkholderia pseudomallei*. Front Microbiol **2:**277.

45. **Chieng S, Carreto L, Nathan S.** 2012. *Burkholderia pseudomallei* transcriptional adaptation in macrophages. BMC Genomics **13:**328.

46. **Harley VS, Dance DA, Tovey G, McCrossan MV, Drasar BS.** 1998. An ultrastructural study of the phagocytosis of *Burkholderia pseudomallei*. Microbios **94:**35-45.

47. **Breitbach K, Rottner K, Klocke S, Rohde M, Jenzora A, Wehland J, Steinmetz I.** 2003. Actin-based motility of *Burkholderia pseudomallei* involves the Arp 2/3 complex, but not N-WASP and Ena/VASP proteins. Cell Microbiol **5:**385-393.

48. **Allwood EM, Devenish RJ, Prescott M, Adler B, Boyce JD.** 2011. Strategies for Intracellular Survival of *Burkholderia pseudomallei*. Front Microbiol **2:**170.

49. **Suparak S, Kespichayawattana W, Haque A, Easton A, Damnin S, Lertmemongkolchai G, Bancroft GJ, Korbsrisate S.** 2005. Multinucleated giant cell formation and apoptosis in infected host cells is mediated by *Burkholderia pseudomallei* type III secretion protein BipB. J Bacteriol **187:**6556-6560.

50. **Schwarz S, Singh P, Robertson JD, Leroux M, Skerrett SJ, Goodlett DR, West TE, Mougous JD.** 2014. VgrG-5 Is a *Burkholderia* Type VI Secretion System-Exported Protein Required for Multinucleated Giant Cell Formation and Virulence. Infect Immun **82:**1445-1452.

51. **Wong KT, Puthucheary SD, Vadivelu J.** 1995. The histopathology of human melioidosis. Histopathology **26:**51-55.

52. **Stevens MP, Stevens JM, Jeng RL, Taylor LA, Wood MW, Hawes P, Monaghan P, Welch MD, Galyov EE.** 2005. Identification of a bacterial factor required for actin-based motility of *Burkholderia pseudomallei*. Mol Microbiol **56:**40-53.

53. **Stevens MP, Wood MW, Taylor LA, Monaghan P, Hawes P, Jones PW, Wallis TS, Galyov EE.** 2002. An Inv/Mxi-Spa-like type III protein secretion system in *Burkholderia pseudomallei* modulates intracellular behaviour of the pathogen. Mol Microbiol **46:**649-659.

54. **Chen Y, Wong J, Sun GW, Liu Y, Tan GY, Gan YH.** 2011. Regulation of type VI secretion system during *Burkholderia pseudomallei* infection. Infect Immun **79:**3064-3073.

55. **Burtnick MN, Brett PJ, Nair V, Warawa JM, Woods DE, Gherardini FC.** 2008. *Burkholderia pseudomallei* type III secretion system mutants exhibit delayed vacuolar escape phenotypes in RAW 264.7 murine macrophages. Infect Immun **76:**2991-3000.

56. **Shalom G, Shaw JG, Thomas MS.** 2007. In vivo expression technology identifies a type VI secretion system locus in *Burkholderia pseudomallei* that is induced upon invasion of macrophages. Microbiology **153:**2689-2699.

57. **Burtnick MN, Brett PJ, Harding SV, Ngugi SA, Ribot WJ, Chantratita N, Scorpio A, Milne TS, Dean RE, Fritz DL, Peacock SJ, Prior JL, Atkins TP, Deshazer D.** 2011. The cluster 1 type VI secretion system is a major virulence determinant in *Burkholderia pseudomallei*. Infect Immun **79:**1512-1525.

58. **Hopf V, Gohler A, Eske-Pogodda K, Bast A, Steinmetz I, Breitbach K.** 2014. BPSS1504, a cluster 1 type VI secretion gene, is involved in intracellular survival and virulence of *Burkholderia pseudomallei*. Infect Immun.

59. **Burtnick MN, DeShazer D, Nair V, Gherardini FC, Brett PJ.** 2010. *Burkholderia mallei* cluster 1 type VI secretion mutants exhibit growth and actin polymerization defects in RAW 264.7 murine macrophages. Infect Immun **78:**88-99.

60. **Burtnick MN, Brett PJ.** 2013. *Burkholderia mallei* and *Burkholderia pseudomallei* cluster 1 type VI secretion system gene expression is negatively regulated by iron and zinc. PLoS One **8:**e76767.

61. **Brett PJ, Burtnick MN, Su H, Nair V, Gherardini FC.** 2008. iNOS activity is critical for the clearance of *Burkholderia mallei* from infected RAW 264.7 murine macrophages. Cell Microbiol **10:**487-498.

62. **Hseu YC, Sung JC, Shieh BS, Chen SC.** 2013. *Burkholderia pseudomallei* infection induces the expression of apoptosis-related genes and proteins in mouse macrophages. J Microbiol Immunol Infect.

63. **Miao EA, Leaf IA, Treuting PM, Mao DP, Dors M, Sarkar A, Warren SE, Wewers MD, Aderem A.** 2010. Caspase-1-induced pyroptosis is an innate immune effector mechanism against intracellular bacteria. Nat Immunol **11:**1136-1142.

64. **Fink SL, Cookson BT.** 2005. Apoptosis, pyroptosis, and necrosis: mechanistic description of dead and dying eukaryotic cells. Infect Immun **73:**1907-1916.

65. **Miao EA, Rajan JV, Aderem A.** 2011. Caspase-1-induced pyroptotic cell death. Immunol Rev **243:**206-214.

66. **Breitbach K, Sun GW, Kohler J, Eske K, Wongprompitak P, Tan G, Liu Y, Gan YH, Steinmetz I.** 2009. Caspase-1 mediates resistance in murine melioidosis. Infect Immun **77:**1589-1595.

67. **Utaisincharoen P, Anuntagool N, Limposuwan K, Chaisuriya P, Sirisinha S.** 2003. Involvement of beta interferon in enhancing inducible nitric oxide synthase production and antimicrobial activity of *Burkholderia pseudomallei*-infected macrophages. Infect Immun **71:**3053-3057.

68. **Tangsudjai S, Pudla M, Limposuwan K, Woods DE, Sirisinha S, Utaisincharoen P.** 2010. Involvement of the MyD88-independent pathway in controlling the intracellular fate of *Burkholderia pseudomallei* infection in the mouse macrophage cell line RAW 264.7. Microbiol Immunol **54:**282-290.

69. **Utaisincharoen P, Tangthawornchaikul N, Kespichayawattana W, Anuntagool N, Chaisuriya P, Sirisinha S.** 2000. Kinetic studies of the production of nitric oxide (NO) and tumour necrosis factor-alpha (TNF-alpha) in macrophages stimulated with *Burkholderia pseudomallei* endotoxin. Clin Exp Immunol **122:**324-329.

70. **Matsuura M, Kawahara K, Ezaki T, Nakano M.** 1996. Biological activities of lipopolysaccharide of *Burkholderia* (*Pseudomonas*) *pseudomallei*. FEMS Microbiol Lett **137:**79-83.

71. **Anuntagool N, Wuthiekanun V, White NJ, Currie BJ, Sermswan RW, Wongratanacheewin S, Taweechaisupapong S, Chaiyaroj SC, Sirisinha S.** 2006. Lipopolysaccharide heterogeneity among *Burkholderia pseudomallei* from different geographic and clinical origins. Am J Trop Med Hyg **74:**348-352.

72. **Breitbach K, Klocke S, Tschernig T, van Rooijen N, Baumann U, Steinmetz I.** 2006. Role of inducible nitric oxide synthase and NADPH oxidase in early control of *Burkholderia pseudomallei* infection in mice. Infect Immun **74:**6300-6309.

73. **Haque A, Easton A, Smith D, O'Garra A, Van Rooijen N, Lertmemongkolchai G, Titball RW, Bancroft GJ.** 2006. Role of T cells in innate and adaptive immunity against murine *Burkholderia pseudomallei* infection. J Infect Dis **193:**370-379.

74. **Easton A, Haque A, Chu K, Lukaszewski R, Bancroft GJ.** 2007. A critical role for neutrophils in resistance to experimental infection with *Burkholderia pseudomallei*. J Infect Dis **195:**99-107.

75. **Woodman ME, Worth RG, Wooten RM.** 2012. Capsule influences the deposition of critical complement C3 levels required for the killing of *Burkholderia pseudomallei* via NADPH-oxidase induction by human neutrophils. PLoS One **7:**e52276.

76. **Laws TR, Smither SJ, Lukaszewski RA, Atkins HS.** 2011. Neutrophils are the predominant cell-type to associate with *Burkholderia pseudomallei* in a BALB/c mouse model of respiratory melioidosis. Microb Pathog **51:**471-475.

77. **Wiersinga WJ, van der Poll T.** 2009. Immunity to *Burkholderia pseudomallei*. Curr Opin Infect Dis **22:**102-108.

78. **Charuchaimontri C, Suputtamongkol Y, Nilakul C, Chaowagul W, Chetchotisakd P, Lertpatanasuwun N, Intaranongpai S, Brett PJ, Woods DE.** 1999. Antilipopolysaccharide II: an antibody protective against fatal melioidosis. Clin Infect Dis **29:**813-818.

79. **Bryan LE, Wong S, Woods DE, Dance DA, Chaowagul W.** 1994. Passive protection of diabetic rats with antisera specific for the polysaccharide portion of the lipopolysaccharide isolated from *Pseudomonas pseudomallei*. Can J Infect Dis **5:**170-178.

80. **Santanirand P, Harley VS, Dance DA, Drasar BS, Bancroft GJ.** 1999. Obligatory role of gamma interferon for host survival in a murine model of infection with *Burkholderia pseudomallei*. Infect Immun **67:**3593-3600.

81. **Leakey AK, Ulett GC, Hirst RG.** 1998. BALB/c and C57Bl/6 mice infected with virulent *Burkholderia pseudomallei* provide contrasting animal models for the acute and chronic forms of human melioidosis. Microb Pathog **24:**269-275.

82. **Liu B, Koo GC, Yap EH, Chua KL, Gan YH.** 2002. Model of differential susceptibility to mucosal *Burkholderia pseudomallei* infection. Infect Immun **70:**504-511.

83. **Lauw FN, Simpson AJ, Prins JM, Smith MD, Kurimoto M, van Deventer SJ, Speelman P, Chaowagul W, White NJ, van der Poll T.** 1999. Elevated plasma concentrations of interferon (IFN)-gamma and the IFN-gamma-inducing cytokines interleukin (IL)-18, IL-12, and IL-15 in severe melioidosis. J Infect Dis **180:**1878-1885.

84. **Mosser DM.** 2003. The many faces of macrophage activation. J Leukoc Biol **73:**209-212.

85. **Schroder K, Hertzog PJ, Ravasi T, Hume DA.** 2004. Interferon-gamma: an overview of signals, mechanisms and functions. J Leukoc Biol **75:**163-189.

86. **Jutras I, Houde M, Currier N, Boulais J, Duclos S, LaBoissiere S, Bonneil E, Kearney P, Thibault P, Paramithiotis E, Hugo P, Desjardins M.** 2008. Modulation of the phagosome proteome by interferon-gamma. Mol Cell Proteomics **7:**697-715.

87. **MacMicking JD.** 2012. Interferon-inducible effector mechanisms in cell-autonomous immunity. Nat Rev Immunol **12:**367-382.

88. **Yates RM, Hermetter A, Taylor GA, Russell DG.** 2007. Macrophage activation downregulates the degradative capacity of the phagosome. Traffic **8:**241-250.

89. **Boehm U, Klamp T, Groot M, Howard JC.** 1997. Cellular responses to interferon-gamma. Annu Rev Immunol **15:**749-795.

90. **Nairz M, Fritsche G, Brunner P, Talasz H, Hantke K, Weiss G.** 2008. Interferon-gamma limits the availability of iron for intramacrophage *Salmonella typhimurium*. Eur J Immunol **38:**1923-1936.

91. **Lee J, Kornfeld H.** 2010. Interferon-gamma Regulates the Death of *M. tuberculosis*-Infected Macrophages. J Cell Death **3:**1-11.

92. **Portnoy DA, Schreiber RD, Connelly P, Tilney LG.** 1989. Gamma interferon limits access of *Listeria monocytogenes* to the macrophage cytoplasm. J Exp Med **170:**2141-2146.

93. **Ouadrhiri Y, Scorneaux B, Sibille Y, Tulkens PM.** 1999. Mechanism of the intracellular killing and modulation of antibiotic susceptibility of *Listeria monocytogenes* in THP-1 macrophages activated by gamma interferon. Antimicrob Agents Chemother **43:**1242-1251.

94. **Lindgren H, Golovliov I, Baranov V, Ernst RK, Telepnev M, Sjostedt A.** 2004. Factors affecting the escape of *Francisella tularensis* from the phagolysosome. J Med Microbiol **53:**953-958.

95. **Myers JT, Tsang AW, Swanson JA.** 2003. Localized reactive oxygen and nitrogen intermediates inhibit escape of *Listeria monocytogenes* from vacuoles in activated macrophages. J Immunol **171:**5447-5453.

96. **Koo GC, Gan YH.** 2006. The innate interferon gamma response of BALB/c and C57BL/6 mice to in vitro *Burkholderia pseudomallei* infection. BMC Immunol **7:**19.

97. **Ulett GC, Ketheesan N, Hirst RG.** 2000. Cytokine gene expression in innately susceptible BALB/c mice and relatively resistant C57BL/6 mice during infection with virulent *Burkholderia pseudomallei*. Infect Immun **68:**2034-2042.

98. **Lertmemongkolchai G, Cai G, Hunter CA, Bancroft GJ.** 2001. Bystander activation of CD8+ T cells contributes to the rapid production of IFN-gamma in response to bacterial pathogens. J Immunol **166:**1097-1105.

99. **Mraheil MA, Billion A, Mohamed W, Rawool D, Hain T, Chakraborty T.** 2011. Adaptation of *Listeria monocytogenes* to oxidative and nitrosative stress in IFN-gamma-activated macrophages. Int J Med Microbiol **301:**547-555.

100. **Fang FC.** 2004. Antimicrobial reactive oxygen and nitrogen species: concepts and controversies. Nat Rev Microbiol **2:**820-832.

101. **Slauch JM.** 2011. How does the oxidative burst of macrophages kill bacteria? Still an open question. Mol Microbiol **80:**580-583.

102. **Geisow MJ, D'Arcy Hart P, Young MR.** 1981. Temporal changes of lysosome and phagosome pH during phagolysosome formation in macrophages: studies by fluorescence spectroscopy. J Cell Biol **89:**645-652.

103. **Utaisincharoen P, Tangthawornchaikul N, Kespichayawattana W, Chaisuriya P, Sirisinha S.** 2001. *Burkholderia pseudomallei* interferes with inducible nitric oxide synthase (iNOS) production: a possible mechanism of evading macrophage killing. Microbiol Immunol **45:**307-313.

104. **Utaisincharoen P, Anuntagool N, Arjcharoen S, Limposuwan K, Chaisuriya P, Sirisinha S.** 2004. Induction of iNOS expression and antimicrobial activity by interferon (IFN)-beta is distinct from IFN-gamma in *Burkholderia pseudomallei*-infected mouse macrophages. Clin Exp Immunol **136:**277-283.

105. **Imlay JA.** 2008. Cellular defenses against superoxide and hydrogen peroxide. Annu Rev Biochem **77:**755-776.

106. **Wiseman H, Halliwell B.** 1996. Damage to DNA by reactive oxygen and nitrogen species: role in inflammatory disease and progression to cancer. Biochem J **313 (Pt 1):**17-29.

107. **Belenky P, Collins JJ.** 2011. Microbiology. Antioxidant strategies to tolerate antibiotics. Science **334:**915-916.

108. **Babior BM, Lambeth JD, Nauseef W.** 2002. The neutrophil NADPH oxidase. Arch Biochem Biophys **397:**342-344.

109. **Nathan C, Shiloh MU.** 2000. Reactive oxygen and nitrogen intermediates in the relationship between mammalian hosts and microbial pathogens. Proc Natl Acad Sci U S A **97:**8841-8848.

110. **Szeto HH.** 2006. Cell-permeable, mitochondrial-targeted, peptide antioxidants. AAPS J **8:**E277-283.

111. **Brown GC, Borutaite V.** 2012. There is no evidence that mitochondria are the main source of reactive oxygen species in mammalian cells. Mitochondrion **12:**1-4.

112. **Touati D.** 2000. Iron and oxidative stress in bacteria. Arch Biochem Biophys **373:**1-6.

113. **Imlay JA.** 2006. Iron-sulphur clusters and the problem with oxygen. Mol Microbiol **59:**1073-1082.

114. **Zhang H, Forman HJ.** 2012. Glutathione synthesis and its role in redox signaling. Semin Cell Dev Biol **23:**722-728.

115. **Forman HJ, Zhang H, Rinna A.** 2009. Glutathione: overview of its protective roles, measurement, and biosynthesis. Mol Aspects Med **30:**1-12.

116. **Meister A.** 1995. Glutathione biosynthesis and its inhibition. Methods Enzymol **252:**26-30.

117. **Lu SC.** 2009. Regulation of glutathione synthesis. Mol Aspects Med **30:**42-59.

118. **Yuan L, Kaplowitz N.** 2009. Glutathione in liver diseases and hepatotoxicity. Mol Aspects Med **30:**29-41.

119. **Ault JG, Lawrence DA.** 2003. Glutathione distribution in normal and oxidatively stressed cells. Exp Cell Res **285:**9-14.

120. **Meister A.** 1995. Glutathione metabolism. Methods Enzymol **251:**3-7.

121. **Masip L, Veeravalli K, Georgiou G.** 2006. The many faces of glutathione in bacteria. Antioxid Redox Signal **8:**753-762.

122. **Kalghatgi S, Spina CS, Costello JC, Liesa M, Morones-Ramirez JR, Slomovic S, Molina A, Shirihai OS, Collins JJ.** 2013. Bactericidal antibiotics induce mitochondrial dysfunction and oxidative damage in Mammalian cells. Sci Transl Med **5:**192ra185.

123. **Stevenson D, Wokosin D, Girkin J, Grant MH.** 2002. Measurement of the intracellular distribution of reduced glutathione in cultured rat hepatocytes using monochlorobimane and confocal laser scanning microscopy. Toxicol In Vitro **16:**609-619.

124. **Doughan AK, Harrison DG, Dikalov SI.** 2008. Molecular mechanisms of angiotensin II-mediated mitochondrial dysfunction: linking mitochondrial oxidative damage and vascular endothelial dysfunction. Circ Res **102:**488-496.

125. **Heller AR, Groth G, Heller SC, Breitkreutz R, Nebe T, Quintel M, Koch T.** 2001. N-acetylcysteine reduces respiratory burst but augments neutrophil phagocytosis in intensive care unit patients. Crit Care Med **29:**272-276.

126. **Griffith OW.** 1981. Depletion of glutathione by inhibition of biosynthesis. Methods Enzymol **77:**59-63.

127. **Plummer JL, Smith BR, Sies H, Bend JR.** 1981. Chemical depletion of glutathione in vivo. Methods Enzymol **77:**50-59.

128. **Meister A.** 1988. Glutathione metabolism and its selective modification. J Biol Chem **263:**17205-17208.

129. **Suzuki H, Hashimoto W, Kumagai H.** 1993. *Escherichia coli* K-12 can utilize an exogenous gamma-glutamyl peptide as an amino acid source, for which gamma-glutamyltranspeptidase is essential. J Bacteriol **175:**6038-6040.

130. **Vergauwen B, Pauwels F, Vaneechoutte M, Van Beeumen JJ.** 2003. Exogenous glutathione completes the defense against oxidative stress in *Haemophilus influenzae*. J Bacteriol **185:**1572-1581.

131. **Suzuki H, Koyanagi T, Izuka S, Onishi A, Kumagai H.** 2005. The yliA, -B, -C, and -D genes of *Escherichia coli* K-12 encode a novel glutathione importer with an ATP-binding cassette. J Bacteriol **187:**5861-5867.

132. **Sherrill C, Fahey RC.** 1998. Import and metabolism of glutathione by *Streptococcus mutans*. J Bacteriol **180:**1454-1459.

133. **Goswami M, Jawali N.** 2010. N-acetylcysteine-mediated modulation of bacterial antibiotic susceptibility. Antimicrob Agents Chemother **54:**3529-3530.

134. **Dhamdhere G, Krishnamoorthy G, Zgurskaya HI.** 2010. Interplay between drug efflux and antioxidants in *Escherichia coli* resistance to antibiotics. Antimicrob Agents Chemother **54:**5366-5368.

135. **Goswami M, Mangoli SH, Jawali N.** 2006. Involvement of reactive oxygen species in the action of ciprofloxacin against *Escherichia coli*. Antimicrob Agents Chemother **50:**949-954.

136. **Goswami M, Mangoli SH, Jawali N.** 2007. Effects of glutathione and ascorbic acid on streptomycin sensitivity of *Escherichia coli*. Antimicrob Agents Chemother **51:**1119-1122.

137. **Paez PL, Becerra MC, Albesa I.** 2010. Effect of the association of reduced glutathione and ciprofloxacin on the antimicrobial activity in *Staphylococcus aureus*. FEMS Microbiol Lett **303:**101-105.

138. **Loprasert S, Whangsuk W, Sallabhan R, Mongkolsuk S.** 2003. Regulation of the katG-dpsA operon and the importance of KatG in survival of *Burkholderia pseudomallei* exposed to oxidative stress. FEBS Lett **542:**17-21.

139. **Vanaporn M, Wand M, Michell SL, Sarkar-Tyson M, Ireland P, Goldman S, Kewcharoenwong C, Rinchai D, Lertmemongkolchai G, Titball RW.** 2011. Superoxide dismutase C is required for intracellular survival and virulence of *Burkholderia pseudomallei*. Microbiology **157:**2392-2400.

140. **Dwyer DJ, Kohanski MA, Collins JJ.** 2009. Role of reactive oxygen species in antibiotic action and resistance. Curr Opin Microbiol **12:**482-489.

141. **Foti JJ, Devadoss B, Winkler JA, Collins JJ, Walker GC.** 2012. Oxidation of the guanine nucleotide pool underlies cell death by bactericidal antibiotics. Science **336:**315-319.

142. **Kohanski MA, Dwyer DJ, Hayete B, Lawrence CA, Collins JJ.** 2007. A common mechanism of cellular death induced by bactericidal antibiotics. Cell **130:**797-810.

143. **Wright GD.** 2007. On the road to bacterial cell death. Cell **130:**781-783.

144. **Kohanski MA, Dwyer DJ, Wierzbowski J, Cottarel G, Collins JJ.** 2008. Mistranslation of membrane proteins and two-component system activation trigger antibiotic-mediated cell death. Cell **135:**679-690.

145. **Shatalin K, Shatalina E, Mironov A, Nudler E.** 2011. H2S: a universal defense against antibiotics in bacteria. Science **334:**986-990.

146. **Grant SS, Kaufmann BB, Chand NS, Haseley N, Hung DT.** 2012. Eradication of bacterial persisters with antibiotic-generated hydroxyl radicals. Proc Natl Acad Sci U S A **109:**12147-12152.

147. **Hassett DJ, Imlay JA.** 2007. Bactericidal antibiotics and oxidative stress: a radical proposal. ACS Chem Biol **2:**708-710.

148. **Wang X, Zhao X.** 2009. Contribution of oxidative damage to antimicrobial lethality. Antimicrob Agents Chemother **53:**1395-1402.

149. **Keren I, Wu Y, Inocencio J, Mulcahy LR, Lewis K.** 2013. Killing by bactericidal antibiotics does not depend on reactive oxygen species. Science **339:**1213-1216.

150. **Liu Y, Imlay JA.** 2013. Cell death from antibiotics without the involvement of reactive oxygen species. Science **339:**1210-1213.

151. **Ezraty B, Vergnes A, Banzhaf M, Duverger Y, Huguenot A, Brochado AR, Su SY, Espinosa L, Loiseau L, Py B, Typas A, Barras F.** 2013. Fe-S cluster biosynthesis controls uptake of aminoglycosides in a ROS-less death pathway. Science **340:**1583-1587.

152. **Owens B.** 2013. Bacteria-killing dispute casts doubt on antibiotic development. Nat Med **19:**954.

CHAPTER 2: RESEARCH RATIONALE AND SPECIFIC AIMS

RESEARCH OVERVIEW

This dissertation presents research aimed at gaining an understanding of the mechanism of immuno-antimicrobial synergistic killing of intracellular *Burkholderia* in the hopes that future treatments and therapies for melioidosis may enhance outcomes through targeting this mechanism. In chapter 3 we explore mechanisms of immuno-antimicrobial synergy. In chapter 4 we examine the role of IFN-γ induced ROS to interact with ceftazidime and synergistically reduce bacterial burden of intracellular *Burkholderia*. We also investigate the mechanism of IFN-γ interference with the normal intracellular lifestyle of *Burkholderia*. In chapter 5 we discover a role for compartmentalized killing in immuno-antimicrobial synergy and therefore focus our investigations on the separate contributions of both IFN-γ and ceftazidime. We also propose a new model to describe the dynamics of our classically used macrophage infection model.

RESEARCH RATIONALE

In vivo, macrophages are an essential cell type for protection against *Burkholderia* infection, capable of direct elimination of the intracellular pathogen as well as secretion of cytokines IL-12 and IL-18 which are potent activators of other cells important for immunity to *Burkholderia* (1, 2). However, in vitro studies show us that macrophages play very little role in controlling intracellular infection without sufficient activation. For instance, Utaisincharoen showed a failure of macrophages to induce iNOS expression or reduce intracellular bacterial

burden when stimulated with *B. pseudomallei* alone (3). The failure of *B. pseudomallei* to sufficiently activate macrophages is thought to be attributed to the structure and components of its LPS and polysaccharide (4, 5). Low activation of immune responses may be a mechanism employed by *Burkholderia* to facilitate its survival in macrophages, perhaps impacting the long latency of chronic infections seen in some hosts (6, 7). However, although *B. pseudomallei* is a poor activator of macrophages on its own, co-stimulation with *Burkholderia* and proper cytokines can strongly activate macrophages, resulting in greatly increased macrophage killing capacity (3, 8, 9). Under these conditions of activation it is more understandable that macrophages in vivo play such an essential role for fighting infection.

Probably the most well known cytokine activator of macrophages is IFN-γ. IFN-γ has been shown to be essential for protection against *Burkholderia* infection, through activation of macrophages and subsequent enhancement of their major microbicidal effectors (1, 2, 10, 11). Despite the importance of IFN-γ and its effects of enhancing host immunity to pathogens, current treatment of melioidosis relies on antibiotic therapy alone.

OVERALL THESIS SPECIFIC AIMS

Our lab understands the critical need for cytokine stimulation to increase macrophage killing potential against *B. pseudomallei*, and has taken the approach of combining the important immune stimulant, IFN-γ, with antibiotics in order to enhance elimination of the pathogen from in vitro and in vivo systems. We previously found that IFN-γ synergized with ceftazidime to kill intracellular *Burkholderia* in infected macrophages and protect against lethal challenge in mice (12). This finding alone has implications for potential enhancement of therapy against melioidosis, however, uncovering the mechanism of this synergistic interaction could further

open new avenues for targeted treatments or immune adjuvants. Therefore our first aim is given below:

Aim 1 (Chapter 3 and 4): **Investigate the mechanism by which IFN-γ activation of macrophages synergizes with ceftazidime to kill intracellular bacteria.**

Our hypothesis was that IFN-γ induced ROS could synergize with ceftazidime to kill intracellular bacteria. In chapter 3 we explore potential mediators of immuno-antimicrobial synergy. We determined a mechanism of the synergistic interaction in chapter 4, namely the macrophage response to IFN-γ which was indispensable for the synergy. However, we still knew very little about the individual contribution of ceftazidime to the synergistic interaction and wanted to further characterize the macrophage response to IFN-γ. Therefore we crafted our second aim:

Aim 2 (Chapter 5): **Investigate the specific and individual contributions of ceftazidime and IFN-γ to the synergistic killing.**

Our hypothesis was that ceftazidime controlled extracellular bacterial burden and IFN-γ controlled intracellular bacterial burden. In chapter 5 we characterized the role of compartmentalized killing in immuno-antimicrobial synergy. We also propose a model to describe the synergistic interaction between ceftazidime and IFN-γ to control total bacterial burden in the macrophage infection model.

REFERENCES

1. **Breitbach K, Klocke S, Tschernig T, van Rooijen N, Baumann U, Steinmetz I.** 2006. Role of inducible nitric oxide synthase and NADPH oxidase in early control of *Burkholderia pseudomallei* infection in mice. Infect Immun **74:**6300-6309.

2. **Haque A, Easton A, Smith D, O'Garra A, Van Rooijen N, Lertmemongkolchai G, Titball RW, Bancroft GJ.** 2006. Role of T cells in innate and adaptive immunity against murine *Burkholderia pseudomallei* infection. J Infect Dis **193:**370-379.

3. **Utaisincharoen P, Anuntagool N, Limposuwan K, Chaisuriya P, Sirisinha S.** 2003. Involvement of beta interferon in enhancing inducible nitric oxide synthase production and antimicrobial activity of *Burkholderia pseudomallei*-infected macrophages. Infect Immun **71:**3053-3057.

4. **Tangsudjai S, Pudla M, Limposuwan K, Woods DE, Sirisinha S, Utaisincharoen P.** 2010. Involvement of the MyD88-independent pathway in controlling the intracellular fate of *Burkholderia pseudomallei* infection in the mouse macrophage cell line RAW 264.7. Microbiol Immunol **54:**282-290.

5. **Matsuura M, Kawahara K, Ezaki T, Nakano M.** 1996. Biological activities of lipopolysaccharide of *Burkholderia* (*Pseudomonas*) *pseudomallei*. FEMS Microbiol Lett **137:**79-83.

6. **Utaisincharoen P, Tangthawornchaikul N, Kespichayawattana W, Anuntagool N, Chaisuriya P, Sirisinha S.** 2000. Kinetic studies of the production of nitric oxide (NO) and tumour necrosis factor-alpha (TNF-alpha) in macrophages stimulated with *Burkholderia pseudomallei* endotoxin. Clin Exp Immunol **122:**324-329.

7. **Utaisincharoen P, Tangthawornchaikul N, Kespichayawattana W, Chaisuriya P, Sirisinha S.** 2001. *Burkholderia pseudomallei* interferes with inducible nitric oxide synthase (iNOS) production: a possible mechanism of evading macrophage killing. Microbiol Immunol **45:**307-313.

8. **Charoensap J, Utaisincharoen P, Engering A, Sirisinha S.** 2009. Differential intracellular fate of *Burkholderia pseudomallei* 844 and *Burkholderia thailandensis* UE5 in human monocyte-derived dendritic cells and macrophages. BMC Immunol **10:**20.

9. **Breitbach K, Sun GW, Kohler J, Eske K, Wongprompitak P, Tan G, Liu Y, Gan YH, Steinmetz I.** 2009. Caspase-1 mediates resistance in murine melioidosis. Infect Immun **77:**1589-1595.

10. **Santanirand P, Harley VS, Dance DA, Drasar BS, Bancroft GJ.** 1999. Obligatory role of gamma interferon for host survival in a murine model of infection with *Burkholderia pseudomallei*. Infect Immun **67:**3593-3600.

11. **Easton A, Haque A, Chu K, Lukaszewski R, Bancroft GJ.** 2007. A critical role for neutrophils in resistance to experimental infection with *Burkholderia pseudomallei*. J Infect Dis **195:**99-107.

12. **Propst KL, Troyer RM, Kellihan LM, Schweizer HP, Dow SW.** 2010. Immunotherapy markedly increases the effectiveness of antimicrobial therapy for treatment of *Burkholderia pseudomallei* infection. Antimicrob Agents Chemother **54:**1785-1792.

CHAPTER 3: POTENTIAL MEDIATORS OF IMMUNO-ANTIMICROBIAL SYNERGY

SUMMARY

B. pseudomallei is a facultative intracellular pathogen that causes severe infections in humans and animals. Since *Burkholderia* is intrinsically resistant to many classes of antibiotics, new treatments are needed to combat melioidosis, the disease caused by *Burkholderia* infection. Our lab previously found that ceftazidime and IFN-γ combined treatment of infected macrophages led to synergistically reduced intracellular bacterial burden and increased survival of infected mice. For several years our lab has investigated the mechanism of this synergistic interaction. The studies presented in this chapter are some of our initial studies to identify a major mediator of the in vitro synergy.

Although IFN-γ stimulation increased CXCL10 protein secretion in a time-dependent manner, we found that synergy between ceftazidime and IFN-γ was still achievable in CXCL10 $^{-/-}$ bone marrow macrophages, suggesting that CXCL10 is not a major mediator of the synergistic interaction between the two treatments. Another AMP, LL-37 was shown to synergistically inhibit *Burkholderia* growth, however only under contrived conditions that are not likely to occur in the macrophages or mice in which we see the synergistic interaction of ceftazidime with IFN-γ. We next investigated IFN-γ induced ROS as a potential mediator of immuno-antimicrobial synergy. We found that subinhibitory ceftazidime and H_2O_2 were able to synergistically inhibit bacterial growth but there was no synergistic interaction between bactericidal concentrations of both compounds. We end the chapter with initial studies to quantitate the levels of intracellular ROS induced by ceftazidime in *Burkholderia*. Although our

preliminary studies showed that ceftazidime could induce ROS in bacteria, recent studies show that the reagent that we used to measure ROS, hydroxyphenyl fluorescein (HPF), is not suitable for that purpose. In conclusion, the results presented in this chapter were aimed at identifying a potential mediator of immuno-antimicrobial synergy. This chapter presents valuable negative data which may help future scientists if they choose to study this topic.

INTRODUCTION

B. pseudomallei is a Gram negative, facultative intracellular pathogen which causes melioidosis, a life-threatening infectious disease (1-3). Since *B. pseudomallei* is intrinsically resistant to many classes of antibiotics (2, 4, 5), new therapies are greatly needed to combat this emerging infectious disease. *Burkholderia* is also resistant to many antimicrobial peptides (AMPs) (6).

AMPs are small charged peptides (anionic or cationic) produced by many cell types as a mechanism of innate immunity for protection against pathogens (7, 8). AMPs can kill microorganisms either through disruption of membranes or direct inhibition of cell wall synthesis, nucleic-acid and protein synthesis, or enzymatic activity similar to antibiotics (7). They can disrupt lipid bilayers either through coating the membrane and breaking it apart or through formation of pores which allow intracellular contents to leak out (7, 9-11). AMPs can exert their antimicrobial effects intracellularly as well as extracellularly as secreted peptides and several studies have shown that AMPs can interact with antibiotics or other AMPs to increase antimicrobial activity against pathogens (12-16).

Some chemokines have been shown to display antimicrobial activity similar to AMPs. In fact in a study of 30 human chemokines, 17 were shown to have antimicrobial activity in vitro

including IFN-γ inducible CXCL10, which showed strong antimicrobial activity against *E. coli* and *Staphylococcus aureus* (17). The strong positive charge of CXCL10 is thought to account for part of its antimicrobial activity against Gram negative and Gram positive bacteria (18).

LL-37 is a linear, α-helical, cationic AMP with broad antimicrobial activity against Gram negative and Gram positive bacteria (7, 19). LL-37 is produced by many cell types such as lung (20) and urinary tract (9, 21, 22) epithelial cells as well as some white blood cells including macrophages (23, 24). The mechanism of action of LL-37 is to lie on membranes and actually induces the membrane to curve inward until a channel is formed (Figure 3.1) (7, 25). Both exogenous LL-37 and endogenous cathelin-related AMP (CRAMP), a homolog of LL-37 in mice, have been shown to increase killing of intracellular mycobacteria in murine macrophages (26).

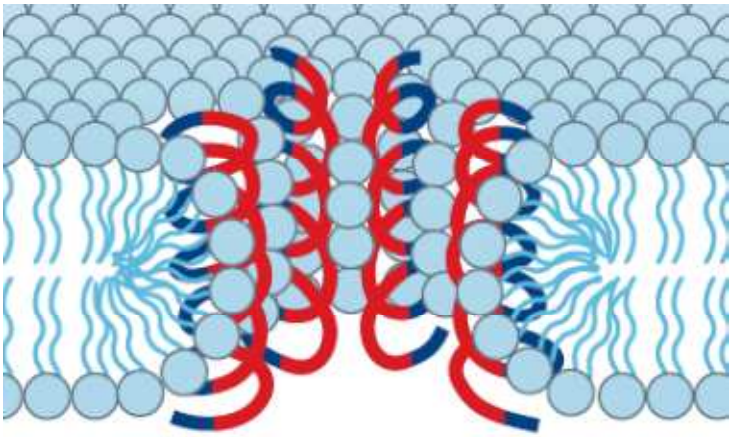

Figure 3.1: Mechanism of action of LL-37: toroidal pore formation. LL-37 attaches to membranes and induces the outer lipid monolayer to bend inward towards the inner lipid monolayer until a channel is formed. LL-37 inserts into the channel so that the hydrophobic portion of its structure is facing the lipids and the hydrophilic portion of its structure is facing the inside of the channel. Image is slightly modified from (7).

B. pseudomallei has been shown to be susceptible to LL-37 at concentrations of 6.25 μM (6). In addition, the AMP has been shown to be more effective at killing *B. pseudomallei* biofilms than high doses of ceftazidime (27).

Our lab has previously found that combined treatment of *Burkholderia* infected macrophages with ceftazidime and IFN-γ led to synergistically reduced intracellular bacterial burden (28). For many years our lab has searched for the major mediator of this immuno-antimicrobial synergy. This chapter summarizes some of our findings during our search for the mediator of the synergistic interaction between ceftazidime and IFN-γ. We caution our readers that in contrast to chapters 4 and 5, most of this chapter contains negative data and may not read as a logical flow from experiment to experiment. At the time of these experiments, we were casting a wide net for potential mediators of the immuno-antimicrobial synergy and therefore we occasionally made abrupt stops to one line of research to focus on a new target. With this said, we believe that the information presented in this chapter is nonetheless important, especially for future scientists that may want to pick up this topic. We hope that this chapter will provide the reader with a background of tried and failed leads for the mediator of immuno-antimicrobial synergy and may save time and frustration for future scientists that may find this information pertinent to their studies.

MATERIALS AND METHODS

Biochemicals.

Ceftazidime hydrate was purchased from Sigma-Aldrich (St. Louis, MO). Other reagents included recombinant murine IFN-γ (Peprotech, Rocky Hill, NJ), γ-D-Glu-mDAP (iE-DAP) and

muramyl dipeptide (MDP; InvivoGen, San Diego, CA), streptavidin-conjugated horseradish peroxidase (SA-HRP; Jackson ImmunoResearch Labs, West Grove, PA), tetramethylbenzidine (TMB; Sigma-Aldrich, St. Louis, MO), and hydroxyphenyl fluorescein (HPF, Life Technologies).

Bacteria.

B. thailandensis E264 was used for these studies (29, 30). Bacteria were grown in Luria-Bertaini broth at 37°C with rotary shaking for 16 hours, and then stored at -80°C with 15% glycerol until needed. Frozen vials of bacteria were thawed and diluted immediately prior to their use. Bacteria were heat killed in an 80°C water bath for 1 hour, and then frozen at -20°C until needed.

Cell lines.

RAW 264.7 macrophage cell line was purchased from American Type Tissue Collection (Manassas, VA). Cell lines were maintained in complete media consisting of minimum essential media (MEM; Life Technologies) supplemented with 10% fetal bovine serum (FBS) (Atlas, Fort Collins, CO), 0.075% sodium bicarbonate (Acros organics, NJ), 1x nonessential amino acids, 0.5x essential amino acids (Life Technologies), and 2 mM L-glutamine (Sigma-Aldrich). Antibiotic additions of 100 Units/ml Penicillin and 100 µg/ml Streptomycin (Life Technologies) were added to media for maintenance of cell lines but all experiments were conducted in antibiotic-free media. All cells were maintained at 37°C with 5% CO_2.

Mice.

Female C57BL/6 and CXCL10 $^{-/-}$ mice were used for these studies. All mice were between 6 to 12 weeks old at the time of their use and were housed under pathogen-free conditions. All animal studies were approved by the Institutional Animal Care and Use Committee at Colorado State University.

Primary bone marrow macrophage culture.

Bone marrow macrophages were generated as previously described (31). Femurs and tibias were aseptically removed from mice, transferred to 50 ml conical tubes containing Hank's buffered salt solution (HBSS) supplemented with 2% FBS, and kept on ice. In a biosafety cabinet, bones were cleaned of tissue and bone marrow was flushed from the bones using needles and syringes filled with HBSS and supplemented with 2% FBS. Bone marrow was gently resuspended with gentle pipetting and passed through a 70 µm nylon filter (BD Biosciences Pharmingen, San Jose, CA). Cells were centrifuged at 1200 rpm for 5 minutes at 4°C. Then supernatant was removed and red blood cells were lysed using 2 ml of ammonium-chloride-potassium (ACK) lysis buffer for 5 minutes, followed immediately by 20 mls of complete MEM with antibiotics and 10% L929-conditioned supernatants to dilute the lysis buffer. Cells were again spun at 1200 rpm for 5 minutes at 4°C. Remaining white blood cells were plated in 24-well plates at a concentration of 2 x 10^6 cells/ml in complete MEM. Cells were allowed to adhere to 24-well plates for 3 hours at 37°C and 5% CO_2 after which, non-adhered cells were washed away three times with room-temperature HBSS supplemented with 2% FBS. Complete media with antibiotics and 10% L929 conditioned media was reapplied to the cells and plates

were returned to the incubator. Addition of 10% L929-conditioned media provided necessary growth factors for differentiation of bone marrow myeloid progenitor cells into the macrophage/monocyte lineage to enrich for these cells. Adherent cells were incubated at 37^{o}C and 5% CO_2 until macrophages reached moderate confluency in wells (approximately 8-12 days).

Macrophage infection assay.

Macrophages were infected and treated as previously described (28). Briefly, macrophages were seeded into 24-well plates with complete MEM (see above) and allowed to adhere overnight. After a 1ml wash with phosphate buffered saline (PBS), *B. thailandensis* was added to macrophages at a multiplicity of infection of 5 and incubated for 1 hour at 37°C in 5% CO_2. Aminoglycosides are not considered to penetrate mammalian cells in short time periods (32), so macrophages were exposed to high-dose kanamycin-sulfate (350 µg/ml) for 1 hour to kill extracellular bacteria. After two 2 ml washes with PBS to remove kanamycin and dead bacteria, treatments were diluted in MEM, applied to macrophages, and incubated for 18 hours. Treatments consisted of individual drugs or combinations of the following: ceftazidime (10 µg/ml), IFN-γ (10 ng/ml), or the combination of both drugs. Although ceftazidime was applied at 10 µg/ml to infected macrophage cell lines, it was applied at 3 µg/ml or 5 µg/ml to infected bone marrow macrophages because 10 µg/ml had too great of an effect at controlling intracellular bacterial burden on its own, and therefore made it harder to determine synergy with IFN-γ. After the 18 hour treatment of infected macrophages, extracellular bacteria were washed off three times with 2 mls of PBS and macrophages were lysed with 1 ml of sterile distilled

water. Intracellular bacterial burden was then assessed by plating serial dilutions of the lysates on LB agar followed by colony counts 24-48 hrs after plating.

CXCL10 ELISA

Enzyme-linked immunosorbent assays (ELISA) were performed to quantitate the concentration of CXCL10 in supernatants after infection and/or stimulation of RAW 264.7 macrophages using a murine CXCL10 (IP-10) ELISA kit (Peprotech, Rocky Hill, NJ). Anti-CXCL10 capture antibody was diluted to 0.5 µg/ml in PBS and added to 96-well Nunc MaxiSorp plates (ebioscience, San Diego, CA). Plates were covered and incubated overnight at room temperature. The next day, wells of plates were washed three times with a solution of 0.05% Tween 20 in PBS (wash buffer). Wells were blocked with 1% bovine serum albumin in PBS for one hour at room temperature and then washed three times in wash buffer. The CXCL10 standard was diluted in 0.1% bovine serum albumin in PBS with 0.05% Tween 20 (diluent) and added to wells in duplicate. The standard ranged from 8 ng/ml to 4 pg/ml. Samples were added to the plate and standards and samples were incubated for two hours at room temperature followed by three washes with wash buffer. Detection antibody was diluted to 0.25 µg/ml and added to wells for two hours at room temperature. After the plates were washed three times with wash buffer, SA-HRP was diluted 1:5,000 in diluent and incubated in plates for 30 minutes at room temperature. Following another three washes in wash buffer, TMB was added to wells at room temperature and the plates were read after color change on a spectrophotometer at 405 nm with a wavelength correction set at 650 nm. Sample concentrations were calculated off of the standard curve.

Bacteria killing assays

In order to determine if treatment of bacteria with one drug may enhance killing by a second, we used a bacteria killing assay and pre-treated *E. coli* with one drug before subjecting bacteria to the second drug. In one set of experiments we pre-treated 125 µl of an overnight culture of *E. coli* with 50-75 ng/ml ceftazidime for 18 hours to induce filamentation. Induction of filamentation of bacteria was confirmed by light microscopy. Previous experiments had determined the resulting bacteria density to be roughly $3x10^7$ CFU/ml after this 18 hour pre-treatment period. We then plated either filamentous or non-filamentous control bacteria into wells of a 96-well plate at a final density of $1x10^7$ CFU/ml in tryptic soy broth (TSB). The second treatment, LL-37 (15 µg/ml) was added to wells so that the total volume per well was 100 µl. Plates were incubated at 37°C with rotary shaking (200-250 rpm) for an additional 2-6 hours. Surviving bacteria were enumerated by plating serial dilutions of remaining bacteria on LB agar and counting colonies 24-48 hours later. Another set of experiments were conducted in which *E. coli* was first pre-treated with LL-37 and then subjected to ceftazidime. Non-filamentous *E. coli* was pre-treated with LL-37 (15 µg/ml) for 1 hour and then washed twice (TSB followed by 1mM sodium phosphate buffer) to remove LL-37 with spins at 10,000xg for 5 minutes at 20°C. Bacteria were added to 96-well plates at a density of $1x10^7$ CFU/ml in wells and ceftazidime (50 ng/ml) was added to wells. Plates were incubated at 37°C with rotary shaking (200-250 rpm) for an additional 6 hours.

Bacteria killing assays were conducted with *B. thailandensis* to determine drug interactions which could enhance killing of bacteria over one drug alone. Bacteria were grown to mid-log phase and plated in 96-well plates with treatment additions as indicated below

specific graphs of data. After the indicated experimental period, surviving bacteria were enumerated by plating well contents on LB agar followed by colony counts 24-48 hours later.

Flow cytometry.

B. thailandensis was grown to mid-log phase and then 1 ml aliquots were treated with ceftazidime (10 µg/ml) for two hours. After the treatment period, 50 µl samples were taken from the 1 ml aliquots, spun down at 5000xg for 5 minutes at 23°C, and stained with 5 µM HPF for 30 minutes at room temperature in the dark. The total volume for staining was 150 µl. After staining, the bacteria were washed twice with 1 ml of bacterial flow buffer and then immediately resuspended in 200-400 µl of bacterial flow buffer and run on flow cytometry. Data was collected on greater than 50,000 cells per sample using a Gallios Flow Cytometer (Beckman Coulter, Brea, CA) and analyzed using FlowJo software version 7.6.5 (Tree Star, Ashland, OR). An untreated, unstained sample was used to set the initial voltages. HPF signal in treated samples was compared to background levels in untreated but stained controls.

Statistical analyses.

Means, standard error of the mean (SEM), and P-values were determined and plotted using Prism software version 5.00 (GraphPad, La Jolla, CA). For comparisons of two groups, a two-tailed Student's t-test was used to determine statistically significant differences. For comparisons of three or more groups the one-way analysis of variance (ANOVA) was used followed by Tukey's post test for multiple comparisons. Grouped data was analyzed by two-way

ANOVA and statistical synergy was determined as before (33) from the interaction P-value of a two-way ANOVA. All differences were considered statistically significant for $P < 0.05$.

RESULTS

IFN-γ stimulates CXCL10 production from macrophages. Our lab had previously observed that ceftazidime and IFN-γ interacted to synergistically reduce intracellular bacterial burden inside *Burkholderia* infected RAW 264.7 macrophages (28) but not J774A.1 macrophages. In order to better understand the mechanism of synergy in RAW 264.7 macrophages, we conducted a microarray to compare differences between gene expression in uninfected RAW 264.7 and J774A.1 cells following treatment with ceftazidime and IFN-γ. The genes encoding CXCL10 and CXCL9 proteins, two chemokines with AMP-like properties (17, 18), were high on the list of genes that were upregulated in RAW 264.7 macrophages but not J774A.1 cells, suggesting a potential role of these proteins as mediators of the immuno-antimicrobial synergy. Our studies turned to CXCL10, an IFN-γ induced protein and chemokine which may also display antimicrobial properties due to its cationic nature. We first wanted to know whether or not IFN-γ could stimulate increased levels of CXCL10 in our macrophage cell line. Therefore, we used an ELISA to determine levels of CXCL10 in supernatants following IFN-γ stimulation of RAW 264.7 macrophages. We showed that IFN-γ stimulation greatly increased CXCL10 protein levels in the supernatants of uninfected macrophages (Figure 3.2). Although we measured extracellular protein levels, we assumed that intracellular levels would also be increased due to this treatment.

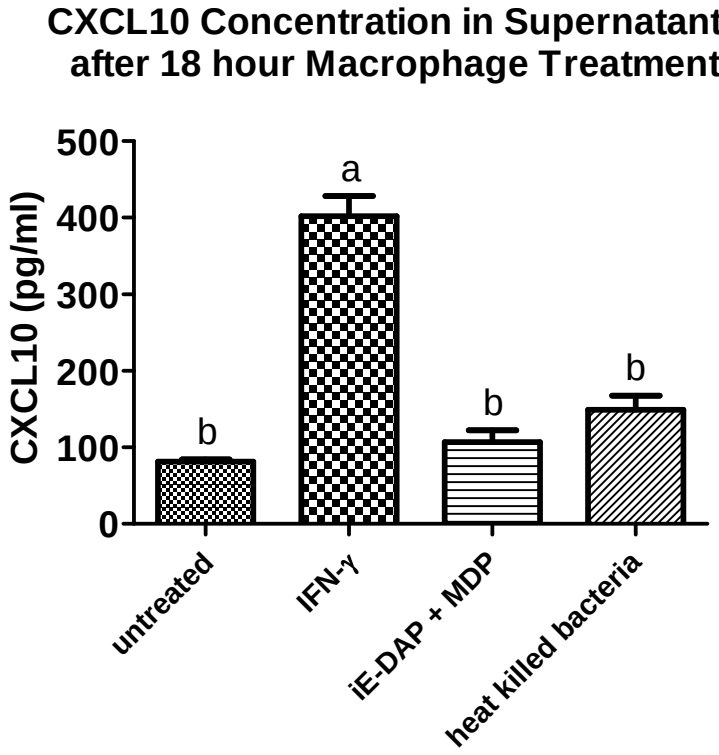

Figure 3.2: IFN-γ stimulates CXCL10 production from uninfected macrophages. Uninfected RAW 264.7 macrophages were stimulated for 18 hours with IFN-γ (10 ng/ml), iE-DAP (10 µg/ml) and MDP (10 µg/ml), or heat killed *B. thailandensis* ($1x10^7$ CFU/ml). After 18 hours, supernatants were collected. An ELISA was performed to determine the concentration of CXCL10 in the collected supernatants. Statistical differences were assessed by one-way ANOVA, ($a > b$, $P < 0.05$). Data are representative of two independent experiments run in triplicate.

Notably, we also showed that neither nucleotide-binding oligomerization domain-containing protein 1 (NOD1) nor NOD2 agonists (iE-DAP and MDP, respectively) were capable of stimulating increased levels of CXCL10 (Figure 3.2). This result suggests that bacteria peptidoglycan sensed intracellularly by NOD1 or NOD2 would be incapable of stimulating increased levels of CXCL10. To confirm that bacterial cell wall components could not increase levels of CXCL10, we showed that heat killed *Burkholderia* were unable to elicit a significant

increase in CXCL10 (Figure 3.2). Taken together these results suggest that IFN-γ but not bacterial cell wall components stimulated increased CXCL10 production from uninfected macrophages.

After showing that IFN-γ increased CXCL10 production in uninfected macrophages, we next determined the extent of increased CXCL10 production in our infected macrophages treated with IFN-γ for 18 hours. Again we found that IFN-γ increased CXCL10 expression as determined by an ELISA of supernatants from infected and treated RAW 264.7 cells (Figure 3.3). We also showed that CXCL10 protein levels increased over time in our *Burkholderia* infected macrophages (Figure A1). Taken together our results show that IFN-γ stimulation increased CXCL10 levels as measured in the supernatants of both uninfected and infected macrophages.

CXCL10 is not likely a major mediator of IFN-γ and ceftazidime immuno-antimicrobial synergy. Although we had shown that IFN-γ could stimulate high levels of secreted CXCL10 protein, we speculated that in our immuno-antimicrobial synergy, intracellular CXCL10 protein would be more likely to synergize with ceftazidime to affect intracellular bacterial burden. We therefore conducted a macrophage infection assay using primary bone marrow derived macrophages from CXCL10 $^{-/-}$ or C57BL/6 control mice. We rationalized that if CXCL10 was a major mechanism of immuno-antimicrobial synergy, macrophages unable to produce CXCL10 would be unable to synergistically control intracellular bacterial burden due to IFN-γ and ceftazidime treatment; or in other words, we would see a reversal of the synergistic

control of intracellular bacterial burden in *Burkholderia* infected macrophages.

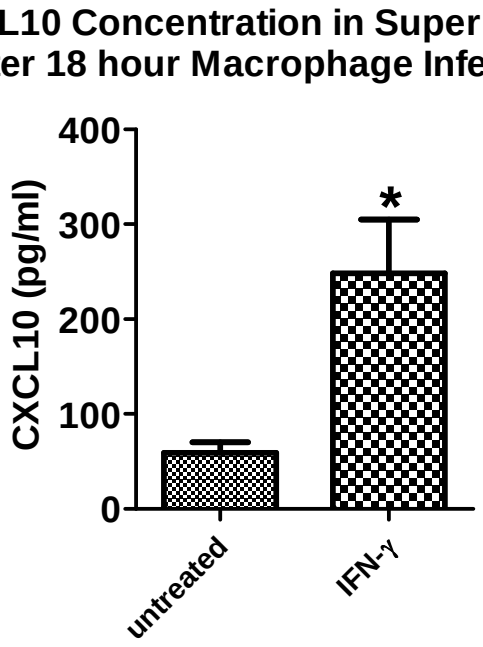

Figure 3.3: IFN-γ stimulates CXCL10 production from *Burkholderia* infected macrophages. RAW 264.7 macrophages were infected with *B. thailandensis* and treated for 18 hours with IFN-γ (10 ng/ml). After 18 hours, supernatants were collected. An ELISA was performed to determine the concentration of CXCL10 in the collected supernatants. Statistical differences were assessed by a two-tailed Student's T-test, (*P = 0.0306). Data are representative of two independent experiments run in triplicate.

However, as shown in Figure 3.4, we found that synergy prevailed in CXCL10 $^{-/-}$ bone marrow macrophages. This result suggested that CXCL10 is not a major mediator of the immuno-antimicrobial synergy observed between IFN-γ and ceftazidime.

Bacteria killing due to interactions between LL-37 and ceftazidime depends on timing of treatment addition. We had just shown that CXCL10 was not likely a major mediator of immuno-antimicrobial synergy, so we turned to another murine cationic AMP which has a homologous protein in humans called LL-37.

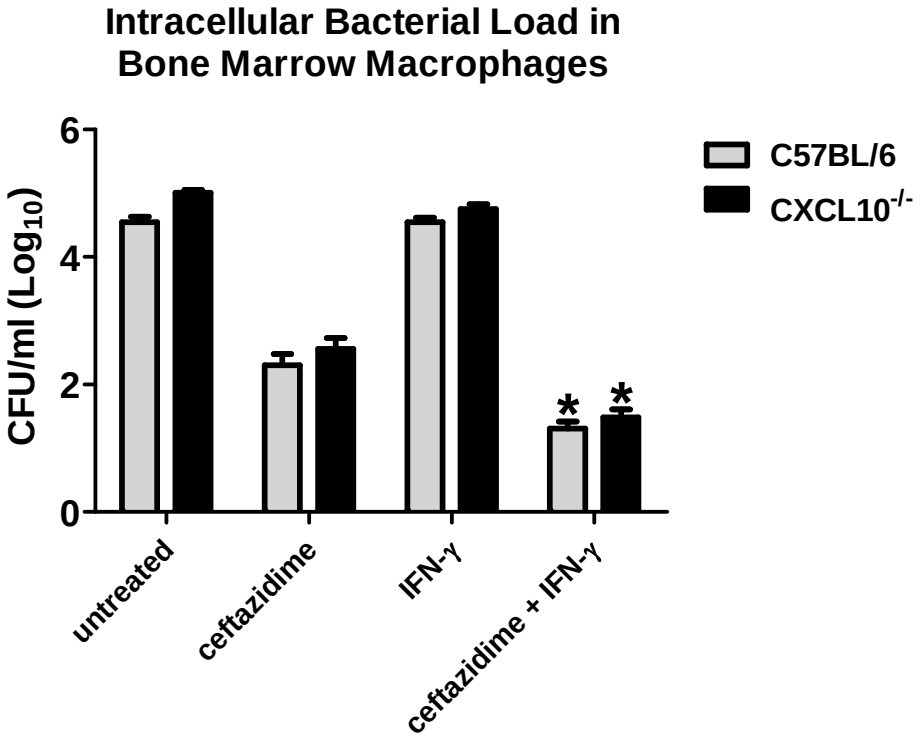

Figure 3.4: Ceftazidime and IFN-γ show synergistic control of intracellular bacterial burden in infected CXCL10 $^{-/-}$ bone marrow macrophages. Primary bone marrow macrophages were cultured from CXCL10 $^{-/-}$ mice or C57BL/6 background-matched control mice. Macrophages were infected with *B. thailandensis* and treated with ceftazidime (3 µg/ml or 5 µg/ml) or IFN-γ (10 ng/ml) or the combination of both ceftazidime and IFN-γ for 18 hours. Intracellular bacterial burden was then assessed by plating serial dilutions of lysates on LB agar followed by colony counts 24-48 hours later. Statistical synergy between ceftazidime and IFN-γ was assessed by two-way ANOVA, *$P < 0.05$. Data is pooled from two similar independent experiments (n >5) in order to increase sample size.

To test whether LL-37 and ceftazidime combination can directly synergize to kill bacteria, we employed a bacteria killing assay which consisted of incubating bacteria with treatments for a designated time and then plating out surviving bacteria. Because *Burkholderia* has inherent resistance to several AMPs (6), we used the more sensitive organism *E. coli* to first determine whether or not ceftazidime and LL-37 may interact to synergistically kill bacteria. We first

showed that ceftazidime and LL-37 showed additive but not synergistic killing of *E. coli* (Figure A2). We next wondered if pre-treating bacteria with one treatment would increase sensitivity to the other. We rationalized that ceftazidime stress and damage to the bacterial cell wall may allow LL-37 better access to the cell membrane. Therefore we pre-treated *E. coli* with low dose ceftazidime for 18 hours to induce filamentation, a typical morphology of Gram negative bacteria observed after exposure to low dose, cell wall active, antibiotics. Then we subjected these filamentous bacteria to LL-37 and were surprised to find that filamentous bacteria were resistant to the inhibitory effects seen by LL-37 treatment of non-filamentous control bacteria (Figure 3.5). We next rationalized that pre-treatment with LL-37 may disrupt the cell wall of bacteria and permit increased access of ceftazidime to inhibit cell wall synthesis. We pre-treated bacteria with LL-37 and then added ceftazidime to the bacteria killing assay. We were again surprised to see that bacteria pre-treated with LL-37 were more resistant to ceftazidime mediated inhibition of growth (Figure A3). Taken together these results suggest that the timing of addition of LL-37 or ceftazidime has a great impact on their level of interaction to inhibit *E. coli* growth.

LL-37 and ceftazidime synergistically inhibit *Burkholderia* growth. After showing additive killing effects of LL-37 and ceftazidime against *E. coli*, we next wanted to determine the interactions between these two compounds against *Burkholderia*. We experimented with several different modifications to the bacteria killing assay, including different types of media and the concentration of treatments. Since LL-37 is a cationic peptide whose mechanism of action is salt sensitive (20, 34), we tried using low-salt media such as 1 mM potassium or sodium phosphate buffer. However, in these low-nutrient buffers, the bacteria would not grow and divide and therefore ceftazidime, was unable to kill bacteria.

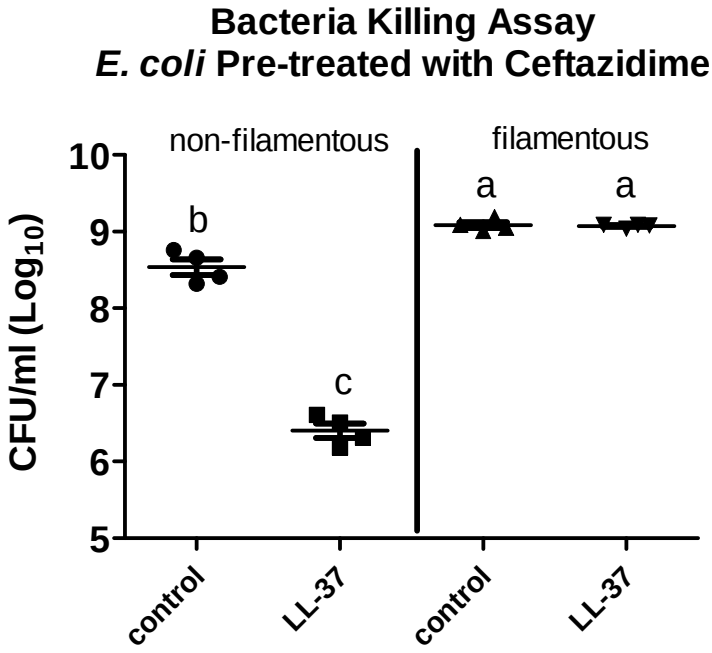

Figure 3.5: Filamentous *E. coli* are more resistant to growth inhibition by LL-37. *E. coli* was treated with low level ceftazidime (50 ng/ml) for 18 hours to induce filamentation. These filamentous bacteria and non-filamentous controls were then exposed to LL-37 (15 µg/ml) in a 96-well plate on a rotary shaker (200 rpm) for six hours with initial starting density of $1x10^7$ CFU/ml. Surviving bacteria were enumerated by plating serial dilutions of remaining bacteria on LB agar followed by colony counts 24-48 hours later. Statistical differences were assessed by one-way ANOVA, $a > b > c$, $P < 0.05$. A similar result was shown when this experiment was repeated using a higher ceftazidime pre-treatment (75 ng/ml) and subsequent 2 hour treatment with LL-37 (15 µg/ml).

We finally showed synergistic killing between LL-37 and ceftazidime when bacteria were first treated with LL-37 in a low-salt media followed shortly after by ceftazidime treatment in a nutrient-rich broth (Figure A4). Since these conditions seemed contrived and unlikely to be present during immuno-antimicrobial synergy in our infected macrophages, we abandoned LL-37 as a major mediator of immuno-antimicrobial synergy.

ROS may synergize with ceftazidime to inhibit bacterial growth but not to kill bacteria. We next turned to another potential mediator of the immuno-antimicrobial synergy which is also increased by IFN-γ stimulation of macrophages---ROS (35-38). Since H_2O_2 is thought to be one of the more stable forms of ROS (39) and is easily added to experiments in vitro, we conducted a bacteria killing assay with *Burkholderia* treated with either ceftazidime, H_2O_2, or the combination of both treatments. Our first attempts at this experiment showed conflicting results. Occasionally the drugs would interact and result in synergistic inhibition of growth, while other times, the effects were only additive and there was no apparent drug interaction. Increasing the sample size to eight replicates, we found that ceftazidime and H_2O_2 did show synergistic inhibition of growth (Figure 3.6). Pooling the data from seven independent experiments also showed a synergistic effect at growth inhibition. We further showed a time course of the growth inhibition over the assay length (Figure A5). We were still skeptical that the interaction between ceftazidime and H_2O_2 was actually synergistic, since it seemed that the assay was extremely sensitive. Furthermore, the assay was particularly sensitive to the exact concentration of treatments used which may indicate that the conditions for synergistic inhibition of growth between H_2O_2 and ceftazidime are not likely present in our macrophages during immuno-antimicrobial synergy. We did uniquely find that H_2O_2 strongly synergized with gentamicin to inhibit bacterial growth (Figure 3.7). Since we had been using subinhibitory doses of both ceftazidime and H_2O_2, we were next curious if there would be a synergistic interaction to kill bacteria if we used higher, bactericidal concentrations of both compounds. In a modified bacteria killing assay, we found that bactericidal concentrations of both ceftazidime and H_2O_2 were unable to interact to enhance killing (Figure A6).

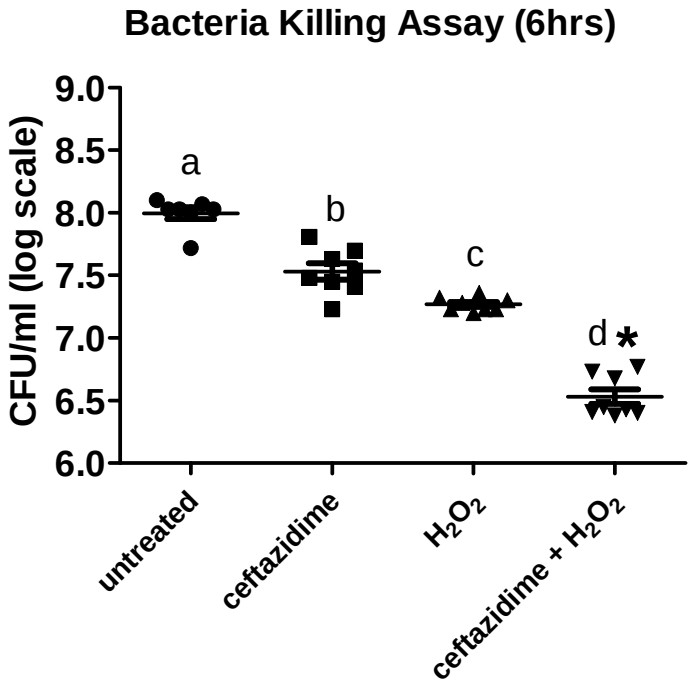

Figure 3.6: H_2O_2 and ceftazidime synergistically inhibit growth of *Burkholderia*. *B. thailandensis* was grown to mid-log phase and then plated into 96-well plates at an initial density of $1x10^6$ CFU/ml. Ceftazidime (750 ng/ml), H_2O_2 (20 µM), or the combination of both treatments were added to wells with bacteria so that the total volume was 200 µl per well in TSB. Plates were incubated for 6 hours at 37°C and then serial dilutions were plated to enumerate surviving bacteria. Statistical differences were assessed by one-way ANOVA, a > b > c > d, $P < 0.05$ and statistical synergy was assessed by two-way ANOVA, $*P < 0.05$. Data is similar in trend to over six independent experiments.

Taken together these results show that the mechanism of immuno-antimicrobial synergy is not likely due to H_2O_2 enhancement of antibiotic-mediated growth-inhibition or antibiotic killing.

Ferrous sulfate interferes with growth inhibition of ceftazidime and H_2O_2. After eliminating a few potential mediators of the immuno-antimicrobial synergy, in particular IFN-γ induced mediators, we began to think more about the role of ceftazidime in the synergy.

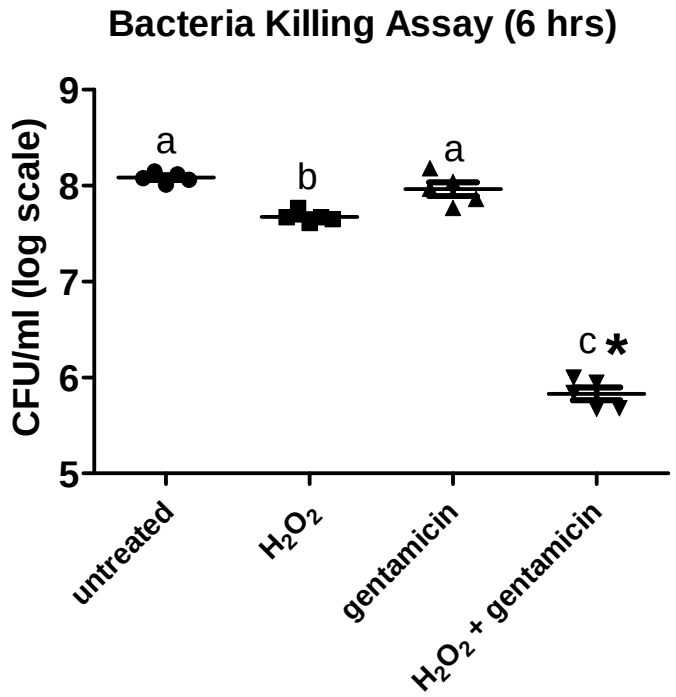

Figure 3.7: H_2O_2 and gentamicin synergistically inhibit growth of *Burkholderia*. *B. thailandensis* was grown to mid-log phase and then plated into 96-well plates at an initial density of $1x10^6$ CFU/ml. Gentamicin (100 µg/ml), H_2O_2 (20 µM), or the combination of both treatments were added to wells with bacteria so that the total volume was 200 µl per well. Plates were incubated for 6 hours at 37°C and then serial dilutions were plated to enumerate surviving bacteria. Statistical differences were assessed by one-way ANOVA, a > b > c > d, $P < 0.05$ and statistical synergy was assessed by two-way ANOVA, *$P < 0.05$. Data is representative of three independent experiments with treatment groups run in duplicate or triplicate.

We learned about the ongoing debate over whether or not all bactericidal antibiotics kill through ROS-mediated pathways. At the time several studies had contributed evidence to suggest that antibiotics may kill bacteria through ROS induced damage (40-42). If ceftazidime was killing bacteria through ROS-mediated pathways, could this be a mechanism by which it could synergize with IFN-γ induced ROS? Perhaps there was a threshold of ROS necessary before bacteria would die from ROS-induced damage. Perhaps ceftazidime and IFN-γ both contributed to increase ROS and perhaps increasing ROS could increase the synergistic control of bacterial

burden seen inside infected macrophages. We therefore added ferrous sulfate to our bacteria killing assay as a form of extra iron. If ceftazidime killed bacteria through a ROS-mediated pathway, then increasing free iron availability should increase production of the deadly hydroxyl radicals and enhance antibiotic killing. On the contrary, we found that ferrous sulfate addition to the bacteria killing assay interfered with the growth inhibition effects of both ceftazidime and H_2O_2 individually as well as their combination (Figure A7). After this result, we realized a flaw in our experiment. Our assay with ceftazidime and H_2O_2 was only inhibiting growth of *Burkholderia*, therefore even if ROS was produced as a mechanism of ceftazidime killing, it was not produced in sufficient quantity in our assay to actually kill bacteria. Therefore, addition of extra free iron in the form of ferrous sulfate would not be expected to increase killing, again, since there was no killing in our assay, only growth inhibition. We proposed that ferrous sulfate may have instead provided the bacteria with the essential nutrient, iron, stimulating increased growth and replication and leading to the increased bacteria burden in wells with increased addition of iron. Conversely, ferrous sulfate may have directly reacted with ceftazidime or H_2O_2, thereby modifying the compounds and inactivating them. Further studies would need to be conducted with bactericidal concentrations of ceftazidime and H_2O_2 in order to determine if ferrous sulfate could increase ROS-mediated bacteria killing. Instead, with our original question unanswered, we turned to flow cytometry to directly determine if ceftazidime induced ROS in bacteria.

Ceftazidime induces ROS production in *Burkholderia*. We used flow cytometry in order to directly detect an increase in intracellular ROS production due to ceftazidime treatment of *Burkholderia*. The cell-permeable reagent, HPF, reacts with highly reactive oxygen species

such as hydroxyl radicals to form a fluorescent compound (43). After treating bacteria with ceftazidime, HPF was added to cultures and fluorescence was detected using flow cytometry. We found that ceftazidime increased the HPF signal inside bacteria compared to untreated controls, with about 30% of ceftazidime treated bacteria staining positive for HPF (Figure 3.8). This result suggested that ceftazidime did induce ROS production in bacteria and supported a role for ROS in the mechanism of antibiotic mediated killing.

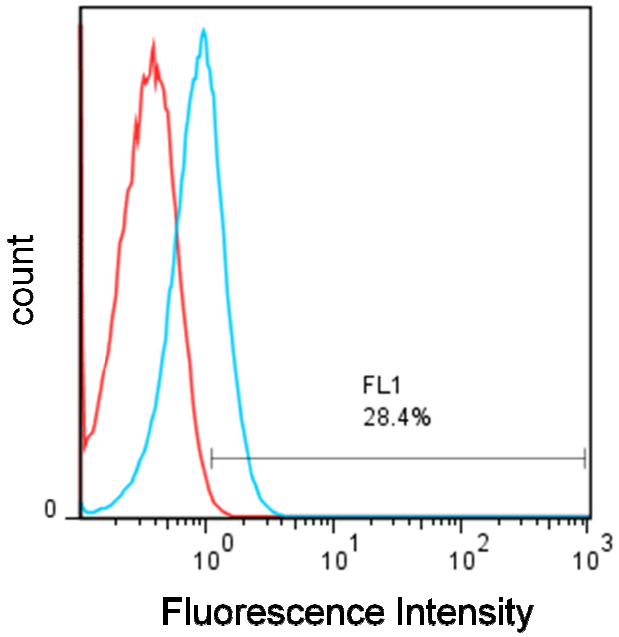

Figure 3.8: Ceftazidime induces ROS production in *Burkholderia*. *B. thailandensis* was treated with 10 µg/ml ceftazidime for 2 hours (blue line) and subsequently stained with HPF to identify levels of ROS compared to an untreated control (red line). Data is representative of at least two independent experiments.

A problem was encountered when we began to look at filamentous *Burkholderia*. Filamentous bacteria were typically formed due to low-dose or sub-lethal doses of ceftazidime treatment. However, even at 10 µg/ml we observed filamentous bacteria at short time periods of 2-3 hours

of antibiotic treatment. We observed that longer filaments contained more HPF signal signifying increased ROS production. However, we could never rule out the possibility that longer filaments contained more ROS per cell simply because each cell was increased in length. It is possible that filaments contained the same proportions of ROS as non-filaments. Therefore we could never determine if increased HPF signal necessarily correlated with increased likelihood of cell death. Another study has recently shown that increased HPF signal does *not* correlate with increased likelihood of cell death and also that HPF could react with other cell contents besides ROS (44, 45). Therefore, the use of HPF as an indicator of ROS has been challenged leading us to question our experimental results with HPF. Furthermore, more recent studies have suggested that antibiotics do *not* kill through oxidative damage (44-46). We therefore abandoned studies using HPF to analyze oxidative damage in ceftazidime treated bacteria, and moved on to the studies presented in chapter 4.

DISCUSSION

In this chapter we discuss several potential mediators of immuno-antimicrobial synergy between ceftazidime and IFN-γ. We first thought that AMPs, namely CXCL10 or LL-37, may interact with ceftazidime in cells to synergistically decrease overall intracellular bacterial burden. We first showed that IFN-γ but not components of bacteria could stimulate increased production of CXCL10 from macrophages. We then showed that CXCL10 was increased over time during our macrophage infection assay due to IFN-γ stimulation of macrophages. However, we found that CXCL10 was not necessary for the immuno-antimicrobial synergy when ceftazidime and IFN-γ still interacted to synergistically reduce intracellular bacteria burden in infected $CXCL10^{-/-}$

bone marrow macrophages. This result suggested that CXCL10 was not a major mechanism of immuno-antimicrobial synergy.

We then turned our attention to AMP LL-37. We hypothesized that LL-37 may enhance ceftazidime killing of bacteria either through increased permeability or through additional insult to the outer membrane or cell wall of the bacteria. Since *Burkholderia* is resistant to several AMPs (6), our initial experiments focused on *E. coli* in order to determine whether or not the two compounds could interact and kill susceptible bacteria. Our major finding using *E. coli* was that the order of addition of LL-37 and ceftazidime to bacteria impacted their abilities to kill. We found that when the two compounds were added simultaneously in the bacteria killing assay, they showed additive inhibition of growth. On the contrary, pre-treatment of bacteria with one compound resulted in subsequent resistance to the growth inhibition effects of the second compound. Although we did not delve into the mechanism of this surprising effect, we may speculate that some sort of compensatory mechanism was induced after injury from the first compound which then protected against the effects of the second compound. Further studies would need to be conducted to understand this effect and it would be important to determine whether this phenomenon is observed with higher, bactericidal concentrations of both compounds as well.

When we switched to a bacteria killing assay with *Burkholderia*, we only observed synergistic inhibition of growth with LL-37 and ceftazidime under very specific, contrived media and timing parameters. Since these conditions are unlikely to occur in the macrophages in our macrophage infection assay, we abandoned LL-37 as a major mediator of the immuno-antimicrobial synergy.

Since IFN-γ stimulation of macrophages is known to increase expression of NADPH phagocyte oxidase subunits and subsequently increase intracellular ROS production (35-38), we thought that H_2O_2, one of the more stable forms of ROS (39) may be able to synergize with ceftazidime to kill intracellular bacteria. In a bacteria killing assay we showed that at subinhibitory concentrations of ceftazidime and H_2O_2, these two compounds could synergistically inhibit bacterial growth. However this result was extremely sensitive to the specific concentrations used and was only partially repeatable. We therefore moved on to look at the interaction of higher, bactericidal concentrations of ceftazidime and H_2O_2 on bacteria killing and found that there was no synergistic interaction between these compounds to kill *Burkholderia* at short time points.

Around this time in the project we learned about the controversy of whether or not antibiotics kill through ROS-mediated pathways. We imagined that if ceftazidime was killing *Burkholderia* through a ROS-mediated pathway, perhaps we could target this pathway to increase ROS due to both ceftazidime and IFN-γ induced ROS and therefore increase killing of bacteria. We first tested if ceftazidime was ROS-mediated by adding free iron in the form of ferrous sulfate to the bacteria killing assay. In cells superoxide can react with iron-sulfur clusters to release free ferrous iron which then reacts with H_2O_2 through Fenton chemistry to create deadly hydroxyl radicals (47-49). We hypothesized that adding an extra source of free ferrous iron could augment hydroxyl radical production and lead to increased killing of bacteria due to ceftazidime treatment. The concentration of ceftazidime we were using was sub-inhibitory, which suggested that ceftazidime was not actually killing bacteria. Therefore, we found that ferrous sulfate only protected against growth inhibition and didn't increase killing since there was no killing in the assay even without ferrous sulfate addition. Further experiments would

need to be conducted with higher bactericidal concentrations of ceftazidime in order to determine if ferrous sulfate addition *could* potentiate the killing effect. Instead, our studies turned to flow cytometry to directly measure intracellular ROS in bacteria due to ceftazidime treatment. We used flow cytometry to show that ceftazidime did increase HPF signal in bacteria, however we later learned that HPF is not a suitable compound for quantization of intracellular ROS (44, 45). Furthermore, recent studies show strong evidence that antibiotics do not kill by a common mechanism of ROS induced death (44-46). Therefore we abandoned studies aimed at quantization of ROS induction due to ceftazidime.

The mixture of studies presented in this chapter provides the framework for the next two chapters. The purpose of this chapter was to show some of the previous studies aimed at understanding the mechanism of immuno-antimicrobial therapy and potential mediators of the synergy between ceftazidime and IFN-γ. Many of the experiments presented here were conducted as initial studies, and as such, may not have been followed up by more in-depth experiments. In some cases there may not have seemed a logical flow from one experiment to the next, though we have tried to rationalize the progression presented here, however we believed these results may be of benefit to future scientists. We hope that some of our negative data and failed attempts to identify the mediator of immuno-antimicrobial synergy may provide some valuable information to future scientists and possibly save them some time and frustration if they choose to pursue similar topics.

REFERENCES

1. **Limmathurotsakul D, Wongratanacheewin S, Teerawattanasook N, Wongsuvan G, Chaisuksant S, Chetchotisakd P, Chaowagul W, Day NP, Peacock SJ.** 2010. Increasing incidence of human melioidosis in Northeast Thailand. Am J Trop Med Hyg **82:**1113-1117.

2. **Wiersinga WJ, Currie BJ, Peacock SJ.** 2012. Melioidosis. N Engl J Med **367:**1035-1044.

3. **Dance DA.** 1991. Melioidosis: the tip of the iceberg? Clin Microbiol Rev **4:**52-60.

4. **Wiersinga WJ, van der Poll T, White NJ, Day NP, Peacock SJ.** 2006. Melioidosis: insights into the pathogenicity of *Burkholderia pseudomallei*. Nat Rev Microbiol **4:**272-282.

5. **Wuthiekanun V, Peacock SJ.** 2006. Management of melioidosis. Expert Rev Anti Infect Ther **4:**445-455.

6. **Tandhavanant S, Thanwisai A, Limmathurotsakul D, Korbsrisate S, Day NP, Peacock SJ, Chantratita N.** 2010. Effect of colony morphology variation of *Burkholderia pseudomallei* on intracellular survival and resistance to antimicrobial environments in human macrophages in vitro. BMC Microbiol **10:**303.

7. **Brogden KA.** 2005. Antimicrobial peptides: pore formers or metabolic inhibitors in bacteria? Nat Rev Microbiol **3:**238-250.

8. **Lai Y, Gallo RL.** 2009. AMPed up immunity: how antimicrobial peptides have multiple roles in immune defense. Trends Immunol **30:**131-141.

9. **Ali AS, Townes CL, Hall J, Pickard RS.** 2009. Maintaining a sterile urinary tract: the role of antimicrobial peptides. J Urol **182:**21-28.

10. **Hancock RE, Chapple DS.** 1999. Peptide antibiotics. Antimicrob Agents Chemother **43:**1317-1323.

11. **Huang Y, Huang J, Chen Y.** 2010. Alpha-helical cationic antimicrobial peptides: relationships of structure and function. Protein Cell **1:**143-152.

12. **Shin SY, Yang ST, Park EJ, Eom SH, Song WK, Kim Y, Hahm KS, Kim JI.** 2002. Salt resistance and synergistic effect with vancomycin of alpha-helical antimicrobial peptide P18. Biochem Biophys Res Commun **290:**558-562.

13. **Darveau RP, Cunningham MD, Seachord CL, Cassiano-Clough L, Cosand WL, Blake J, Watkins CS.** 1991. Beta-lactam antibiotics potentiate magainin 2 antimicrobial activity in vitro and in vivo. Antimicrob Agents Chemother **35:**1153-1159.

14. **Yan H, Hancock RE.** 2001. Synergistic interactions between mammalian antimicrobial defense peptides. Antimicrob Agents Chemother **45:**1558-1560.

15. **Giacometti A, Cirioni O, Barchiesi F, Fortuna M, Scalise G.** 1999. In-vitro activity of cationic peptides alone and in combination with clinically used antimicrobial agents against *Pseudomonas aeruginosa*. J Antimicrob Chemother **44:**641-645.

16. **Rishi P, Preet S, Bharrhan S, Verma I.** 2011. In vitro and in vivo synergistic effects of cryptdin 2 and ampicillin against *Salmonella*. Antimicrob Agents Chemother **55:**4176-4182.

17. **Yang D, Chen Q, Hoover DM, Staley P, Tucker KD, Lubkowski J, Oppenheim JJ.** 2003. Many chemokines including CCL20/MIP-3alpha display antimicrobial activity. J Leukoc Biol **74:**448-455.

18. **Esche C, Stellato C, Beck LA.** 2005. Chemokines: key players in innate and adaptive immunity. J Invest Dermatol **125:**615-628.

19. **Bucki R, Leszczynska K, Namiot A, Sokolowski W.** 2010. Cathelicidin LL-37: a multitask antimicrobial peptide. Arch Immunol Ther Exp (Warsz) **58:**15-25.

20. **Bals R, Wang X, Zasloff M, Wilson JM.** 1998. The peptide antibiotic LL-37/hCAP-18 is expressed in epithelia of the human lung where it has broad antimicrobial activity at the airway surface. Proc Natl Acad Sci U S A **95:**9541-9546.

21. **Saemann MD, Horl WH, Weichhart T.** 2007. Uncovering host defences in the urinary tract: cathelicidin and beyond. Nephrol Dial Transplant **22:**347-349.

22. **Chromek M, Slamova Z, Bergman P, Kovacs L, Podracka L, Ehren I, Hokfelt T, Gudmundsson GH, Gallo RL, Agerberth B, Brauner A.** 2006. The antimicrobial peptide cathelicidin protects the urinary tract against invasive bacterial infection. Nat Med **12:**636-641.

23. **Wah J, Wellek A, Frankenberger M, Unterberger P, Welsch U, Bals R.** 2006. Antimicrobial peptides are present in immune and host defense cells of the human respiratory and gastrointestinal tracts. Cell Tissue Res **324:**449-456.

24. **Agerberth B, Charo J, Werr J, Olsson B, Idali F, Lindbom L, Kiessling R, Jornvall H, Wigzell H, Gudmundsson GH.** 2000. The human antimicrobial and chemotactic peptides LL-37 and alpha-defensins are expressed by specific lymphocyte and monocyte populations. Blood **96:**3086-3093.

25. **Burton MF, Steel PG.** 2009. The chemistry and biology of LL-37. Nat Prod Rep **26:**1572-1584.

26. **Sonawane A, Santos JC, Mishra BB, Jena P, Progida C, Sorensen OE, Gallo R, Appelberg R, Griffiths G.** 2011. Cathelicidin is involved in the intracellular killing of mycobacteria in macrophages. Cell Microbiol **13:**1601-1617.

27. **Kanthawong S, Bolscher JG, Veerman EC, van Marle J, de Soet HJ, Nazmi K, Wongratanacheewin S, Taweechaisupapong S.** 2012. Antimicrobial and antibiofilm activity of LL-37 and its truncated variants against *Burkholderia pseudomallei*. Int J Antimicrob Agents **39:**39-44.

28. **Propst KL, Troyer RM, Kellihan LM, Schweizer HP, Dow SW.** 2010. Immunotherapy markedly increases the effectiveness of antimicrobial therapy for treatment of *Burkholderia pseudomallei* infection. Antimicrob Agents Chemother **54:**1785-1792.

29. **Brett PJ, Deshazer D, Woods DE.** 1997. Characterization of *Burkholderia pseudomallei* and *Burkholderia pseudomallei*-like strains. Epidemiol Infect **118:**137-148.

30. **DeShazer D, Brett PJ, Carlyon R, Woods DE.** 1997. Mutagenesis of *Burkholderia pseudomallei* with Tn5-OT182: isolation of motility mutants and molecular characterization of the flagellin structural gene. J Bacteriol **179:**2116-2125.

31. **Bosio CM, Dow SW.** 2005. *Francisella tularensis* induces aberrant activation of pulmonary dendritic cells. J Immunol **175:**6792-6801.

32. **Tulkens PM.** 1991. Intracellular distribution and activity of antibiotics. Eur J Clin Microbiol Infect Dis **10:**100-106.

33. **Slinker BK.** 1998. The statistics of synergism. J Mol Cell Cardiol **30:**723-731.

34. **Dorschner RA, Lopez-Garcia B, Peschel A, Kraus D, Morikawa K, Nizet V, Gallo RL.** 2006. The mammalian ionic environment dictates microbial susceptibility to antimicrobial defense peptides. FASEB J **20:**35-42.

35. **Schroder K, Hertzog PJ, Ravasi T, Hume DA.** 2004. Interferon-gamma: an overview of signals, mechanisms and functions. J Leukoc Biol **75:**163-189.

36. **Jutras I, Houde M, Currier N, Boulais J, Duclos S, LaBoissiere S, Bonneil E, Kearney P, Thibault P, Paramithiotis E, Hugo P, Desjardins M.** 2008. Modulation of the phagosome proteome by interferon-gamma. Mol Cell Proteomics **7:**697-715.

37. **Mraheil MA, Billion A, Mohamed W, Rawool D, Hain T, Chakraborty T.** 2011. Adaptation of *Listeria monocytogenes* to oxidative and nitrosative stress in IFN-gamma-activated macrophages. Int J Med Microbiol **301:**547-555.

38. **Fang FC.** 2004. Antimicrobial reactive oxygen and nitrogen species: concepts and controversies. Nat Rev Microbiol **2:**820-832.

39. **Slauch JM.** 2011. How does the oxidative burst of macrophages kill bacteria? Still an open question. Mol Microbiol **80:**580-583.

40. **Dwyer DJ, Kohanski MA, Hayete B, Collins JJ.** 2007. Gyrase inhibitors induce an oxidative damage cellular death pathway in *Escherichia coli*. Mol Syst Biol **3:**91.

41. **Kohanski MA, Dwyer DJ, Hayete B, Lawrence CA, Collins JJ.** 2007. A common mechanism of cellular death induced by bactericidal antibiotics. Cell **130:**797-810.

42. **Kohanski MA, Dwyer DJ, Wierzbowski J, Cottarel G, Collins JJ.** 2008. Mistranslation of membrane proteins and two-component system activation trigger antibiotic-mediated cell death. Cell **135:**679-690.

43. **Setsukinai K, Urano Y, Kakinuma K, Majima HJ, Nagano T.** 2003. Development of novel fluorescence probes that can reliably detect reactive oxygen species and distinguish specific species. J Biol Chem **278:**3170-3175.

44. **Keren I, Wu Y, Inocencio J, Mulcahy LR, Lewis K.** 2013. Killing by bactericidal antibiotics does not depend on reactive oxygen species. Science **339:**1213-1216.

45. **Liu Y, Imlay JA.** 2013. Cell death from antibiotics without the involvement of reactive oxygen species. Science **339:**1210-1213.

46. **Ezraty B, Vergnes A, Banzhaf M, Duverger Y, Huguenot A, Brochado AR, Su SY, Espinosa L, Loiseau L, Py B, Typas A, Barras F.** 2013. Fe-S cluster biosynthesis controls uptake of aminoglycosides in a ROS-less death pathway. Science **340:**1583-1587.

47. **Imlay JA.** 2008. Cellular defenses against superoxide and hydrogen peroxide. Annu Rev Biochem **77:**755-776.

48. **Touati D.** 2000. Iron and oxidative stress in bacteria. Arch Biochem Biophys **373:**1-6.

49. **Imlay JA.** 2006. Iron-sulphur clusters and the problem with oxygen. Mol Microbiol **59:**1073-1082.

CHAPTER 4: INTERACTION OF IFN-γ INDUCED REACTIVE OXYGEN SPECIES WITH CEFTAZIDIME LEADS TO SYNERGISTIC KILLING OF INTRACELLULAR *BURKHOLDERIA*

SUMMARY

Burkholderia pseudomallei, a facultative intracellular pathogen, causes severe infections and is inherently refractory to many antibiotics. Previous studies have shown that IFN-γ interacts synergistically with the antibiotic ceftazidime to kill bacteria in infected macrophages. The present study aimed to identify the underlying mechanism of that interaction. We first showed that blocking ROS pathways reversed IFN-γ and ceftazidime mediated killing. Through flow cytometry we observed that IFN-γ, but not ceftazidime, induced significant ROS responses in infected macrophages, which led to the hypothesis that synergistic killing of intracellular *Burkholderia* was mediated by the interaction of ceftazidime with IFN-γ induction of ROS. Consistent with our hypothesis, we also observed that BSO, another inducer of ROS, could substitute for IFN-γ to similarly potentiate the effect of ceftazidime on intracellular killing. To investigate the exact role of ROS responses, we used microscopy to analyze the effect of IFN-γ stimulation on intracellular *Burkholderia* and observed both a lack of vacuolar escape and a lack of actin polymerization compared to controls. These effects were recapitulated using BSO in place of IFN-γ which supports the role of ROS involvement. Based upon these results, we propose a model by which IFN-γ induced ROS responses interact with ceftazidime to synergistically kill intracellular bacteria. Prevention of actin polymerization and vacuolar escape due to IFN-γ induced ROS may be a mechanism for increased phagolysosomal killing of

intracellular *Burkholderia*. Our findings suggest an alternative means of enhancing antibiotic activity against *Burkholderia* through combination with drugs that induce ROS pathways.

INTRODUCTION

B. pseudomallei, the causative agent of melioidosis, is a gram negative, facultative intracellular pathogen that causes potentially lethal acute infections and occasionally chronic systemic infections in humans and animals (1-3). *B. pseudomallei* can invade and thrive inside professional phagocytes and non-phagocytic cells alike (4-6) and the stages of its intracellular pathogenesis are well defined (7-9). After uptake into a cell, *Burkholderia* escape from the phagosome into the cytoplasm where they replicate, polymerize host-cell actin, and spread to neighboring cells usually causing cell fusion and MNGC formation (5, 9-13).

Treatment of *B. pseudomallei* infection currently involves in-hospital administration of intravenous antibiotics followed by a lengthy eradication phase with oral antibiotics (2, 3, 14). With such an invasive and expensive treatment regimen there is a greater chance of non-compliance which can lead to persistent infection. Therefore, there is a need to identify new treatments which may make treatment administration more practical in areas where access to healthcare may be limited. Therapies which could potentially accelerate the time to recovery or decrease the length or dose of intravenous antibiotics could be good candidates for new treatments against melioidosis.

Although current melioidosis treatments rely exclusively on antibiotics and antimicrobials, much research has focused on understanding and characterizing the natural host immune responses to *B. pseudomallei* infection, specifically in regards to the effects of IFN-γ. Studies show that IFN-γ is absolutely necessary for protection against acute disease (15-17).

There is also a known role for ROS responses due to IFN-γ stimulation in controlling early infection with *Burkholderia* (16, 18). While the effects of IFN-γ on infected macrophages have been studied in great detail, there are few studies that look at the combination of immune stimulation with antibiotic treatment, even though this scenario is realistically encountered in patients treated for melioidosis. Our lab has studied these immuno-antimicrobial interactions and has previously shown that treatment with IFN-γ can synergistically enhance the effect of ceftazidime treatment on infected macrophages, reducing intracellular bacterial burden beyond either drug alone (19). For the following study we used a combination of in vitro and in vivo techniques to investigate the underlying mechanism of the interaction between IFN-γ and ceftazidime. From these studies we developed a new model by which IFN-γ induces host antimicrobial pathways which synergize with antibiotics to kill intracellular pathogens.

MATERIALS AND METHODS

Biochemicals.

Ceftazidime hydrate, *N*-acetyl-L-cysteine (NAC), reduced L-glutathione (GSH), L-Buthionine-sulfoximine (BSO) were purchased from Sigma-Aldrich (St. Louis, MO). Other reagents included recombinant murine IFN-γ (Peprotech, Rocky Hill, NJ), ketamine (Fort Dodge Animal Health, Overland Park, KS), and xylazine (Ben Venue Labs, Bedford, OH). For flow cytometry and fluorescent microscopy, we purchased the following biochemicals from Life Technologies (Carlsbad, CA): Alexa Fluor 488 conjugated phalloidin, ProLong Gold Anti-fade mounting media with DAPI, Di(Acetoxymethyl Ester) (6-Carboxy-2',7'-Dichlorodihydrofluorescein Diacetate)(carboxy-H2DCFDA), monochlorobimane (mBCl), Alexa

Fluor 488 streptavidin-conjugated antibody, and trypsin with EDTA. Other reagents included lysosome-associated membrane protein (LAMP) antibody (ebioscience, San Diego, CA), Alexa Fluor 647 conjugated anti-mouse CD11b antibody (BD Biosciences Pharmingen, San Jose, CA), rabbit polyclonal anti-*B. pseudomallei* antibody (provided by D. Waag from USAMRIID), and goat anti-rabbit secondary IgG antibody conjugated to Cy3 (Jackson ImmunoResearch Labs, West Grove, PA).

Bacteria.

B. thailandensis E264 and *B. pseudomallei* 1026b strains were used for these studies (20, 21). Both strains were grown in Luria-Bertaini broth at 37°C with rotary shaking for 16 hours, and then stored at -80°C with 15% glycerol until needed. Frozen vials of bacteria were thawed and diluted immediately prior to their use.

Cell lines.

RAW 264.7 and J774A.1 macrophage cell lines and murine fibroblast cell line L929 were purchased from American Type Tissue Collection (Manassas, VA). Cell lines were maintained in complete media consisting of minimum essential media (MEM; Life Technologies) supplemented with 10% fetal bovine serum (FBS) (Atlas, Fort Collins, CO), 0.075% sodium bicarbonate (Acros organics, NJ), 1x nonessential amino acids, 0.5x essential amino acids (Life Technologies), and 2 mM L-glutamine (Sigma-Aldrich). Antibiotic additions of 100 Units/ml Penicillin and 100 µg/ml Streptomycin (Life Technologies) were added to media for

maintenance of cell lines but all experiments were conducted in antibiotic-free media. All cells were maintained at 37°C with 5% CO_2.

Mice.

Female BALB/c, C57BL/6 and ICR mice were used for these studies. The BALB/c and C57BL/6 mice were purchased from Jackson Laboratories (Bar Harbor, ME). The ICR mice were purchased from Harlan Laboratories (Indianapolis, IN). All mice were between 6 to 12 weeks old at the time of their use and were housed under pathogen-free conditions. All animal studies were approved by the Institutional Animal Care and Use Committee at Colorado State University.

Primary bone marrow macrophage culture.

Bone marrow macrophages were generated as previously described (22). Femurs and tibias were aseptically removed from mice, transferred to 50 ml conical tubes containing Hank's buffered salt solution (HBSS) supplemented with 2% FBS, and kept on ice. In a biosafety cabinet, bones were cleaned of tissue and bone marrow was flushed from the bones using needles and syringes filled with HBSS and supplemented with 2% FBS. Bone marrow was gently resuspended with gentle pipetting and passed through a 70 µm nylon filter (BD Biosciences Pharmingen, San Jose, CA). Cells were centrifuged at 1200 rpm for 5 minutes at 4°C. Then supernatant was removed and red blood cells were lysed using 2 ml of ammonium-chloride-potassium (ACK) lysis buffer for 5 minutes, followed immediately by 20 mls of complete MEM with antibiotics and 10% L929-conditioned supernatants to dilute the lysis buffer. Cells were

again spun at 1200 rpm for 5 minutes at 4°C. Remaining white blood cells were plated in 24-well plates at a concentration of 2 x 10^6 cells/ml in complete MEM. Cells were allowed to adhere to 24-well plates for 3 hours at 37°C and 5% CO_2 after which, non-adhered cells were washed away three times with room-temperature HBSS supplemented with 2% FBS. Complete media with antibiotics and 10% L929 conditioned media was reapplied to the cells and plates were returned to the incubator. Addition of 10% L929-conditioned media provided necessary growth factors for differentiation of bone marrow myeloid progenitor cells into the macrophage/monocyte lineage to enrich for these cells. Adherent cells were incubated at 37^{o}C and 5% CO_2 until macrophages reached moderate confluency in wells (approximately 8-12 days).

Macrophage infection assay.

Macrophages were infected and treated as previously described (19). Briefly, macrophages were seeded into 24-well plates with complete MEM (see above) and allowed to adhere overnight. After a 1ml wash with phosphate buffered saline (PBS), *B. thailandensis* was added to macrophages at a multiplicity of infection of 5 and incubated for 1 hour at 37°C in 5% CO_2. Aminoglycosides are not considered to penetrate mammalian cells in short time periods (23), so macrophages were exposed to high-dose kanamycin-sulfate (350 µg/ml) for 1 hour to kill extracellular bacteria. After two 2 ml washes with PBS to remove kanamycin and dead bacteria, treatments were diluted in MEM, applied to macrophages, and incubated for 18 hours. Treatments consisted of individual drugs or combinations of the following: ceftazidime (10 µg/ml), IFN-γ (10 ng/ml), NAC (25, 50, 100 mM), GSH (10, 25, 50 mM), or BSO (5 mM). Because the effect of BSO is to deplete GSH by preventing its biosynthesis, BSO treatment was

applied as an 18-24 hour pre-treatment of uninfected macrophages prior to the start of the macrophage infection assay in order to effectively deplete GSH. BSO was also added at the same concentration with the other treatments for the 18 hours post-infection treatment. Although ceftazidime was applied at 10 µg/ml to infected macrophage cell lines, it was applied at 3 µg/ml to infected bone marrow macrophages because 10 µg/ml had too great of an effect at controlling intracellular bacterial burden on its own, and therefore made it harder to determine synergy with IFN-γ. After the 18 hour treatment of infected macrophages, extracellular bacteria were washed off three times with 2 mls of PBS and macrophages were lysed with 1 ml of sterile distilled water. Intracellular bacterial burden was then assessed by plating serial dilutions of the lysates on LB agar followed by colony counts 24-48 hrs after plating.

Fluorescent microscopy.

RAW 264.7 macrophages were seeded into chamber slides, infected, and treated as previously described for the macrophage infection assay. At indicated times, chamber slides containing *B. thailandensis* infected macrophages were fixed with a solution of 2% paraformaldehyde in PBS for 20 minutes, and subsequently permeabilized with 1 ml of 0.1% triton-X in PBS for 5 minutes. Cells were then incubated overnight at 4°C with Alexa Fluor 647 conjugated anti-mouse CD11b antibody and rabbit anti-*Burkholderia* serum. The next morning, a blocking buffer consisting of 0.5% bovine serum albumin in PBS was applied to wells for 30 minutes at room temperature. For experiments including LAMP staining, the blocking buffer used was 5% Donkey serum in PBS with 0.05% Tween applied to wells for 1 hour at room temperature. When LAMP staining was necessary, wells were also blocked with streptavidin (Vector Laboratories, Burlingame, CA) for 15 minutes followed by biotin (Vector Laboratories)

for 15 minutes at room temperature. Phalloidin was added to wells at 5 units/well in PBS for 30 minutes to stain actin filaments. Lysosome compartments were identified by incubation for 1 hour with a 1/400 dilution of a biotinylated anti-mouse LAMP antibody followed by a 1/500 dilution of Alexa Fluor 488 or Alexa Fluor 647 streptavidin-conjugated antibody for 1 hour. To identify *Burkholderia*, we applied a 1/1000 dilution of a goat anti-rabbit IgG antibody conjugated to Cy3. This secondary antibody was applied with the secondary antibody for LAMP identification. Wells were washed between steps with either 0.5% bovine serum albumin in PBS or PBS with 0.05% Tween (for experiments involving LAMP staining). Coverslips were applied with mounting media containing DAPI to stain nuclei. Images were acquired with a Leica DM 4500B microscope (Leica Microsystems, Buffalo Grove, IL) fitted with a Retiga 2000R camera (QImaging, Surrey, BC, Canada) and using QCapture Pro software (QImaging). Adobe Photoshop CS3 version 10.0.1 (Adobe, San Jose, CA) was used to create color overlay images as well as make global manipulations to the linear parameters of black-point and individual color brightness for each experiment.

Flow cytometry.

Macrophages were treated in 24-well plates at a density of $4x10^5$ cells/ml. Treatments included ceftazidime (10 µg/ml), IFN-γ (10 ng/ml), NAC (20 mM), or BSO (5 mM). Macrophages were pre-treated with BSO (5 mM) 18-24 hours prior to infection as well as 18-24 hours post infection. After indicated treatment times the cells were washed with PBS and detached with 0.25% trypsin with EDTA. We made several attempts to use the reagent hydroxyphenyl fluorescein (HPF, Life Technologies) to detect intracellular ROS in mammalian cells, however our negative controls were always positive for the HPF stain. Therefore we

turned to carboxy-H2DCFDA to measure intracellular ROS instead. Cells were incubated with either 5 μM carboxy-H2DCFDA for 30 min at 37^{o}C to detect total intracellular ROS or with 40 μM mBCl for 20 minutes at room temperature in the dark, as previously done (24). The reagent mBCl is used to detect intracellular thiols, of which GSH is the most abundant. Data was collected on greater than 50,000 cells per sample using a Gallios Flow Cytometer (Beckman Coulter, Brea, CA) and analyzed using FlowJo software version 7.6.5 (Tree Star, Ashland, OR).

In vivo challenge model.

BALB/c mice were anesthetized with 100 mg/kg ketamine plus 10 mg/kg xylazine administered intraperitoneally. The *B. pseudomallei* challenge dose was thawed from a frozen stock, diluted in PBS, and delivered intranasally in a volume of 20 μl for a total of 5.7 x 10^3 CFU/mouse. This dose was determined retrospectively by serial dilution, plating onto LB agar, and counting colonies 24-48 hours later. Ceftazidime was administered through the intraperitoneal route (IP) at 25 mg/kg of body weight 6 hrs after initial infection and subsequently every 12 hrs for a total of six treatments total. BSO was administered IP to mice at 2 mmol/kg once daily starting the day before infection and continuing through two days after the infection. Mice were monitored twice daily for signs of disease and were euthanized according to predetermined humane end points. All procedures were performed in a biosafety level 3 (BSL-3) facility, following approved protocols for BSL-3 research and select agent use.

Statistical analyses.

Means, standard error of the mean (SEM), and P-values were determined and plotted using Prism software version 5.00 (GraphPad, La Jolla, CA). For comparisons of two groups, a two-tailed Student's t-test was used to determine statistically significant differences. For comparisons of three or more groups the one-way analysis of variance (ANOVA) was used followed by Tukey's post test for multiple comparisons. Grouped data was analyzed by two-way ANOVA and statistical synergy was determined as before (25) from the interaction P-value of a two-way ANOVA. All differences were considered statistically significant for $P < 0.05$. In-vivo survival rates were plotted by Kaplan-Meier analysis. To determine statistical differences between two survival curves we compared P-values from the log-rank test to the Bonferroni-corrected threshold for multiple comparisons.

RESULTS

IFN-γ combination with ceftazidime significantly reduces intracellular bacteria burden in infected macrophages. Previously, we found that the combination of IFN-γ with ceftazidime synergistically reduced intracellular bacterial burden of *B. thailandensis*-infected AMJ macrophages after 18 hours of treatment (19). We confirmed the IFN-γ and ceftazidime synergistic interaction using a different macrophage cell line, RAW 264.7, (Figure 4.1A) as well as primary bone marrow macrophages from C57BL/6, BALB/c, and ICR mice (Figure 4.1B-D). For each source of macrophage, the combination of IFN-γ plus ceftazidime controlled the intracellular bacteria burden by 3-4 Log_{10} units compared to untreated controls. Although β-lactam antibiotics can be unstable in solution, we showed that supernatants from ceftazidime

wells were still bactericidal at the end of the 18 hour incubation (K. Mosovsky and S. Dow, unpublished data), which confirmed that the activity of ceftazidime was not compromised during our experiments due to its instability. Surprisingly, IFN-γ and ceftazidime combination failed to reduce bacterial burden in the murine fibroblast cell line, L929, compared to untreated controls (Figure 4.2).

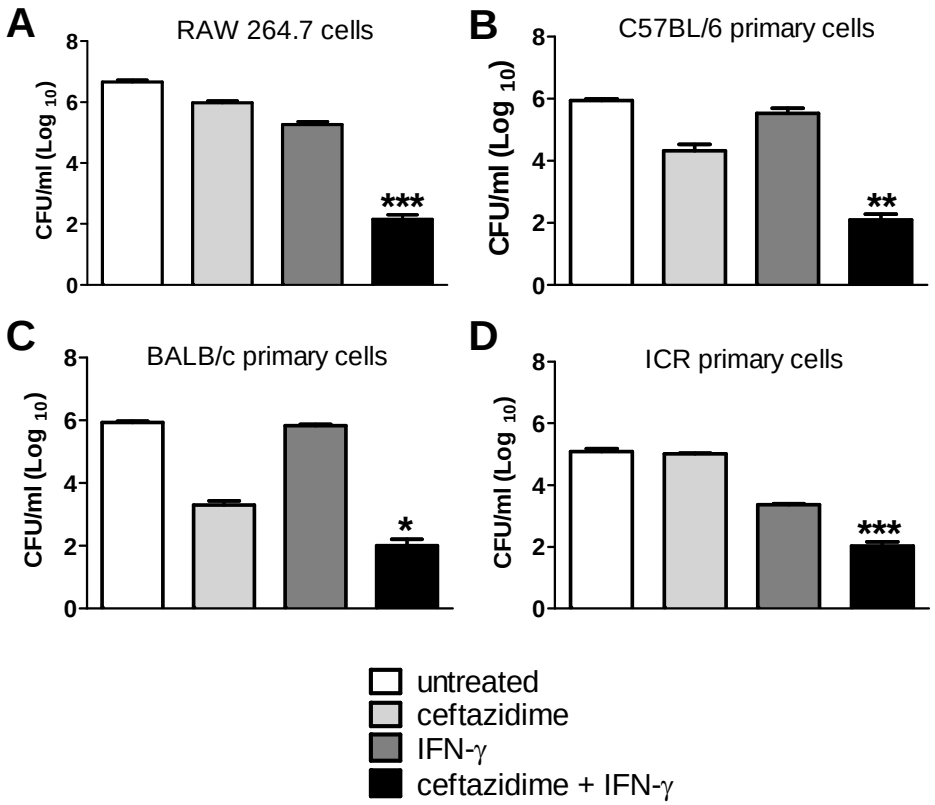

Figure 4.1: Ceftazidime and IFN-γ induce synergistic killing of intracellular bacteria in macrophages. Adherent RAW 264.7 cells (A) or primary bone marrow macrophages from C57BL/6 mice (B) BALB/c mice (C) or ICR mice (D) were infected with *B. thailandensis* and treated with ceftazidime (10 µg/ml for RAW 264.7 cells, 3 µg/ml for bone marrow macrophages), IFN-γ (10 ng/ml) or the combination of ceftazidime plus IFN-γ for 18 hours. Intracellular bacteria were then enumerated by plating macrophage lysates. Synergistic interactions between ceftazidime and IFN-γ were determined by two-way ANOVA (* $P < 0.01$, ** $P < 0.001$, *** $P < 0.0001$). Graphs are representative of data from two or more independent experiments with treatment groups run in triplicate.

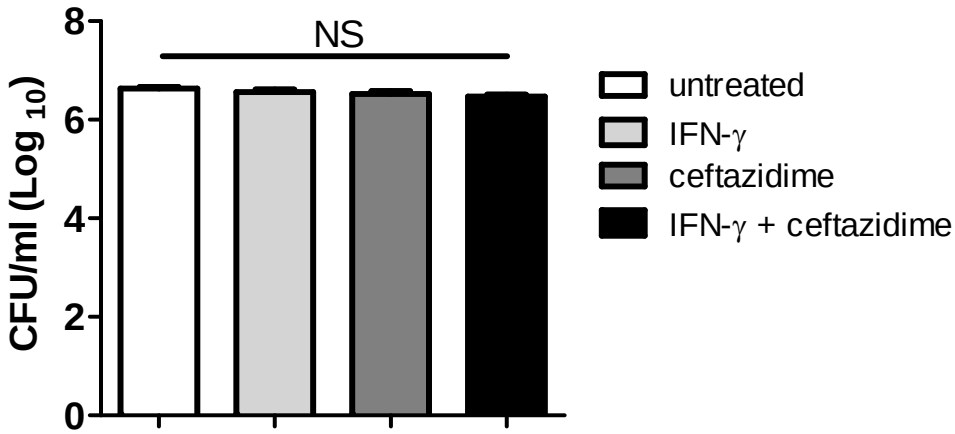

Figure 4.2: Ceftazidime and IFN-γ fail to kill intracellular bacteria in L929 fibroblast cells. L929 fibroblast cells were infected with *B. thailandensis* and treated with ceftazidime (10 µg/ml), IFN-γ (10 ng/ml), or the combination of ceftazidime plus IFN-γ for 18 hrs. Intracellular bacteria were then enumerated by plating macrophage lysates. Significant differences were determined by one-way ANOVA. Graph is representative of data from three independent experiments with treatment groups run in triplicate.

IFN-γ treatment of L929 cells has been shown to protect cells from intracellular pathogens (26, 27), though some properties of IFN-γ activation, such as increased major histocompatibility complex, inhibition of cell growth, and clearance of pathogens may be deficient in L929 cells (27, 28). Taken together these results demonstrate that the interaction between IFN-γ and ceftazidime is exhibited by macrophages but not by non-phagocytic cells.

Inhibitors of ROS pathway reverse synergistic interaction between IFN-γ and ceftazidime. We considered several mechanisms by which IFN-γ, with no direct bactericidal effects itself, could trigger the synergistic interaction with ceftazidime. These included induction of nitric oxide, autophagy, increased uptake of ceftazidime, or induction of ROS responses in

IFN-γ-stimulated macrophages. Increased nitric oxide and increased autophagy were eliminated as potential mechanisms of synergy after specific inhibitors of these pathways failed to reverse the combination therapy synergy (R. Troyer and S. W. Dow, data not shown). Furthermore, direct quantitation of intracellular ceftazidime concentrations showed an average of 0.0272 µg/ml after ceftazidime treatment, approximately 50 fold below the MIC, with no increased uptake of ceftazidime due to IFN-γ stimulation, a similar result to studies by Miyagi et. al. (18). We were then left to explore IFN-γ induction of ROS pathways as a mechanism of synergy.

We reasoned that if IFN-γ synergizes with ceftazidime through a ROS-mediated pathway, blocking ROS pathways using specific antioxidant inhibitors should abolish the synergy (Figure 4.3).

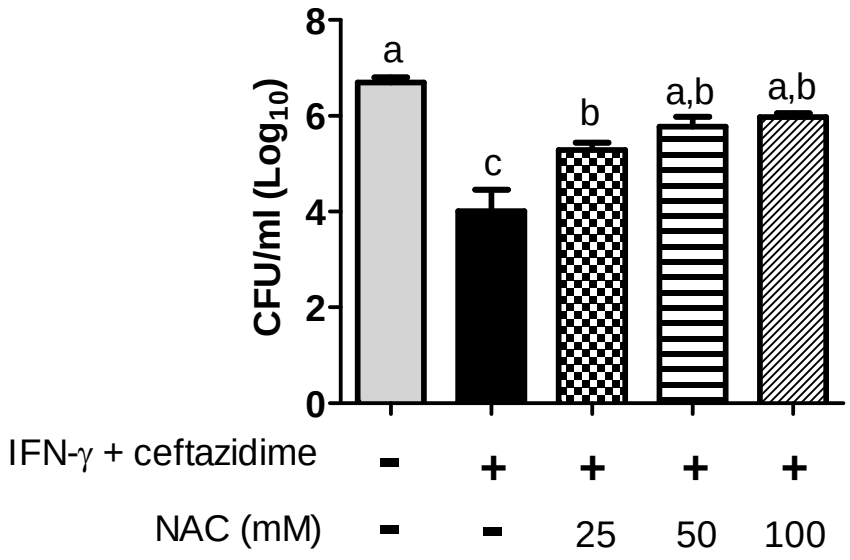

Figure 4.3: NAC reverses IFN-γ and ceftazidime synergy. NAC reversed the intracellular killing effect of IFN-γ (10 ng/ml) plus ceftazidime (10 µg/ml) combination therapy on *B. thailandensis*-infected macrophages in a dose-dependent manner. Statistical differences were assessed by one-way ANOVA, a > b > c, $P < 0.05$. Results are representative of results from at least two independent experiments.

NAC, an antioxidant and cysteine precursor for GSH synthesis (29-31) (see Figure 1.3), reversed the synergistic killing of the combination therapy in a concentration-dependent manner (Figure 4.3). We also observed this effect in *B. pseudomallei* 1026b (data not shown). We hypothesized that NAC was functioning through increased production of GSH, a prominent cellular antioxidant and ROS scavenger in macrophages (29, 32-38). To test this hypothesis, we measured intracellular GSH levels using mBCl and confirmed that treatment with NAC increased GSH content (Figure 4.4A) and also decreased total ROS levels in IFN-γ and ceftazidime treated macrophages (Figure 4.4B).

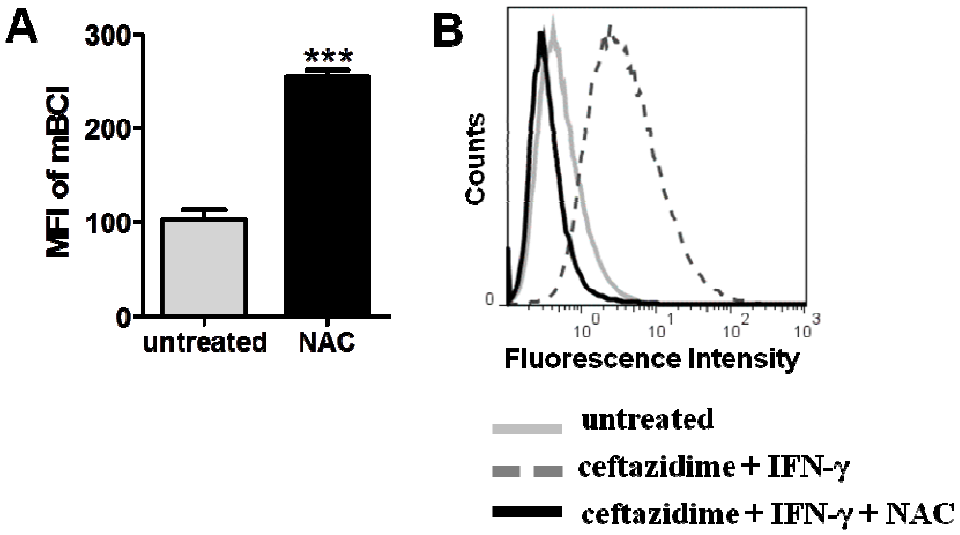

Figure 4.4: NAC increases intracellular GSH and reduces intracellular ROS. (A) Mean fluorescent intensity of mBCl after treatment of uninfected RAW cells with NAC (20 mM) for 2 hrs (P = 0.0004) (B) Intracellular ROS levels (as detected by carboxy-H2DCFDA) in RAW 264.7 cells after 10 hr treatment with ceftazidime plus IFN-γ, with or without NAC (20 mM). Results are representative of results from at least two independent experiments.

Finally, when GSH was substituted for NAC, we observed a similar titratable effect for reversing the IFN-γ and ceftazidime synergistic killing of intracellular *B. thailandensis* (Figure 4.5) and *B. pseudomallei* (data not shown). Based on these findings, we concluded that

inhibitors of ROS pathways can reverse the killing effect of IFN-γ and ceftazidime, which is in agreement with a ROS-mediated mechanism of synergy.

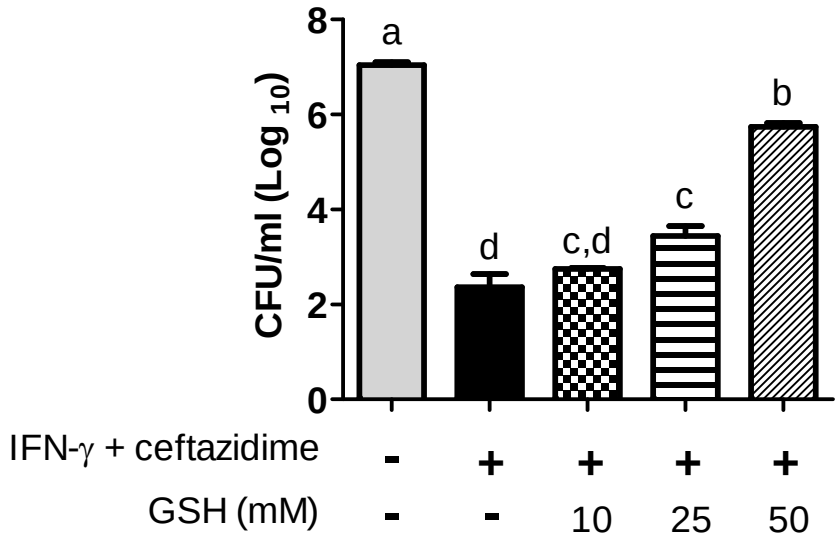

Figure 4.5: GSH reverses IFN-γ and ceftazidime synergy. GSH reversed the intracellular killing effect of IFN-γ (10 ng/ml) plus ceftazidime (10 µg/ml) combination therapy on *B. thailandensis*-infected macrophages in a dose-dependent manner. Statistical differences were assessed by one-way ANOVA, a > b > c > d, $P < 0.05$. Results are representative of results from at least two independent experiments.

IFN-γ induces ROS production in macrophages. We confirmed increased levels of intracellular ROS due to IFN-γ stimulation in uninfected macrophages and found that IFN-γ increases ROS as early as 6 hrs post-stimulation with increasing levels through 24 hrs (Figure 4.6A). Significantly, the time required for the start of ROS induction, 6 hrs, coincides with the time it takes for the combination of IFN-γ plus ceftazidime to begin control of intracellular bacteria burden as seen in our previous study (19). We also observed increased ROS in bone marrow macrophages due to IFN-γ stimulation (E. Silva and S. W. Dow, data not shown). In infected macrophages, IFN-γ but not ceftazidime increased intracellular ROS levels (Figure

4.6B). Combined, these results indicate that uninfected and infected macrophages increase production of ROS due to stimulation with IFN-γ.

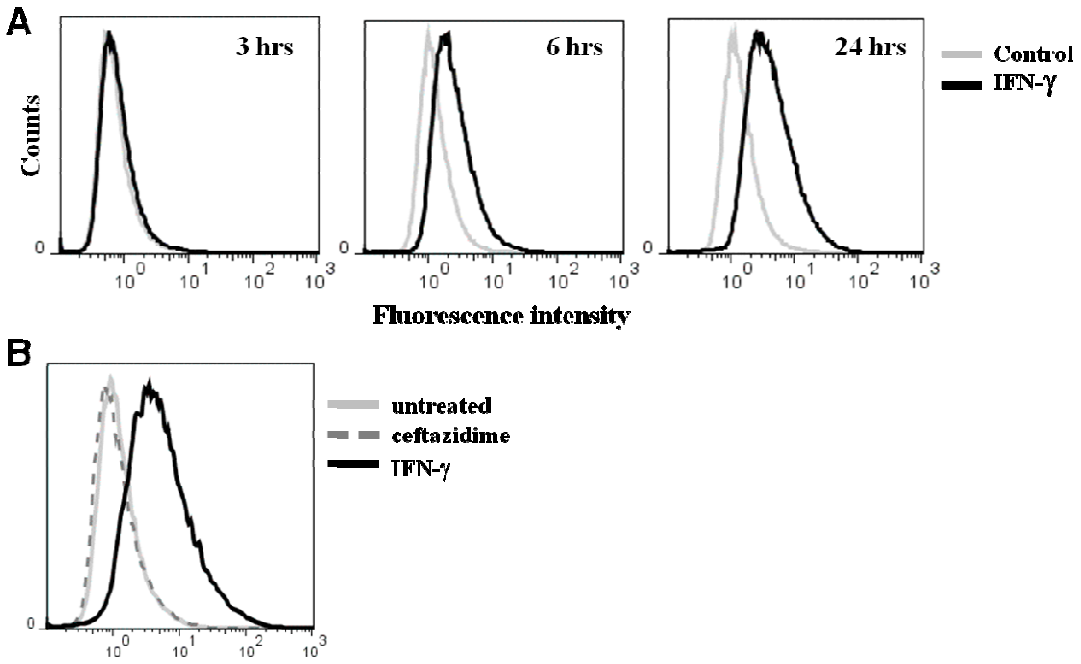

Figure 4.6: Stimulation with IFN-γ induces ROS production in macrophages. (A-B) Histogram overlays of ROS responses as measured with carboxy-H2DCFDA by flow cytometry. (A) IFN-γ elicited ROS responses from uninfected RAW 264.7 macrophages starting 6 hrs post-stimulation with a peak response at 24 hrs. (B) RAW 264.7 macrophages were infected with *B. thailandensis*, treated with IFN-γ (10 ng/ml) or ceftazidime (10 μg/ml) for 18 hrs, and then analyzed for ROS responses. Results are representative of results from at least two independent experiments.

Inducers of ROS can interact with ceftazidime to increase killing of intracellular *Burkholderia*. We next argued that if the IFN-γ effect is ROS-mediated, then other pro-oxidant drugs that increased ROS should also interact with ceftazidime to enhance killing of intracellular *Burkholderia*. BSO specifically inhibits the rate-limiting step in GSH synthesis (29), depleting GSH content through prevention of biosynthesis and resulting in increased intracellular ROS as a result of decreased antioxidant activity (39-44) (see Figure 4.7).

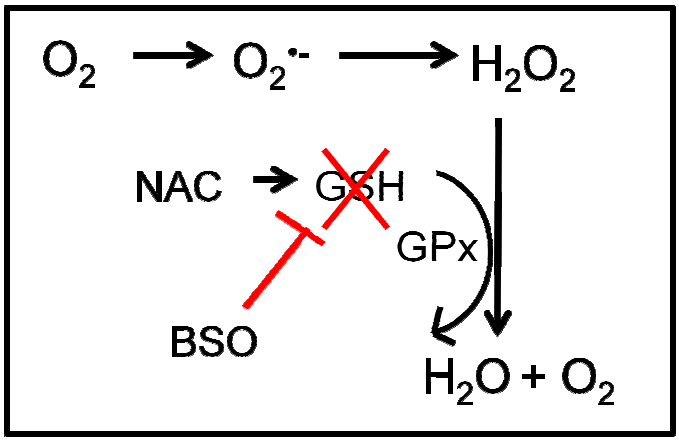

Figure 4.7: Pathway by which BSO should decrease intracellular GSH concentrations. BSO specifically inhibits the first step in GSH synthesis. By blocking GSH synthesis, the cell will have fewer antioxidants to degrade ROS, and therefore BSO should indirectly increase ROS levels in the cell.

BSO was combined with ceftazidime and/or IFN-γ in *B. thailandensis* infected macrophages (Figure 4.8) and the effect on intracellular bacterial burden was assessed

The combination of BSO with ceftazidime produced the same level of killing inside macrophages as the combination of IFN-γ with ceftazidime. Furthermore the combination of the three drugs significantly increased intracellular killing beyond the effect of IFN-γ plus ceftazidime alone (Figure 4.8). We confirmed that treatment with BSO increased levels of ROS in *B. thailandensis* infected macrophages and further increased ROS levels due to IFN-γ (Figure 4.9A). Analysis of these results corroborates the hypothesis that BSO was acting as a pro-oxidant in our macrophage infection model. Finally, we showed that treatment with BSO decreases intracellular GSH levels as predicted (Figure 4.9B). These results demonstrate that inducers of ROS can both substitute for IFN-γ and augment the IFN-γ plus ceftazidime synergistic interaction on intracellular killing.

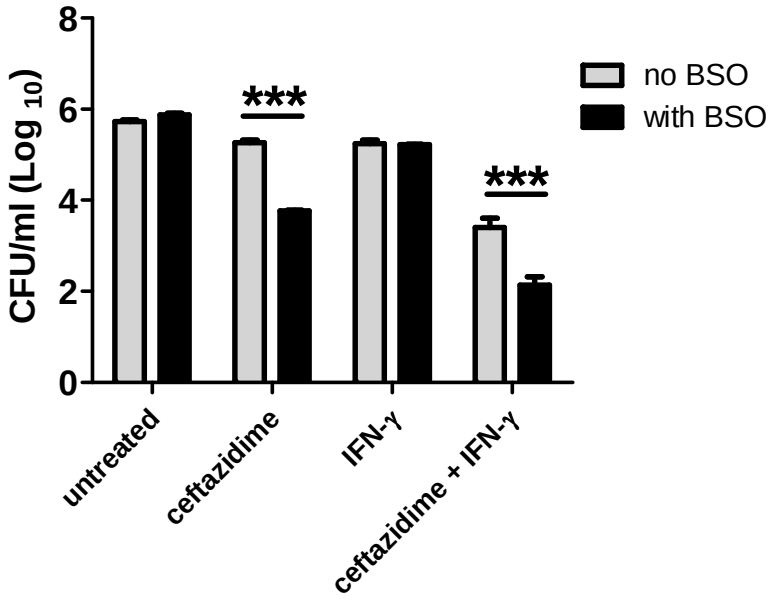

Figure 4.8: BSO enhances antibiotic killing of intracellular *Burkholderia*. RAW 264.7 cells were pre-treated with BSO (5 mM) overnight for 18-24 hrs, infected with *B. thailandensis*, and treated with IFN-γ (10 ng/ml), ceftazidime (10 µg/ml), or the combination of IFN-γ plus ceftazidime for another 18 hrs, with or without BSO (5 mM). Significant differences were assessed between groups treated with or without BSO by Student's T-test, *** $P < 0.001$.

BSO enhances antibiotic-mediated survival of mice challenged with lethal dose of *B. pseudomallei*. To validate observations made in vitro we evaluated the interaction of BSO plus ceftazidime in vivo using an intranasal challenge model. Mice treated with the combination of BSO plus ceftazidime were completely protected from a lethal challenge with *B. pseudomallei* (Figure 4.10). This result was consistent with our previous finding that ceftazidime plus IFN-γ greatly enhanced protection of mice from a lethal challenge of *B. pseudomallei* (19) and strongly suggests a role for ROS in enhancing antibiotic therapy in vivo.

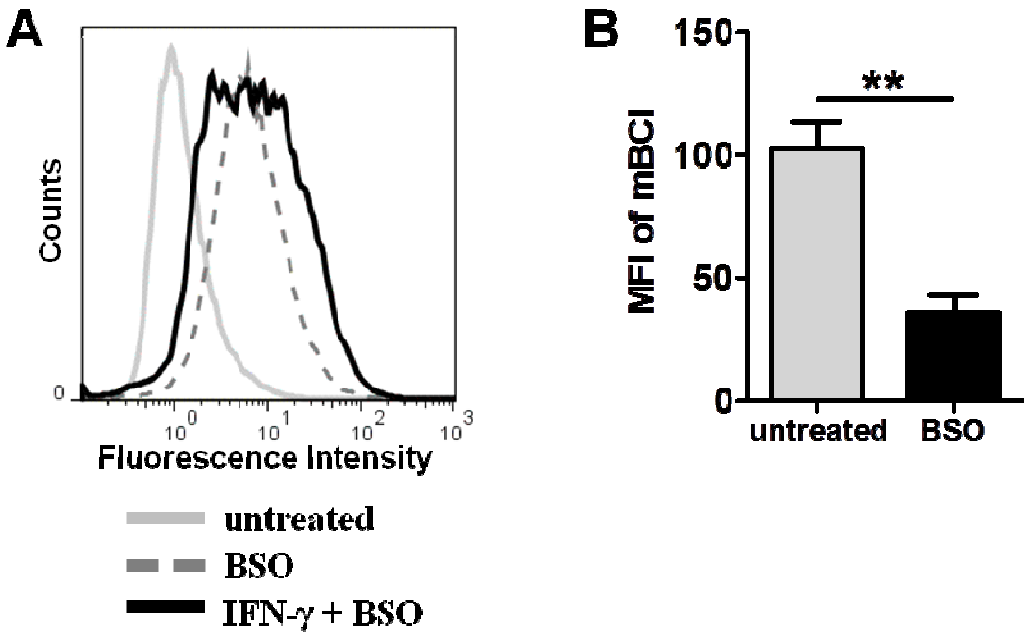

Figure 4.9: BSO induces intracellular ROS and decreases intracellular GSH.
(A) Histogram overlays of intracellular ROS, as measured by carboxy-H2DCFDA and flow cytometry, after macrophage infection with *B. thailandensis* and subsequent treatment with BSO (5 mM) or the combination of IFN-γ + BSO for 12 hrs. All BSO groups were also pre-treated with BSO (5 mM) overnight for 18-24 hrs. (B) MFI of intracellular thiols, as measured by mBCl, after 18 hrs of treatment with 5 mM BSO (** P = 0.0079). All data are representative of at least two independent experiments.

Taken together, our in vitro and in vivo results provide strong evidence for IFN-γ induction of ROS responses as the mechanism of the interaction between IFN-γ and ceftazidime on intracellular control of bacterial burden. We next investigated the specific mechanisms by which the increased ROS could affect bacterial burden.

***Burkholderia* fail to escape the phagosome and polymerize actin inside IFN-γ treated macrophages.** In order to understand how IFN-γ induced ROS could interact with ceftazidime and increase killing of intracellular bacteria, we turned to fluorescent microscopy. We revealed a failure of *Burkholderia* to polymerize host cell actin due to IFN-γ (Figure 4.11).

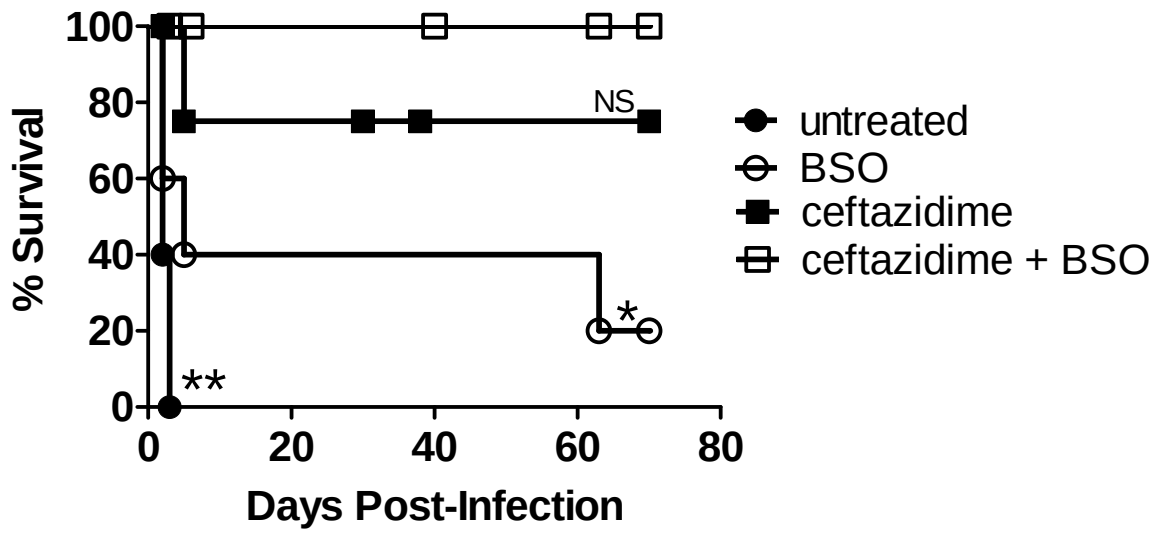

Figure 4.10: The combination of BSO with ceftazidime fully protects mice from lethal *B. pseudomallei* infection. BALB/c mice (n = 5 per group) were challenged with 5.7 X 10^3 bacteria administered intranasally and subsequently treated with IP ceftazidime (25 mg/kg), BSO (2 mmol/kg), or the combination of both drugs. Percent survival was tracked over 70 days. Statistical significance between survival curves was assessed by log-rank test and the Bonferroni-corrected threshold for multiple comparisons ($P < 0.01667$).

This effect was recapitulated with BSO treatment (Figure 4.12) suggesting ROS involvement. Since *Burkholderia* polymerize host cell actin only after vacuolar escape into the cytoplasm (9-11) (see Figure 1.2), an investigation was prompted to determine whether bacteria inside IFN-γ treated macrophages failed to escape the phagosome. Since the phagolysosome would be the only intracellular compartment we would expect to find both LAMP-1 and bacteria (see Figure 4.13), we used fluorescent microscopy to quantitate the ratio of bacteria inside IFN-γ treated macrophages that co-localized with LAMP-1 compared to untreated controls. Indeed, we found that IFN-γ treated macrophages had a higher proportion of bacteria that colocalized with LAMP-1 containing vacuoles suggesting that bacteria failed to escape the phagosome in IFN-γ treated groups (Figure 4.14 and Figure A8). This explanation is consistent with the lack of actin tails on *Burkholderia* inside macrophages treated with IFN-γ or BSO.

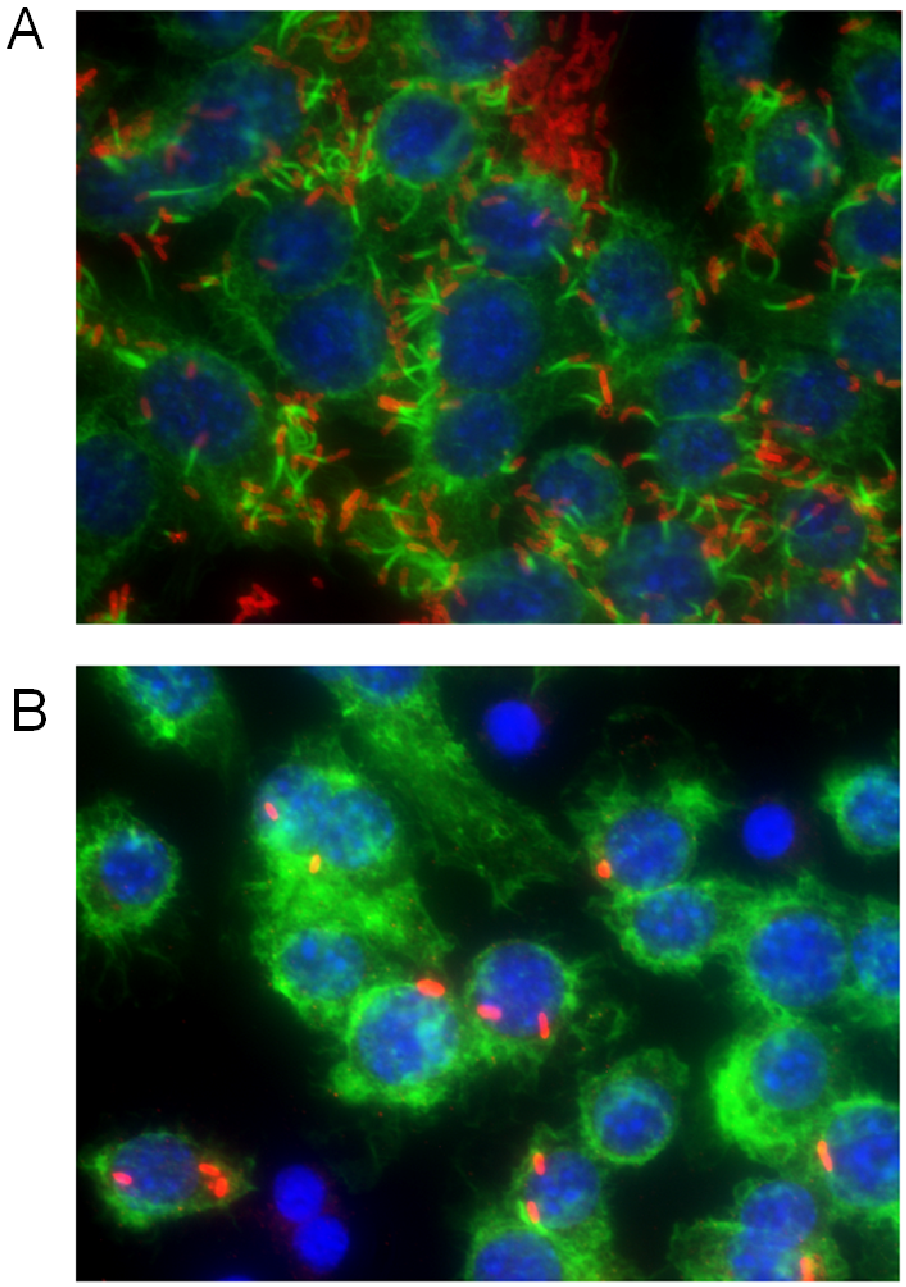

Figure 4.11: *B. thailandensis* fails to form actin tails inside IFN-γ-treated macrophages. RAW cells were infected with *B. thailandensis* and left untreated (A) or treated with IFN-γ (10 ng/ml) (B) for 12 hours. Macrophages were fixed, permeabilized, and stained with phalloidin to identify host cell actin (green), DAPI to stain nuclei (blue), and anti-*Burkholderia* serum followed by secondary antibody conjugated to Cy3 to stain *B. thailandensis* (red). Images were captured under 100x magnification. Actin tails are seen as bright green protrusions from the red bacteria in (A). Images are representative of data from three independent experiments.

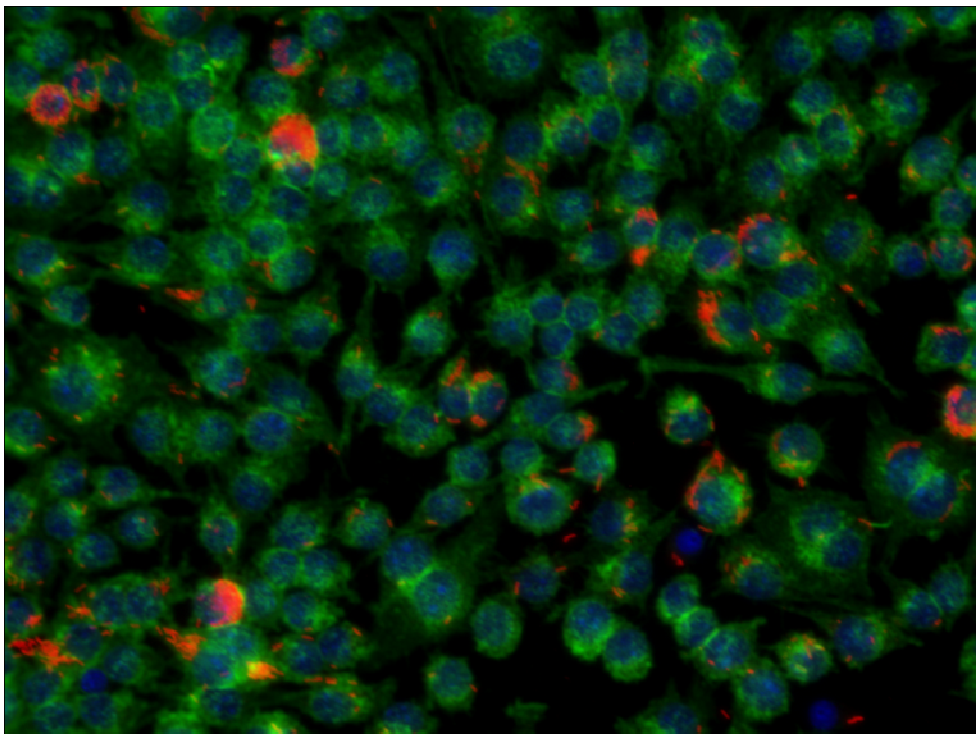

Figure 4.12: *B. thailandensis* fails to form actin tails inside BSO-treated macrophages. RAW 264.7 cells were pre-treated with BSO (5 mM) for 18-24 hrs to deplete intracellular ROS before infection with *B. thailandensis* and subsequent treatment for 18 hrs BSO (5 mM). Macrophages were then fixed and stained for host cell actin (green), nuclei (blue), and *B. thailandensis* (red) and images were captured under 40x magnification. Image is representative of data from two independent experiments.

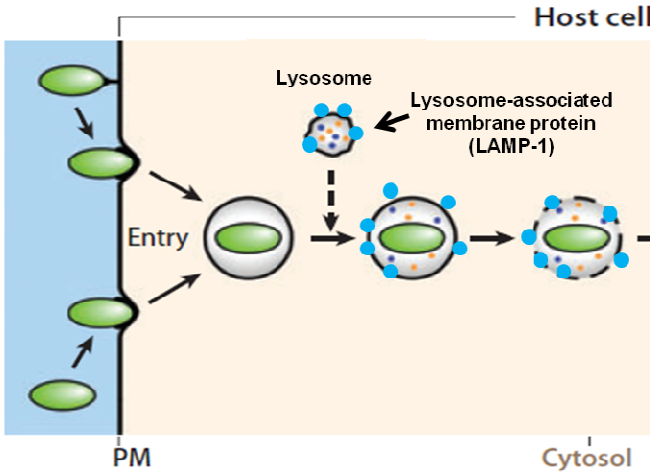

Figure 4.13: Diagram of LAMP-1 expression on phagolysosomes. LAMP-1 is enriched on lysosomes, late endosomes, and phagolysosomes. Phagolysosomes, therefore, are the only compartment in which bacteria should share co-localization with LAMP-1 staining. Image modified from (12).

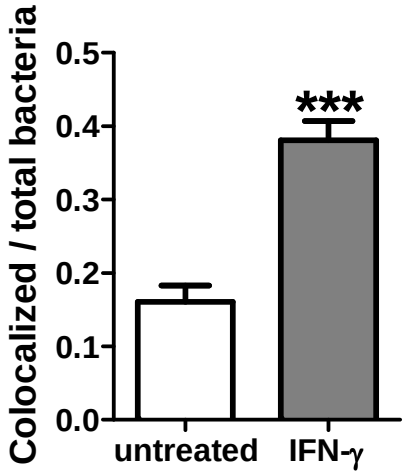

Figure 4.14: *Burkholderia* inside IFN-γ treated macrophages have higher proportion of LAMP-1 colocalization than untreated control. Quantitation of *B. thailandensis* colocalization with LAMP-1 antibody after 8 hr IFN-γ treatment of infected macrophages. Data is represented as the ratio of colocalized bacteria (with LAMP-1) to total bacteria per field of view. Data represents 10 fields of view for each treatment group ($P < 0.0001$) and results are representative of 2 independent experiments.

DISCUSSION

We previously described a novel therapeutic approach for melioidosis which combined immune stimulation by IFN-γ with the routinely administered antibiotic, ceftazidime, to synergistically enhance killing of intracellular *Burkholderia* (19). Here we have shown that the mechanism of synergy between IFN-γ and ceftazidime is mediated by IFN-γ induced ROS responses in infected macrophages. Evidence of ROS involvement is supported by our experiments in which ROS inhibitors reversed the synergistic killing of IFN-γ and ceftazidime while inducers of ROS not only potentiated the killing but could completely substitute for IFN-γ with equal effect (see Figure 4.15).

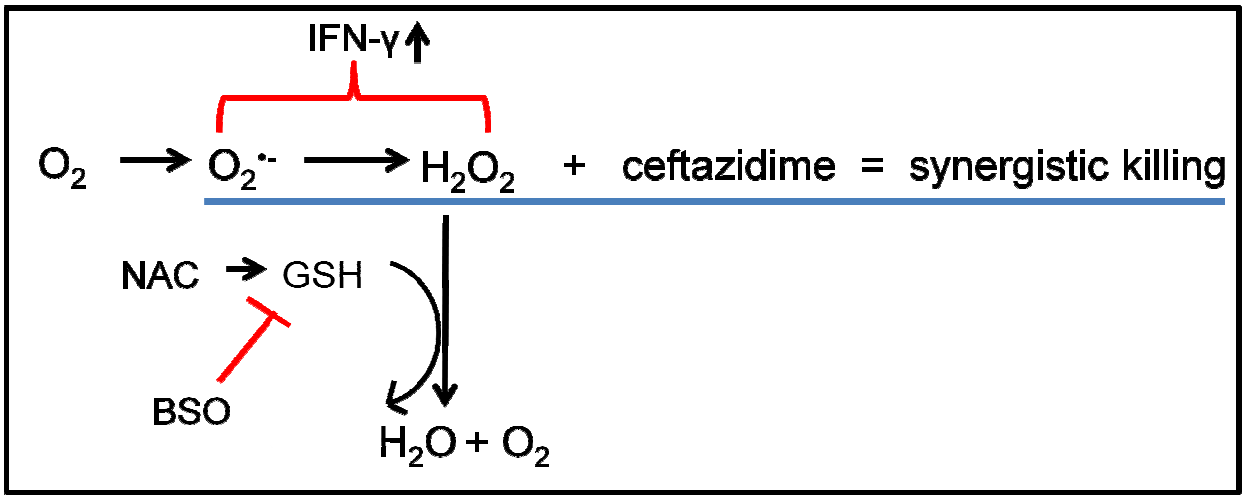

Figure 4.15: Diagram of major findings related to ROS production and degradation. The blue line underlines our original hypothesis that IFN-γ induced ROS synergizes with ceftazidime to synergistically kill intracellular *Burkholderia*. All of our findings in Chapter 4 are in line with this hypothesis. We first showed that IFN-γ increases intracellular ROS in infected macrophages. We next showed that antioxidants such as NAC and GSH could remove ROS and therefore reverse the synergism. Finally, we showed that BSO could inhibit GSH synthesis, to indirectly increase ROS and lead to synergy, even in the absence of IFN-γ.

We further showed evidence that IFN-γ induced ROS prevented bacteria from escaping the phagosome and polymerizing host cell actin, two steps which are deemed necessary for intracellular replication and cell-to-cell spread of the infection (5, 9, 10, 45, 46) (see Figure 4.16). In this way IFN-γ may be able to contain bacteria in the toxic environment of the phagolysosome where macrophage defenses can more effectively eliminate them, while also controlling replication and intercellular spread of bacteria.

However, we cannot exclude the possibility that what we observe to be IFN-γ prevention of vacuolar escape is simply an increased frequency or speed of phagosome-lysosome fusion events that kills *Burkholderia* before it is capable of escaping the phagosome. However due to a similar phenotype with BSO treatment, which is not known to increase phagosome-lysosome fusion events, we believe that the effect is in fact a prevention of vacuolar escape due to ROS.

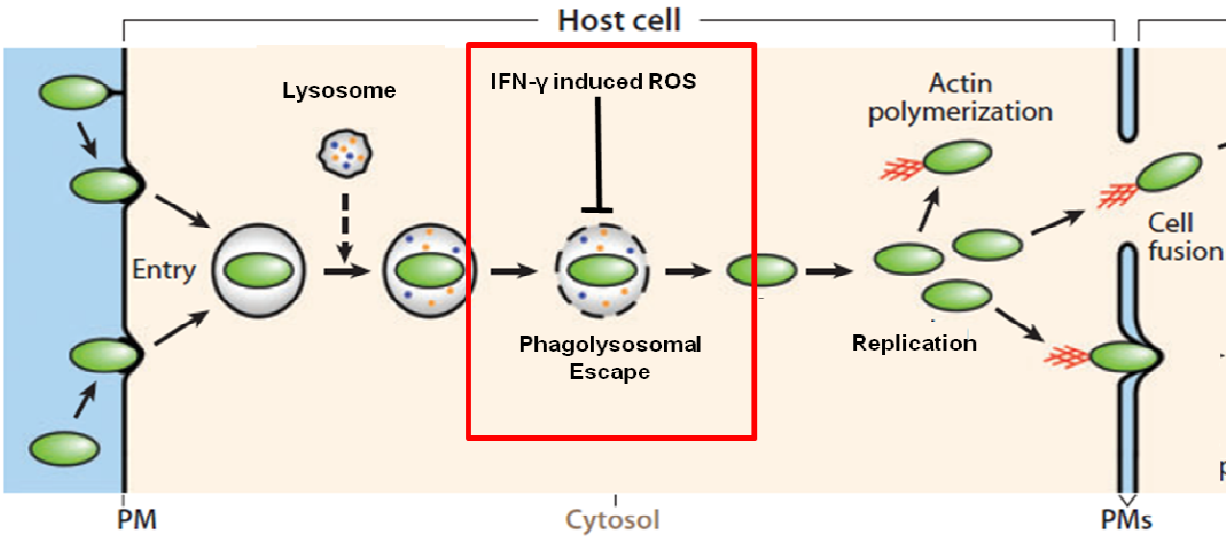

Figure 4.16: Diagram of major findings related to IFN-γ interference with *Burkholderia* intracellular lifestyle. IFN-γ induced ROS was shown to prevent phagolysosomal escape of bacteria due to lack of actin polymerization associated with bacteria in IFN-γ treated macrophages, as well as an increased proportion of bacteria co-localized with LAMP-1 in IFN-γ treated macrophages.

Furthermore, several other studies have shown a role for IFN-γ prevention of vacuolar escape in macrophages infected with other intracellular bacteria pathogens (47-49). Similar to our results, Myers et. al. showed that ROS inhibitors could partially reverse this IFN-γ effect, which is consistent with a ROS-mediated mechanism (49). Taken together, our results support an already established role for IFN-γ induced ROS to interfere with intracellular pathogen lifestyles.

Although we used high concentrations of NAC and GSH to reverse the synergistic effect, we do not believe that our concentrations were unreasonably high or physiologically irrelevant. Studies using NAC to enhance athletic performance in humans have used NAC infusions up to 150mg/kg (31). Additionally, NAC has been used in prevention and treatment of a number of health related problems at doses of up to 6 grams per day (50). Therefore, we believe that our highest concentration of 100 mM NAC is likely within the realm of achievable concentrations at

least in local environments. In most cells, GSH can range in concentration from 1-10 mM (36). Since we have seen that IFN-γ induces increased ROS production, we believe that 50 mM GSH, the highest concentration used in our studies, was a reasonable dose to scavenge and degrade the increased ROS produced due to IFN-γ.

There is strong evidence that IFN-γ treatment of macrophages can greatly increase killing of intracellular *B. pseudomallei* (51-55), however we show here that IFN-γ, by itself, has a negligible role in controlling intracellular bacterial burden. We believe this discrepancy can be easily explained by differences in macrophage infection models, in particular, the relative order and timing of IFN-γ stimulation to macrophage infection. We and others who pre-activate macrophages prior to infection have always seen a strong role for IFN-γ to increase antimicrobial responses and killing of intracellular bacteria (51-55), whereas the infection model used for the current study consisted of macrophage infection followed by activation by IFN-γ. While pre-activation with IFN-γ produces a clear advantage to study the specific antimicrobial effects of *fully* activated macrophages, it is likely that pre-activating macrophages in the absence of bacteria elicits a different antimicrobial response than macrophages activated in the presence of bacteria and IFN-γ (56).

We believe our system of infection, in which macrophages are infected and subsequently treated with IFN-γ might more closely mimic the timing in a natural infection by which a host is infected first and an immune response is mounted second. However, an obvious disadvantage of this infection model is that treatment of infected macrophages with IFN-γ has never elicited a strong killing effect on its own which makes it difficult to determine the mechanism behind any IFN-γ mediated antimicrobial responses. Fortunately, our current study focused on the mechanism of the *combination* of IFN-γ with ceftazidime which elicited an effect with large

enough magnitude to easily study. As to why IFN-γ stimulation doesn't control infection after macrophage infection, we suspect that by the time ROS is maximally induced by IFN-γ stimulation, the macrophages are already overwhelmed by the infection and so it becomes an issue of too little too late. However, even increased ROS due to BSO depletion of GSH was unable to increase IFN-γ stimulated intracellular killing without the presence of ceftazidime, which suggests a critical and perhaps underestimated role for ceftazidime in our infection model. After all, even though we have found IFN-γ induced ROS are an important component of the synergistic killing, ceftazidime is a very large component of that synergy that we did not focus on in this chapter. It is important to uncover the specific contributions of both ceftazidime and IFN-γ to the synergistic interaction and chapter 5 will address these points.

In the current study we have shown substantial evidence of a role for IFN-γ induced ROS responses to synergize with ceftazidime to control *B. pseudomallei* infection in macrophages. While there is a well documented role for IFN-γ induced RNS responses in the killing of *B. pseudomallei*, typically through induction of inducible nitric oxide synthase (iNOS) (18, 51, 54, 55, 57), far fewer studies support a role for IFN-γ induced ROS responses. Although less frequently evaluated, ROS responses have been implicated in control of *Burkholderia* infection in the past. For example, in vivo knock-out studies by Breitbach and colleagues showed that NADPH oxidase, but not iNOS, was important for controlling mortality during acute phase infection with *B. pseudomallei* (16). Furthermore, two studies have shown a role for IFN-γ induced ROS response control of bacterial burden during acute phase infection with *B. pseudomallei* (16, 18). Finally, connections between contraction of melioidosis and patients with chronic granulomatous disease, who lack a functional NADPH phagocyte oxidase, suggest a role for NADPH phagocyte oxidase generated ROS responses in protection of hosts (58, 59). While

the issue of IFN-γ induced antimicrobial mechanisms is inarguably complex, we believe there may be a role for both IFN-γ induced RNS and ROS responses which at least partially depends on the current activation state of the host immune cells at the time of initial infection.

In conclusion, we have shown that IFN-γ induced ROS can synergize with ceftazidime to increase intracellular killing of *Burkholderia*. The effect of IFN-γ to keep the bacteria in the phagolysosome and prevent their escape into the cytoplasm suggests that IFN-γ may inhibit further spread and replication of this intracellular pathogen. We believe our results show that IFN-γ induced ROS is a likely factor involved with preventing escape from the phagolysosome. Our results also suggest that pro-oxidant drugs that increase intracellular ROS responses may have similar antibiotic enhancing effects. Continuation of these studies on immuno-antimicrobial interactions may lead to discovery of alternative therapies for treating melioidosis which make use of pro-oxidant, ROS inducing drugs as non-specific enhancers of antibiotic activity to either speed recovery or decrease the physical and economical burden of intravenous antibiotic treatment.

REFERENCES

1. **Wuthiekanun V, Peacock SJ.** 2006. Management of melioidosis. Expert Rev Anti Infect Ther **4:**445-455.

2. **Limmathurotsakul D, Peacock SJ.** 2011. Melioidosis: a clinical overview. Br Med Bull **99:**125-139.

3. **Fisher DA, Harris PN.** 2013. Melioidosis: refining management of a tropical time bomb. Lancet.

4. **Jones AL, Beveridge TJ, Woods DE.** 1996. Intracellular survival of *Burkholderia pseudomallei*. Infect Immun **64:**782-790.

5. **Kespichayawattana W, Rattanachetkul S, Wanun T, Utaisincharoen P, Sirisinha S.** 2000. *Burkholderia pseudomallei* induces cell fusion and actin-associated membrane protrusion: a possible mechanism for cell-to-cell spreading. Infect Immun **68:**5377-5384.

6. **Stevens MP, Galyov EE.** 2004. Exploitation of host cells by *Burkholderia pseudomallei*. Int J Med Microbiol **293:**549-555.

7. **Chieng S, Carreto L, Nathan S.** 2012. *Burkholderia pseudomallei* transcriptional adaptation in macrophages. BMC Genomics **13:**328.

8. **French CT, Toesca IJ, Wu TH, Teslaa T, Beaty SM, Wong W, Liu M, Schroder I, Chiou PY, Teitell MA, Miller JF.** 2011. Dissection of the *Burkholderia* intracellular life cycle using a photothermal nanoblade. Proc Natl Acad Sci U S A **108:**12095-12100.

9. **Allwood EM, Devenish RJ, Prescott M, Adler B, Boyce JD.** 2011. Strategies for Intracellular Survival of *Burkholderia pseudomallei*. Front Microbiol **2:**170.

10. **Burtnick MN, DeShazer D, Nair V, Gherardini FC, Brett PJ.** 2010. *Burkholderia mallei* cluster 1 type VI secretion mutants exhibit growth and actin polymerization defects in RAW 264.7 murine macrophages. Infect Immun **78:**88-99.

11. **Burtnick MN, Brett PJ, Nair V, Warawa JM, Woods DE, Gherardini FC.** 2008. *Burkholderia pseudomallei* type III secretion system mutants exhibit delayed vacuolar escape phenotypes in RAW 264.7 murine macrophages. Infect Immun **76:**2991-3000.

12. **Galyov EE, Brett PJ, DeShazer D.** 2010. Molecular insights into *Burkholderia pseudomallei* and *Burkholderia mallei* pathogenesis. Annu Rev Microbiol **64:**495-517.

13. **Wiersinga WJ, van der Poll T, White NJ, Day NP, Peacock SJ.** 2006. Melioidosis: insights into the pathogenicity of *Burkholderia pseudomallei*. Nat Rev Microbiol **4:**272-282.

14. **Schweizer HP.** 2012. Mechanisms of antibiotic resistance in *Burkholderia pseudomallei*: implications for treatment of melioidosis. Future Microbiol **7:**1389-1399.

15. **Santanirand P, Harley VS, Dance DA, Drasar BS, Bancroft GJ.** 1999. Obligatory role of gamma interferon for host survival in a murine model of infection with *Burkholderia pseudomallei*. Infect Immun **67:**3593-3600.

16. **Breitbach K, Klocke S, Tschernig T, van Rooijen N, Baumann U, Steinmetz I.** 2006. Role of inducible nitric oxide synthase and NADPH oxidase in early control of *Burkholderia pseudomallei* infection in mice. Infect Immun **74:**6300-6309.

17. **Haque A, Easton A, Smith D, O'Garra A, Van Rooijen N, Lertmemongkolchai G, Titball RW, Bancroft GJ.** 2006. Role of T cells in innate and adaptive immunity against murine *Burkholderia pseudomallei* infection. J Infect Dis **193:**370-379.

18. **Miyagi K, Kawakami K, Saito A.** 1997. Role of reactive nitrogen and oxygen intermediates in gamma interferon-stimulated murine macrophage bactericidal activity against *Burkholderia pseudomallei*. Infect Immun **65:**4108-4113.

19. **Propst KL, Troyer RM, Kellihan LM, Schweizer HP, Dow SW.** 2010. Immunotherapy markedly increases the effectiveness of antimicrobial therapy for treatment of *Burkholderia pseudomallei* infection. Antimicrob Agents Chemother **54:**1785-1792.

20. **Brett PJ, Deshazer D, Woods DE.** 1997. Characterization of *Burkholderia pseudomallei* and *Burkholderia pseudomallei*-like strains. Epidemiol Infect **118:**137-148.

21. **DeShazer D, Brett PJ, Carlyon R, Woods DE.** 1997. Mutagenesis of *Burkholderia pseudomallei* with Tn5-OT182: isolation of motility mutants and molecular characterization of the flagellin structural gene. J Bacteriol **179:**2116-2125.

22. **Bosio CM, Dow SW.** 2005. *Francisella tularensis* induces aberrant activation of pulmonary dendritic cells. J Immunol **175:**6792-6801.

23. **Tulkens PM.** 1991. Intracellular distribution and activity of antibiotics. Eur J Clin Microbiol Infect Dis **10:**100-106.

24. **Webb C, Bedwell C, Guth A, Avery P, Dow S.** 2006. Use of flow cytometry and monochlorobimane to quantitate intracellular glutathione concentrations in feline leukocytes. Vet Immunol Immunopathol **112:**129-140.

25. **Slinker BK.** 1998. The statistics of synergism. J Mol Cell Cardiol **30:**723-731.

26. **Mujtaba MG, Patel CB, Patel RA, Flowers LO, Burkhart MA, Waiboci LW, Martin J, Haider MI, Ahmed CM, Johnson HM.** 2006. The gamma interferon (IFN-gamma) mimetic peptide IFN-gamma (95-133) prevents encephalomyocarditis virus infection both in tissue culture and in mice. Clin Vaccine Immunol **13:**944-952.

27. **Turco J, Winkler HH.** 1983. Cloned mouse interferon-gamma inhibits the growth of *Rickettsia prowazekii* in cultured mouse fibroblasts. J Exp Med **158:**2159-2164.

28. **Hemmi S, Peghini P, Metzler M, Merlin G, Dembic Z, Aguet M.** 1989. Cloning of murine interferon gamma receptor cDNA: expression in human cells mediates high-affinity binding but is not sufficient to confer sensitivity to murine interferon gamma. Proc Natl Acad Sci U S A **86:**9901-9905.

29. **Meister A.** 1995. Glutathione metabolism. Methods Enzymol **251:**3-7.

30. **Samuni Y, Goldstein S, Dean OM, Berk M.** 2013. The chemistry and biological activities of N-acetylcysteine. Biochim Biophys Acta **1830:**4117-4129.

31. **Kerksick C, Willoughby D.** 2005. The antioxidant role of glutathione and N-acetyl-cysteine supplements and exercise-induced oxidative stress. J Int Soc Sports Nutr **2:**38-44.

32. **Meister A.** 1988. Glutathione metabolism and its selective modification. J Biol Chem **263:**17205-17208.

33. **Kaplowitz N, Aw TY, Ookhtens M.** 1985. The regulation of hepatic glutathione. Annu Rev Pharmacol Toxicol **25:**715-744.

34. **Noctor G, Queval G, Mhamdi A, Chaouch S, Foyer CH.** 2011. Glutathione. Arabidopsis Book **9:**e0142.

35. **Foyer CH, Noctor G.** 2011. Ascorbate and glutathione: the heart of the redox hub. Plant Physiol **155:**2-18.

36. **Forman HJ, Zhang H, Rinna A.** 2009. Glutathione: overview of its protective roles, measurement, and biosynthesis. Mol Aspects Med **30:**1-12.

37. **Lu SC.** 2009. Regulation of glutathione synthesis. Mol Aspects Med **30:**42-59.

38. **Zhang H, Forman HJ.** 2012. Glutathione synthesis and its role in redox signaling. Semin Cell Dev Biol **23:**722-728.

39. **Griffith OW.** 1981. Depletion of glutathione by inhibition of biosynthesis. Methods Enzymol **77:**59-63.

40. **Meister A.** 1995. Glutathione biosynthesis and its inhibition. Methods Enzymol **252:**26-30.

41. **Armstrong JS, Steinauer KK, Hornung B, Irish JM, Lecane P, Birrell GW, Peehl DM, Knox SJ.** 2002. Role of glutathione depletion and reactive oxygen species generation in apoptotic signaling in a human B lymphoma cell line. Cell Death Differ **9:**252-263.

42. **Ault JG, Lawrence DA.** 2003. Glutathione distribution in normal and oxidatively stressed cells. Exp Cell Res **285:**9-14.

43. **Brodie AE, Reed DJ.** 1985. Buthionine sulfoximine inhibition of cystine uptake and glutathione biosynthesis in human lung carcinoma cells. Toxicol Appl Pharmacol **77:**381-387.

44. **Stevenson D, Wokosin D, Girkin J, Grant MH.** 2002. Measurement of the intracellular distribution of reduced glutathione in cultured rat hepatocytes using monochlorobimane and confocal laser scanning microscopy. Toxicol In Vitro **16:**609-619.

45. **Breitbach K, Rottner K, Klocke S, Rohde M, Jenzora A, Wehland J, Steinmetz I.** 2003. Actin-based motility of *Burkholderia pseudomallei* involves the Arp 2/3 complex, but not N-WASP and Ena/VASP proteins. Cell Microbiol **5:**385-393.

46. **Stevens MP, Wood MW, Taylor LA, Monaghan P, Hawes P, Jones PW, Wallis TS, Galyov EE.** 2002. An Inv/Mxi-Spa-like type III protein secretion system in *Burkholderia pseudomallei* modulates intracellular behaviour of the pathogen. Mol Microbiol **46:**649-659.

47. **Portnoy DA, Schreiber RD, Connelly P, Tilney LG.** 1989. Gamma interferon limits access of *Listeria monocytogenes* to the macrophage cytoplasm. J Exp Med **170:**2141-2146.

48. **Lindgren H, Golovliov I, Baranov V, Ernst RK, Telepnev M, Sjostedt A.** 2004. Factors affecting the escape of *Francisella tularensis* from the phagolysosome. J Med Microbiol **53:**953-958.

49. **Myers JT, Tsang AW, Swanson JA.** 2003. Localized reactive oxygen and nitrogen intermediates inhibit escape of *Listeria monocytogenes* from vacuoles in activated macrophages. J Immunol **171:**5447-5453.

50. **Kelly GS.** 1998. Clinical applications of N-acetylcysteine. Altern Med Rev **3:**114-127.

51. **Breitbach K, Wongprompitak P, Steinmetz I.** 2011. Distinct roles for nitric oxide in resistant C57BL/6 and susceptible BALB/c mice to control *Burkholderia pseudomallei* infection. BMC Immunol **12:**20.

52. **Breitbach K, Sun GW, Kohler J, Eske K, Wongprompitak P, Tan G, Liu Y, Gan YH, Steinmetz I.** 2009. Caspase-1 mediates resistance in murine melioidosis. Infect Immun **77:**1589-1595.

53. **Charoensap J, Utaisincharoen P, Engering A, Sirisinha S.** 2009. Differential intracellular fate of *Burkholderia pseudomallei* 844 and *Burkholderia thailandensis* UE5 in human monocyte-derived dendritic cells and macrophages. BMC Immunol **10:**20.

54. **Utaisincharoen P, Tangthawornchaikul N, Kespichayawattana W, Chaisuriya P, Sirisinha S.** 2001. *Burkholderia pseudomallei* interferes with inducible nitric oxide

synthase (iNOS) production: a possible mechanism of evading macrophage killing. Microbiol Immunol **45:**307-313.

55. **Utaisincharoen P, Anuntagool N, Arjcharoen S, Limposuwan K, Chaisuriya P, Sirisinha S.** 2004. Induction of iNOS expression and antimicrobial activity by interferon (IFN)-beta is distinct from IFN-gamma in *Burkholderia pseudomallei*-infected mouse macrophages. Clin Exp Immunol **136:**277-283.

56. **Mosser DM.** 2003. The many faces of macrophage activation. J Leukoc Biol **73:**209-212.

57. **Tangsudjai S, Pudla M, Limposuwan K, Woods DE, Sirisinha S, Utaisincharoen P.** 2010. Involvement of the MyD88-independent pathway in controlling the intracellular fate of *Burkholderia pseudomallei* infection in the mouse macrophage cell line RAW 264.7. Microbiol Immunol **54:**282-290.

58. **Renella R, Perez JM, Chollet-Martin S, Sarnacki S, Fischer A, Blanche S, Casanova JL, Picard C.** 2006. *Burkholderia pseudomallei* infection in chronic granulomatous disease. Eur J Pediatr **165:**175-177.

59. **Tarlow MJ, Lloyd J.** 1971. Melioidosis and chronic granulomatous disease. Proc R Soc Med **64:**19-20.

CHAPTER 5: THE ROLE OF COMPARTMENTALIZED KILLING IN IMMUNO-ANTIMICROBIAL SYNERGY AGAINST *BURKHOLDERIA*

SUMMARY

Burkholderia pseudomallei, the causative agent of melioidosis, is a facultative intracellular pathogen of phagocytes and non-phagocytes that causes severe infections in humans and animals. In chapter 4 we showed a role for IFN-γ induced ROS in the interaction of IFN-γ and ceftazidime which synergistically kills intracellular *Burkholderia*. In the present chapter we further extended our investigation into the specific and individual contributions of both IFN-γ and ceftazidime to the synergy. We first used fluorescent microscopy to show that IFN-γ treated macrophages appeared to control the intracellular bacterial burden, whereas ceftazidime treated macrophages did not. We therefore hypothesized that ceftazidime primarily controlled extracellular bacterial burden and IFN-γ primarily controlled intracellular bacterial burden. We next tracked extracellular numbers of bacteria during our macrophage infection and found a role for ceftazidime to control extracellular bacteria, an effect that was synergistically enhanced with co-treatment with IFN-γ. Using a macrophage-free bacteria killing assay we determined that ceftazidime alone kills *Burkholderia*, which meant that IFN-γ activated macrophages, but not IFN-γ itself, helps to control extracellular bacterial burden. We then studied these IFN-γ activated macrophages to show their ability to kill intracellular bacteria. We found no role of macrophages pre-treated with ceftazidime to reduce intracellular numbers, suggesting that IFN-γ alone controls intracellular bacterial burden. Taken together, our results suggest that the effects

of IFN-γ and ceftazidime treatment can be simplified to individual compartments, such that IFN-γ stimulates killing of intracellular *Burkholderia* and prevents further spread and replication, while ceftazidime kills extracellular bacteria, thereby reducing the pool of bacteria that can further infect healthy host cells. In summary, it is only with the combination of intracellular killing by IFN-γ induced ROS, and ceftazidime-mediated extracellular killing, that we see synergistic reductions in bacterial burden in the system as a whole as well as overall maintained health of the host cells.

INTRODUCTION

B. pseudomallei is a facultative intracellular pathogen and the causative agent of melioidosis, a severe and often life-threatening emerging infectious disease (1-3). *B. pseudomallei* is inherently resistant to many classes of antibiotics as well as host-derived antimicrobial defenses (4-8). Suggested treatment of melioidosis includes intravenous administration of either ceftazidime or meropenem for two weeks followed by an oral eradication therapy of trimethoprim and sulfamethoxazole for an additional three months (6, 9). However, even with antibiotic treatment, recurrent infections due to relapse are not uncommon (10-12). Therefore there is a critical need for new therapies which can enhance antibiotic efficacy or interfere with *Burkholderia* pathogenesis.

Burkholderia can infect and survive inside both phagocytes and non-phagocytes and its specific intracellular lifestyle is well characterized (13, 14). *Burkholderia* utilizes host microfilaments to facilitate its entry into vacuoles or phagosomes within minutes of contact with host cells (15-18). Bacteria then lyse the vacuole and escape into the host cell cytoplasm where

they replicate, polymerize host cell actin, and form MNGCs through induction of cell fusion and cell-to-cell spread (7, 15, 18, 19). Macrophages eventually rupture, releasing bacteria back into the extracellular space (15).

IFN-γ, which is obligatory for resistance to *Burkholderia* infection (20-23), has a well recognized role for activating macrophages to enhance killing of intracellular *Burkholderia* through either increased ROS or RNS (24, 25). Studies also show that IFN-γ is capable of interfering with the normal intracellular lifestyle of *Burkholderia* by almost completely preventing cell fusion and MNGC formation (26, 27). In chapter 4 we also showed that IFN-γ prevents bacterial escape from the phagolysosome. Taken together, there is a strong role for IFN-γ in the resistance to *Burkholderia* and control of infection.

In a previous study we showed that IFN-γ could interact with ceftazidime to synergistically reduce bacterial burden of *Burkholderia* inside infected macrophage and also protect mice from a lethal challenge with *B. pseudomallei* (28). Since IFN-γ is not known to have antimicrobial effects on its own, we suspected a role for IFN-γ activation of macrophages to synergize with ceftazidime. In chapter 4 we showed that IFN-γ induced ROS contributes to the mechanism of synergistic intracellular killing, but the role of ceftazidime in the synergy was still unknown. Here we expand our investigation to the individual contributions of both IFN-γ and ceftazidime to the synergistic killing and we further evaluate the role of ROS. We show that while IFN-γ and ceftazidime synergistically interact to reduce bacterial burden intracellularly, they also interact to reduce extracellular bacterial burden. Surprisingly, their effects seem to be compartmentalized to either the intracellular or extracellular effects, although killing in one compartment does affect the other. In the end, we propose a new model to describe the dynamics of our macrophage infection model which is consistent with our results.

MATERIALS AND METHODS

Biochemicals.

Ceftazidime hydrate, *N*-Acetyl-L-cysteine (NAC), and reduced L-Glutathione (GSH) were purchased from Sigma-Aldrich (St. Louis, MO). Other reagents included recombinant murine IFN-γ (Peprotech, Rocky Hill, NJ), Alexa Fluor 488 conjugated phalloidin (Life Technologies, Carlsbad, CA), ProLong Gold Anti-fade mounting media with DAPI (Life Technologies), rabbit polyclonal anti-*B. pseudomallei* antibody (provided by D. Waag from USAMRIID), and goat anti-rabbit secondary IgG antibody conjugated to Cy3 (Jackson ImmunoResearch Labs, West Grove, PA).

Bacteria.

B. thailandensis E264 was used in all studies (29). Bacteria were grown in trypticase soy broth (BD Biosciences, San Jose, CA) at 37°C with rotary shaking for 16 hours and stored at -80°C in 15% glycerol until needed. Mid-logarithmic phase bacteria were grown for approximately 3 hours with rotary shaking from a 1 to 25 dilution of an overnight culture until an optical density of 0.5-0.8 was reached.

Cell lines.

RAW 264.7 macrophages (ATCC, Manassas, VA) were maintained at 37°C with 5% CO_2 and used for all studies. Cell lines were grown and maintained in complete media (cMEM) consisting of minimum essential media (MEM; Life Technologies) supplemented with 10% fetal

bovine serum (Atlas, Fort Collins, CO), 0.075% sodium bicarbonate (Acros organics, NJ), 0.5x essential amino acids, 1x nonessential amino acids (Life Technologies, Carlsbad, CA), and 2 mM L-glutamine (Sigma-Aldrich). Penicillin (100 Units/ml) and Streptomycin (100 µg/ml) (Life Technologies) were added to media for maintenance of cell lines but all experiments were conducted in antibiotic-free cMEM.

Resting macrophage infection assay.

Macrophages were infected and treated as previously described (28). Briefly, macrophages were seeded into 24-well plates with antibiotic-free cMEM and allowed to adhere overnight. Macrophages were infected with *B. thailandensis* E264 at a multiplicity of infection of 5 for 1 hour followed by a 1 ml wash with phosphate buffered saline (PBS). High dose kanamycin monosulfate (Thermo Fisher Scientific, Waltham, MA) was then applied for 1 hour to kill extracellular bacteria. The MIC of kanamycin for *B. thailandensis* E264 is 128 µg/ml, and the concentration used to kill extracellular bacteria in this assay was 350 µg/ml (30). Macrophages were then washed twice with 2 mls PBS to remove kanamycin and dead bacteria and then incubated with IFN-γ (10 ng/ml), ceftazidime (10 µg/ml), or the combination of both treatments in cMEM for 18 hours. The MIC of ceftazidime for *B. thailandensis* E264 is 1.75 µg/ml (31). After the treatment period, cells were washed three times with 2 mls PBS and lysed with 1 ml sterile distilled water. Intracellular bacterial burden was quantified by plating serial dilutions of the lysates on Luria-Bertaini (LB) agar (BD Biosciences) followed by colony counts 24-48 hours later. In experiments aimed to determine synergy between IFN-γ and other antibiotics, the following antibiotics and concentrations were tested: piperacillin (10 µg/ml, 100 µg/ml), imipenem (1 µg/ml, 10 µg/ml), ciprofloxacin(0.1 µg/ml, 0.3 µg/ml), gentamicin (200

µg/ml), chloramphenicol (1 µg/ml, 3 µg/ml), doxycydine (1 µg/ml, 3 µg/ml), trimethoprim (0.1 µg/ml, 1 µg/ml). Single antibiotic titration studies were conducted on infected macrophages and the above antibiotic concentrations were chosen for synergy studies because they had a small or negligible effect on reducing intracellular bacterial burden compared to untreated controls. All of the antibiotic concentrations used to determine synergism with IFN-γ had less than a 2 $\log_{10}$ effect at controlling intracellular bacterial burden on their own. For experiments that aimed to quantitate extracellular bacteria numbers after the 18 hour treatment period, supernatants were first gently pipetted up and down to resuspend bacteria in wells without disturbing the adhered macrophages. Then extracellular bacteria were quantitated by plating serial dilutions of the supernatants onto LB agar, followed by colony counts 24-48 hours later.

Pre-activated macrophage infection assay.

In order to specifically study the intracellular antimicrobial effects of fully activated macrophages, we pre-activated adhered macrophages with IFN-γ (10 ng/ml) or pre-treated macrophages with ceftazidime (10 µg/ml) for 18 hours prior to infection. Following the 18 hour pre-treatment, macrophages were infected with *B. thailandensis* E264 at a multiplicity of infection of 5 for 30 minutes. Since we expected rapid killing of bacteria in IFN-γ pre-activated macrophages, the infection time was only 30 minutes (instead of the 1 hour infection we typically use for our resting macrophage infection assays) so that we could more quickly observe killing effects. Following the 30 minute infection, macrophages were washed once with 2 mls of PBS and high dose kanamycin monosulfate (350 µg/ml) was applied to kill extracellular bacteria for 1 hour. Macrophages were then washed twice with 2 mls of PBS and cMEM was applied to the macrophages for up to 6 hours. In order to ensure that only pre-treatment effects were

evaluated, no treatments were present during the infection nor the 6 hour assay length. When NAC (50 mM) or GSH (50 mM) were used in the pre-activated macrophage infection assay, these additional treatments were added for 3 hours prior to infection and washed off with 1 ml PBS prior to the infection. We used this timing of treatments to ensure that NAC and GSH additions would work to decrease the maximal production of ROS due to IFN-γ activation of macrophages. The length of the assay was shortened to 6 hours from the 18 hour resting macrophage infection assay because we expected rapid killing of intracellular bacteria. The use of the pre-activated macrophage infection assay helped determine how fully activated macrophages might react to intracellular pathogens when there is no lag-time for initiation of activation. Therefore, we used the pre-activated macrophage infection assay to help predict what might be occurring in our resting macrophage infection assay after full IFN-γ activation of the macrophages.

Extracellular bacteria killing assay.

In order to evaluate the effects of the treatments on bacterial killing alone, we used a bacterial killing assay consisting of only bacteria and treatments, and in the complete absence of macrophages. Our goal was to simulate the exact extracellular environment of our resting macrophage infection model but in the absence of macrophages. Therefore we used the same treatment concentrations (see below), the same media (cMEM) and volume of media in wells (500 µl), and the same incubation conditions and times (see below). Treatments were pre-prepared, diluted in cMEM, and added to 24-well plates at a total volume of 100 µl for treatments. Treatments were ceftazidime (10 µg/ml), IFN-γ (10 ng/ml), or GSH (10, 25, 50 mM)

or combinations of these treatments. Meanwhile, *B. thailandensis* was grown to mid-logarithmic phase from an overnight culture, diluted in cMEM, and 400 µls were added to the 24-well plate already containing the treatments. The initial density of bacteria was 1 x 10^7 CFU/well and a total of 500 µl was present in each well. Plates were incubated at 37°C with 5% CO_2 for 18 hours to simulate the same incubation conditions as our resting macrophage infection assay. After 18 hours, well contents were resuspended by slowly pipetting up and down, and surviving bacteria were enumerated by plating serial dilutions of well contents on LB agar and counting colonies after 24-48 hours.

Fluorescent microscopy.

RAW 264.7 resting macrophages were seeded onto chamber slides, infected and treated the same as in the resting macrophage infection assay, and after 12 hours were fixed with a 1 ml of a 2% paraformaldehyde solution for 20 minutes at room temperature. Cells were permeabilized with 1 ml of 0.1% triton-X in PBS for 5 minutes and subsequently incubated with a 1/15,000 dilution of rabbit anti-*Burkholderia* serum at 4°C overnight in the dark. Chamber slides were then blocked with a 0.5% solution of bovine serum albumin in PBS for 30 minutes at room temperature. Host cell actin was stained with phalloidin at 5 units/well in PBS for 30 minutes in the dark, followed by three 10 minute wash steps with PBS. Then a goat anti-rabbit IgG antibody conjugated to Cy3 was diluted 1/1000, added to the chamber slides, and incubated for 1 hour in the dark. After three 3 minute washes with room temperature PBS in the dark, the slides were left to dry and then nuclei were stained with 15 µl of DAPI-containing mounting media applied with the coverslip. Images were acquired with a Leica DM 4500B microscope (Leica Microsystems, Buffalo Grove, IL) fitted with a Retiga 2000R camera (QImaging, Surrey,

BC, Canada) and using QCapture Pro software (QImaging). Adobe Photoshop CS3 version 10.0.1 (Adobe, San Jose, CA) was used to create triple-color overlay images as well as make global manipulations to the linear parameters of black-point and individual color brightness for each image.

Primary bone marrow macrophage culture.

Bone marrow macrophages were generated as previously described (32). Femurs and tibias were aseptically removed from mice, transferred to 50 ml conical tubes containing Hank's buffered salt solution (HBSS) supplemented with 2% FBS, and kept on ice. In a biosafety cabinet, bones were cleaned of tissue and bone marrow was flushed from the bones using needles and syringes filled with HBSS and supplemented with 2% FBS. Bone marrow was gently resuspended with gentle pipetting and passed through a 70 µm nylon filter (BD Biosciences Pharmingen, San Jose, CA). Cells were centrifuged at 1200 rpm for 5 minutes at 4°C. Then supernatant was removed and red blood cells were lysed using 2 ml of ammonium-chloride-potassium (ACK) lysis buffer for 5 minutes, followed immediately by 20 mls of complete MEM with antibiotics and 10% L929-conditioned supernatants to dilute the lysis buffer. Cells were again spun at 1200 rpm for 5 minutes at 4°C. Remaining white blood cells were plated in 24-well plates at a concentration of 2×10^6 cells/ml in complete MEM. Cells were allowed to adhere to 24-well plates for 3 hours at 37°C and 5% CO_2 after which, non-adhered cells were washed away three times with room-temperature HBSS supplemented with 2% FBS. Complete media with antibiotics and 10% L929 conditioned media was reapplied to the cells and plates were returned to the incubator. Addition of 10% L929-conditioned media provided necessary

growth factors for differentiation of bone marrow myeloid progenitor cells into the macrophage/monocyte lineage. Adherent cells were incubated at 37^{o}C and 5% CO_2 until macrophages reached moderate confluency in wells (approximately 8-12 days).

Statistical analyses.

Unless otherwise noted, all data is represented by the mean +/- standard error of the mean (SEM). Means, SEM, and P-values were determined and plotted using Prism software version 5.00 (GraphPad, La Jolla, CA). A two-tailed Student's t-test was used to determine statistically significant differences between two groups. For comparisons of three or more groups, the one-way analysis of variance (ANOVA) was used followed by Tukey's post test for multiple comparisons. Grouped data was analyzed by two-way ANOVA and statistical synergy was determined as before (33) from the interaction P-value of a two-way ANOVA. The term synergy describes an interaction between two drugs which is greater than either drug alone or the additive effects of the drugs combined. It is determined statistically by comparing the untreated group, both single treatment groups, and the combination treatment group. All differences were considered statistically significant for $P < 0.05$.

RESULTS

IFN-γ synergizes with other bactericidal antibiotics to kill intracellular *Burkholderia*. Our previous investigations of immuno-antimicrobial therapy have focused solely on the ability of the antibiotic ceftazidime to synergize with IFN-γ (28). We explored

interactions between IFN-γ and other antibiotics in our macrophage infection model and found a surprising ability of sub-therapeutic bactericidal but not bacteriostatic antibiotics to similarly synergize with IFN-γ to reduce intracellular bacterial burden (R. Troyer and S. Dow, data unpublished). Furthermore, the synergistic effect with IFN-γ broadly encompassed several classes of bactericidal antibiotics including cephalosporins, penicillins, carbapenems, fluoroquinolones, and aminoglycosides, many of which *B. pseudomallei* are resistant to alone (results summarized in Table 5.1). We also observed immuno-antimicrobial synergy in macrophages infected with *E. coli* (A. Melia, K. Mosovsky, and S. Dow, data not shown). These results imply that immuno-antimicrobial synergy between IFN-γ and antibiotics is widely observed over several classes of bactericidal antibiotics and may be relevant to other Gram negative intracellular pathogens.

Table 5.1: IFN-γ synergizes with bactericidal antibiotics.

Antibiotic	Drug Class	Static/Cidal	Synergy?
Ceftazidime	Cephalosporin	Cidal	Yes
Piperacillin	Penicillin	Cidal	Yes
Imipenem	Carbapenem	Cidal	Yes
Ciprofloxacin	Fluoroquinolone	Cidal	Yes
Gentamicin	Aminoglycoside	Cidal	Yes
Chloramphenicol	Phenicol	Static	No
Doxycycline	Tetracycline	Static	No
Trimethoprim	DHFR inhibitor	Static	No

Ceftazidime does not control intracellular replication of *Burkholderia*. Previous studies had shown that IFN-γ played a major role in controlling intracellular replication of *Burkholderia*. Microscopy of RAW 264.7 infected cells visually confirmed that these IFN-γ

effects were reproduced with its combination with ceftazidime, but not by ceftazidime alone (Figure 5.1). Untreated macrophages formed large multinucleated giant cells (MNGC), with large hubs of densely replicating bacteria. Bacteria around the edges of the MNGC had polymerized actin tails, signifying their attempt to spread to neighboring cells. The macrophages and bacteria in the ceftazidime-treated group looked very similar, however, any group treated with IFN-γ appeared much different. We confirmed the lack of actin polymerization in IFN-γ treated cells that we had seen before, and also observed a lack of MNGC from both IFN-γ treated groups. It appeared that without MNGC formation, IFN-γ treated macrophages appeared to have been able to control the intracellular infection much better than untreated controls or ceftazidime treatment (Figure 5.1). Noting the similarities of appearance between ceftazidime and untreated controls, we hypothesized that the main contribution of ceftazidime to the synergism must be entirely through extracellular killing, while the role of IFN-γ may be more focused on intracellular control of bacterial burden. We first conducted experiments to determine the specific contribution of ceftazidime extracellular control of bacterial burden.

Ceftazidime primarily controls extracellular bacterial burden. We first analyzed the ability of ceftazidime to control extracellular replication of *Burkholderia* during the macrophage infection. We were surprised to find that ceftazidime appeared to play a role in controlling extracellular bacterial burden during macrophage infection (Figure 5.2A). We were also surprised to show that while IFN-γ had no effect on extracellular bacterial burden itself, it significantly enhanced the ceftazidime effect to control extracellular bacteria. This result prompted us to investigate whether IFN-γ increased antibiotic killing or could kill bacteria itself.

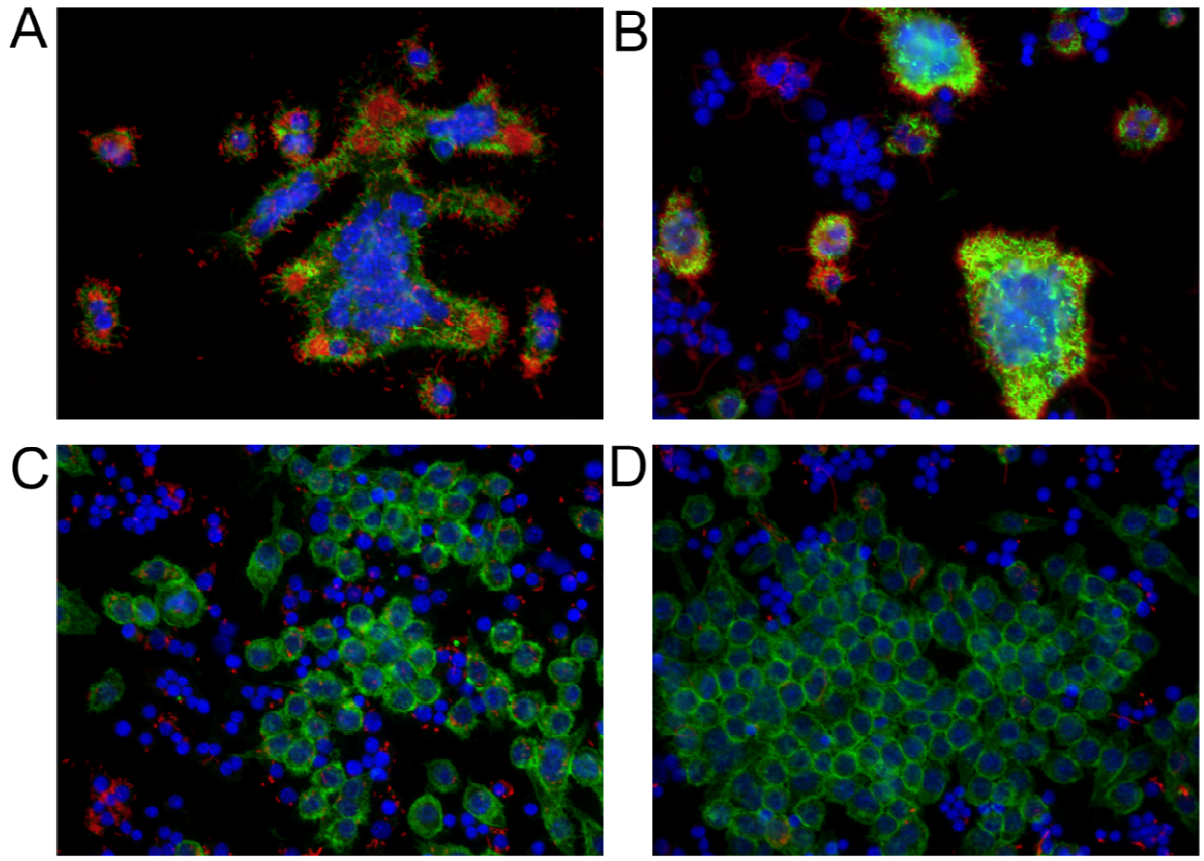

Figure 5.1: IFN-γ alone controls intracellular replication of *Burkholderia*. RAW 264.7 macrophages were infected with *B. thailandensis* for 1 hr and subsequently treated for 12 hrs with (A) no treatment, (B) ceftazidime (10 μg/ml), (C) IFN-γ (10 ng/ml), or (D) the combination of ceftazidime and IFN-γ. Cells were then fixed, permeabilized, and stained with phalloidin to identify host cell actin (green), DAPI to stain nuclei (blue) and anti-*Burkholderia* serum followed by a secondary antibody conjugated to Cy3 to identify *B. thailandensis* (red). Images were captured at 40x magnification and are representative of at least two independent experiments. The blue nuclei which are not associated with green actin filaments are thought to be dead or dying cells due to *B. pseudomallei* toxicity (19, 34, 35), since the loss of filamentous actin precedes cell death (36).

In our extracellular bacteria killing assay we reproduced the same in vitro culture conditions, this time in a macrophage-*free* system (see Materials and Methods), and found that ceftazidime alone killed *B. thailandensis* cultures (Figure 5.2B). IFN-γ had no bactericidal effects alone and did not significantly increase killing due to ceftazidime.

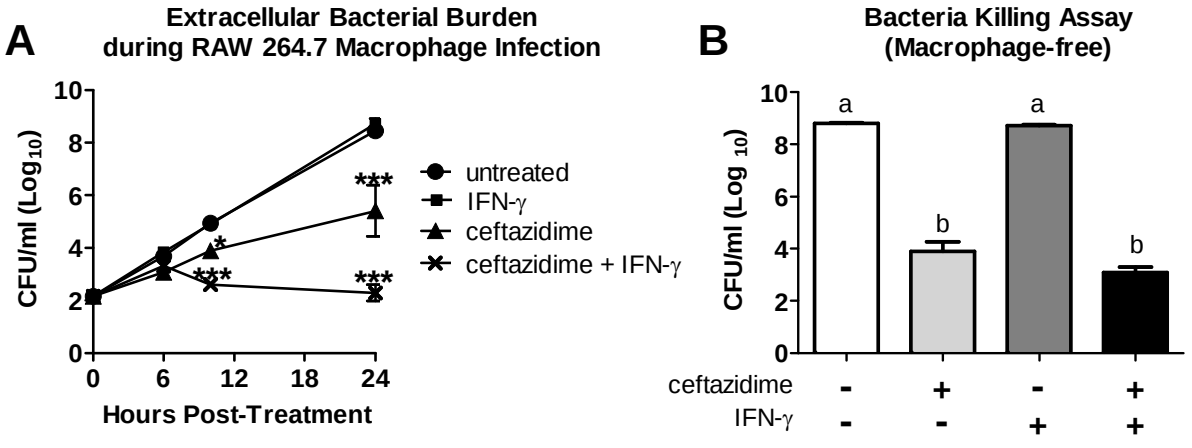

Figure 5.2: Ceftazidime primarily controls extracellular bacterial burden. (A) RAW 264.7 cells were infected with *B. thailandensis* and treated for 24 hours with IFN-γ (10 ng/ml), ceftazidime (10 µg/ml), or the combination of ceftazidime and IFN-γ. During the macrophage infection, extracellular bacterial burden was assessed at 0, 6, 10, and 24 hrs post-treatment by plating serial dilutions of well supernatants (see Materials and Methods for more details). Significant differences were assessed at all time points by two-way repeated measures ANOVA and compared to untreated control (*P < 0.05, ***P < 0.001). (B) *B. thailandensis* was treated with ceftazidime (10 µg/ml), IFN-γ (10ng/ml) or the combination of ceftazidime and IFN-γ for 18 hours in the absence of macrophages. Surviving bacteria were enumerated by plating dilutions of remaining bacteria after 18 hrs of treatment. Significant differences were assessed by one-way ANOVA, a > b (P < 0.0001). Both graphs are representative of two independent experiments with treatment groups run in triplicate or quadruplicate.

This meant that the IFN-γ enhanced antibiotic effect to reduce extracellular bacterial numbers, seen in Figure 5.2A, must have been due to IFN-γ activation of macrophages, and not IFN-γ itself. Taken together these results show that ceftazidime primarily kills extracellular bacteria in our macrophage infection model, though IFN-γ activation of macrophages can contribute to reduction of extracellular numbers. We had previously shown that IFN-γ and ceftazidime can interact synergistically to control intracellular bacterial burden, but we had also just shown a synergistic interaction to control extracellular bacterial burden.

IFN-γ, but not ceftazidime, kills intracellular *Burkholderia* and prevents intracellular replication. After showing that ceftazidime primarily controls extracellular bacterial burden we began to suspect that the role of IFN-γ and IFN-γ induced ROS may be strictly intracellular control of bacteria. To investigate this hypothesis, we turned to a pre-activated macrophage infection model to determine the intracellular killing power of macrophages fully activated by IFN-γ. Shortening the assay to 6 hrs instead of 18 hrs enabled us to more accurately describe killing in the intracellular compartment without confounding by extracellular bacteria. Macrophages were pre-activated with IFN-γ for 18 hours and then infected with *B. thailandensis* (see Materials and Methods for further details). Bacteria that had been taken up into the intracellular compartment during the initial infection were steadily killed over the entire 6 hr assay (Figure 5.3A). Conversely, *Burkholderia* actually replicated inside untreated macrophages over the 6 hours. This result clearly showed that IFN-γ activation of macrophages could induce killing responses to control intracellular killing and prevent replication. The difference in intracellular bacteria numbers at time T = 0 between untreated and pre-activated macrophages was likely due to the 1.5 hour time lapse between the start of infection and the start of the 6 hour experiment. We suspect that *Burkholderia* invaded untreated and pre-activated macrophages equally, but pre-activated macrophages likely began killing bacteria immediately after infection and throughout the 1 hour kanamycin step (see Materials and Methods), leading to the small, but significant difference in intracellular burden at time T = 0.

We next evaluated the ability of ceftazidime to control intracellular bacterial burden. Microscopy images of infected macrophages showed that ceftazidime didn't appear to play a major role in control of intracellular bacteria numbers (Figure 5.1).

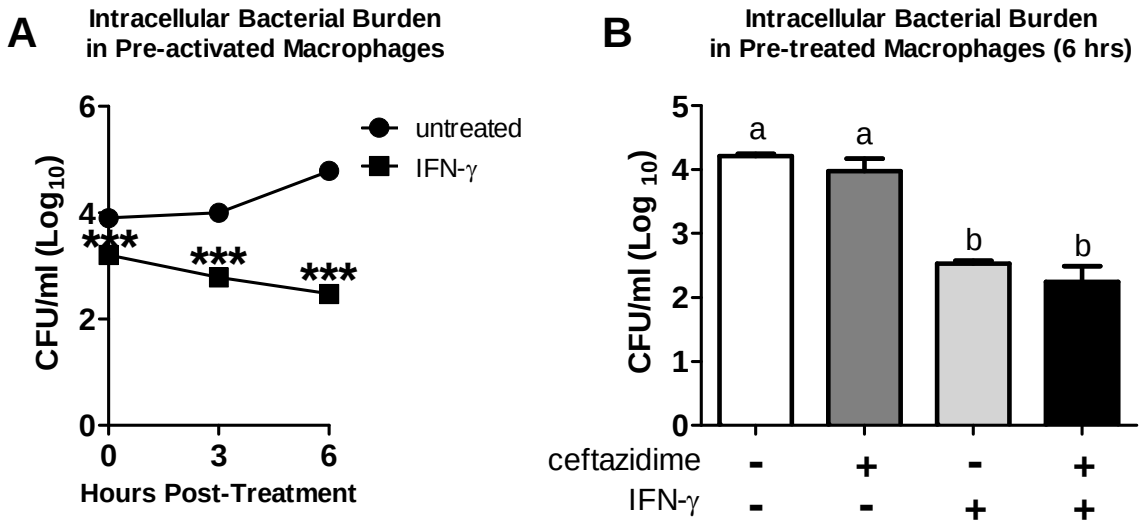

Figure 5.3: IFN-γ alone kills intracellular bacteria and prevents replication. (A-B) RAW 264.7 macrophages were pre-activated with IFN-γ (10 ng/ml) or pre-treated with ceftazidime (10 µg/ml) for 18 hrs prior to infection with *B. thailandensis*. At indicated times lysates were plated to enumerate surviving intracellular bacteria. (A) Time course of intracellular killing due to pre-activation with IFN-γ prior to infection. Significant differences compared to untreated control were assessed at each time point by two-way ANOVA (***P < 0.001). (B) Intracellular bacterial burden after 6 hours of infection. Statistical differences were assessed by one-way ANOVA, a > b (***P < 0.0001). Both graphs are representative of two independent experiments run in triplicate or quadruplicate.

Furthermore, we had previously found that whole cell intracellular concentrations of ceftazidime (either alone or without IFN-γ stimulation) were more than 50 fold below the MIC of ceftazidime (R. Troyer and S. Dow, unpublished data). However, if ceftazidime was taken up into specific compartments, the localized concentration of ceftazidime could be much higher. To determine the contribution of ceftazidime to intracellular killing, we pre-treated macrophages for 18 hours with IFN-γ (as before), or ceftazidime, or the combination of both drugs. We then removed all treatments and infected the macrophages with *B. thailandensis*. After 6 hours we lysed the macrophages and determined surviving bacteria by plating dilutions of lysates onto LB agar. Only macrophages pre-treated with IFN-γ showed intracellular killing of *Burkholderia*

during the 6 hour assay (Figure 5.3B). Macrophages pre-treated with ceftazidime were both unable to control intracellular bacterial burden and unable to enhance the killing effect seen with IFN-γ activation. These results suggest that over 18 hours ceftazidime is unable to accumulate in macrophages to an extent that could reduce bacterial numbers. Taken together these results support a role for IFN-γ but not ceftazidime in contributing to killing in the intracellular compartment.

IFN-γ induced ROS kills intracellular bacteria. We had now shown a role for ceftazidime to kill extracellular bacteria and a role for IFN-γ to kill and prevent replication of intracellular bacteria. However we had not specifically investigated the role for ROS in either of these compartments. In chapter 4 we had shown that IFN-γ induced ROS responses were involved in the mechanism of immuno-antimicrobial synergy by showing that antioxidants NAC and GSH could reverse the synergistic intracellular killing. However, now that we had gained an appreciation of the role for compartmentalized killing in the immuno-antimicrobial synergy, we began to speculate whether NAC and GSH were specifically reversing the IFN-γ intracellular killing, the ceftazidime extracellular killing, or both. Or in other words, was ROS important for the IFN-γ effect, the ceftazidime effect, or both?

We first evaluated the role of ROS in IFN-γ activated macrophages. We showed that antioxidants NAC and GSH could both partially reverse the intracellular killing of *Burkholderia* due to IFN-γ-activated macrophages (Figure 5.4). Furthermore, using the bone marrow macrophages from phox$^{-/-}$ mice, which lack a functional NADPH phagocyte oxidase, we showed that synergy between ceftazidime and IFN-γ was partially reversed in these mice compared to the

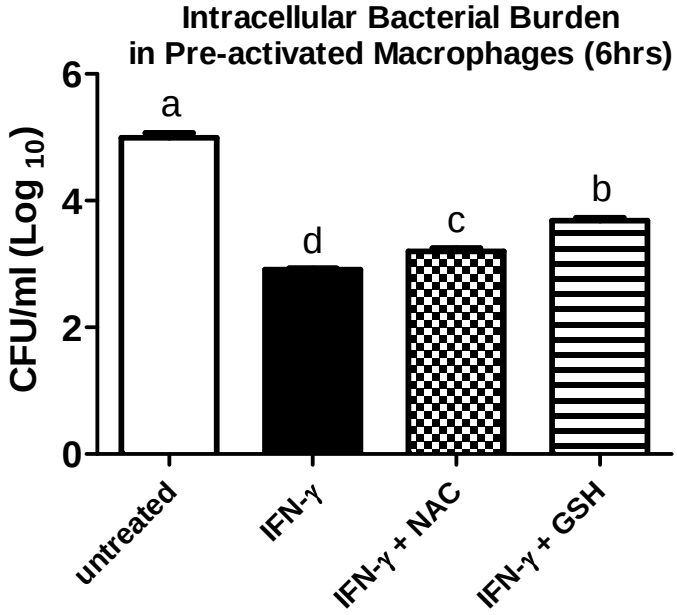

Figure 5.4: IFN-γ mediated intracellular killing is partially dependent on ROS. RAW 264.7 macrophages were pre-activated with IFN-γ (10 ng/ml) for 18 hrs and treated with NAC (50 mM) or GSH (50 mM) for the last 3 hrs of the pre-treatment period. Treatments were then washed away and macrophages were infected with *B. thailandensis*. Intracellular bacterial burden was assessed 6 hours after MEM was reapplied to macrophages by plating serial dilutions of lysates (see Materials and Methods for more details). $a > b > c > d$ ($P < 0.05$). Data is representative of two independent experiments run in quadruplicate.

C57BL/6 background-matched controls (Figure 5.5). Taken together, these results suggest a partial role for ROS in the mechanism of IFN-γ mediated killing of intracellular bacteria.

GSH reverses ceftazidime killing of bacteria. After showing only a partial role for GSH to reverse IFN-γ mediated intracellular killing, we were especially interested in whether or not GSH could reverse ceftazidime mediated extracellular killing.

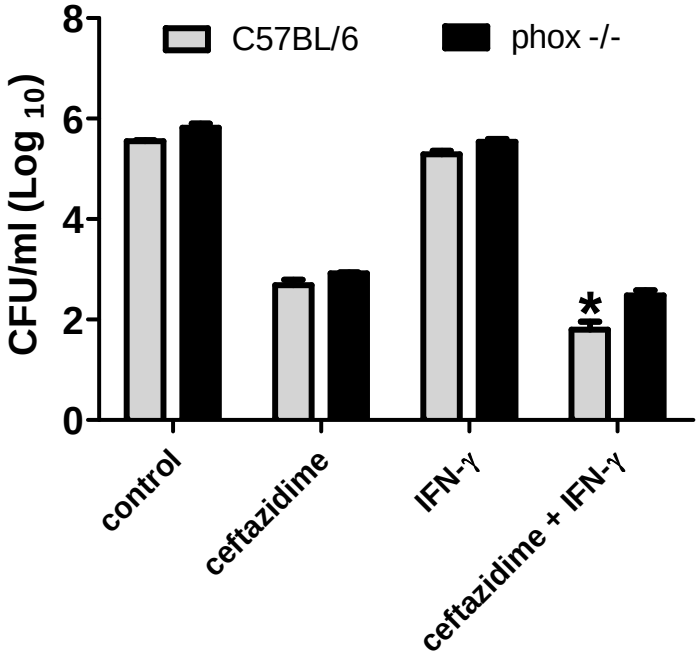

Figure 5.5: IFN-γ induced ROS kills intracellular *Burkholderia*. Resting bone marrow macrophages from C57BL/6 or phox KO mice were infected with *B. thailandensis* for 1 hr and subsequently treated with ceftazidime (3 μg/ml) or IFN-γ (10 ng/ml) for 18 hrs. Cell lysates were then plated to determine remaining intracellular bacteria burden. Synergy between IFN-γ and ceftazidime was determined separately for C57BL/6 macrophages and phox $^{-/-}$ macrophages. Statistically synergistic interactions were assessed by two-way ANOVA (*P = 0.0164).

In our macrophage-free bacteria killing assay, we showed that GSH reversed ceftazidime mediated killing in a dose-dependent manner, with complete reversal of killing at 100 mM (Figure 5.6). Although we do not suspect that this result implies that the mechanism of ceftazidime killing is ROS-mediated, further investigation into the mechanism of this reversal is required to fully understand this effect. Taken together, these results with GSH reversal of both IFN-γ and ceftazidime mediated killing in separate compartments, suggests a dual role for this antioxidant to interfere with immuno-antimicrobial synergy either through scavenging IFN-γ induced ROS, or by some yet unknown mechanism of interference with ceftazidime killing.

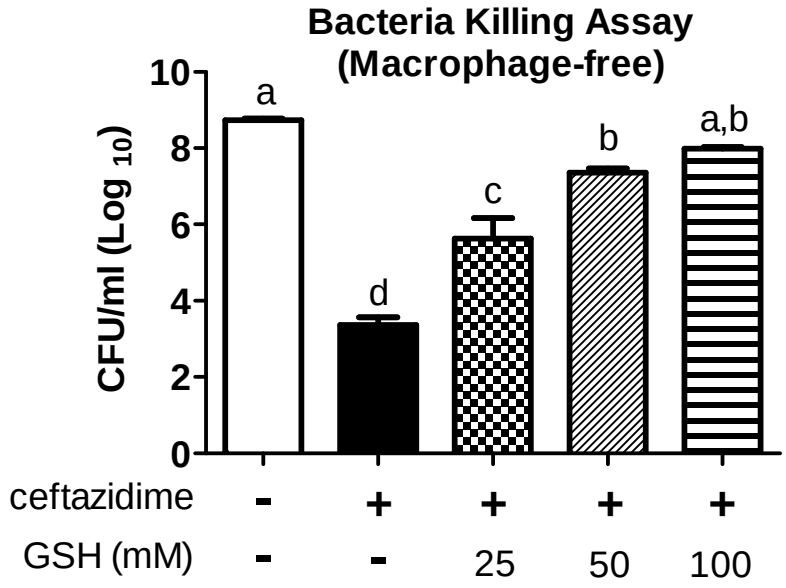

Figure 5.6: GSH reverses ceftazidime killing of *Burkholderia*. *B. thailandensis* was incubated for 18 hours with ceftazidime (10 µg/ml) with or without GSH in a macrophage-free bacteria killing assay. Surviving bacteria were enumerated by plating dilutions of remaining bacteria in wells. Significant differences were assessed by one-way ANOVA, a > b > c > d ($P < 0.05$). Graph is representative of two independent experiments with treatment groups run in triplicate or quadruplicate.

DISCUSSION

We have shown previously that IFN-γ synergizes with ceftazidime to control intracellular bacterial burden from *Burkholderia* infected macrophages as well as protect mice from lethal infection with *Burkholderia* (28). In chapter 4 we showed that IFN-γ induced ROS was essential for the synergy observed between IFN-γ and ceftazidime, and furthermore, that this ROS response prevented vacuolar escape of *Burkholderia*. In the present chapter we expanded on the individual contributions of both ceftazidime and IFN-γ to the synergistic interaction. We show that while IFN-γ and ceftazidime synergistically interact to reduce bacterial burden intracellularly, we also show that they synergistically interact to reduce extracellular bacterial

burden. We found that each drug contributes primarily to control of bacterial numbers in either the extracellular or intracellular compartment, but also that numbers of bacteria in one compartment can impact the other compartment.

We first discovered that other bactericidal, but not bacteriostatic, antibiotics were capable of interacting with IFN-γ to synergistically reduce bacterial burden inside infected macrophages. This result showed that immuno-antimicrobial synergy is a broadly observed interaction with other classes of bactericidal antibiotics. We then showed that ceftazidime primarily controls the extracellular bacterial burden in our macrophage infection model. Through experiments that measured extracellular bacterial burden either with or without the presence of infected macrophages (Figure 5.2), we showed that ceftazidime was responsible for the reduced extracellular bacteria numbers. We showed that IFN-γ activated macrophages, but not IFN-γ itself, only contributed to enhanced reduction of extracellular bacterial burden when ceftazidime was present. Although we have speculated that IFN-γ induced ROS may cross the membrane and interact with ceftazidime in the extracellular environment, we have already taken steps towards confirming a lack of interaction between ceftazidime and ROS in the extracellular compartment. We combined supernatants from IFN-γ activated macrophages with ceftazidime, in a modified and shortened bacteria killing assay, and found no evidence of interaction resulting in increased control of bacterial burden (Figure A9). Although supernatants from IFN-γ activated *and infected* macrophages may combine with ceftazidime to increase control of bacterial burden, we suspect that this is not the case, since there was no effect and not even a trend for an effect in Figure A9 using uninfected cells. Therefore, we suggest that the IFN-γ activated macrophage ability to contribute to ceftazidime control of extracellular bacterial burden

is specifically due to IFN-γ prevention of replication, cell-to-cell spread, or decreased macrophage lysis.

We then showed that IFN-γ activated macrophages killed intracellular *Burkholderia* and also prevented intracellular replication, while ceftazidime pre-treated macrophages were unable to significantly control intracellular bacterial burden. IFN-γ also appeared to inhibit cell-to-cell spread of infection in microscopy images of *Burkholderia* infected macrophages. In these three ways, it is clear that IFN-γ, and IFN-γ alone, controlled intracellular bacterial burden. We also observed a partial reversal of the IFN-γ mediated killing effect of IFN-γ activated macrophages owing to NAC or GSH, suggesting a partial role for ROS in the IFN-γ mediated killing of intracellular *Burkholderia*.

Our results enable us to present a novel model to describe the dynamics of the macrophage infection assay (Figure 5.7). In the absence of antibiotic, extracellular bacteria replicate and are a source for further infection of macrophages. In the absence of IFN-γ, and more specifically IFN-γ induced ROS, intracellular replication and cell-to-cell spread both go unchecked and eventually high bacteria numbers may rupture the macrophages, spilling back into the extracellular compartment. Therefore we predict there is some level of constant exchange of bacteria between the intracellular and extracellular compartments which makes the control of one compartment's killing inadequate to reduce overall numbers in the system as a whole. It is only when both extracellular and intracellular bacteria numbers are controlled simultaneously that the synergistic interaction is achieved. This explanation also clarifies why bacteriostatic antibiotics were not synergistic with IFN-γ.

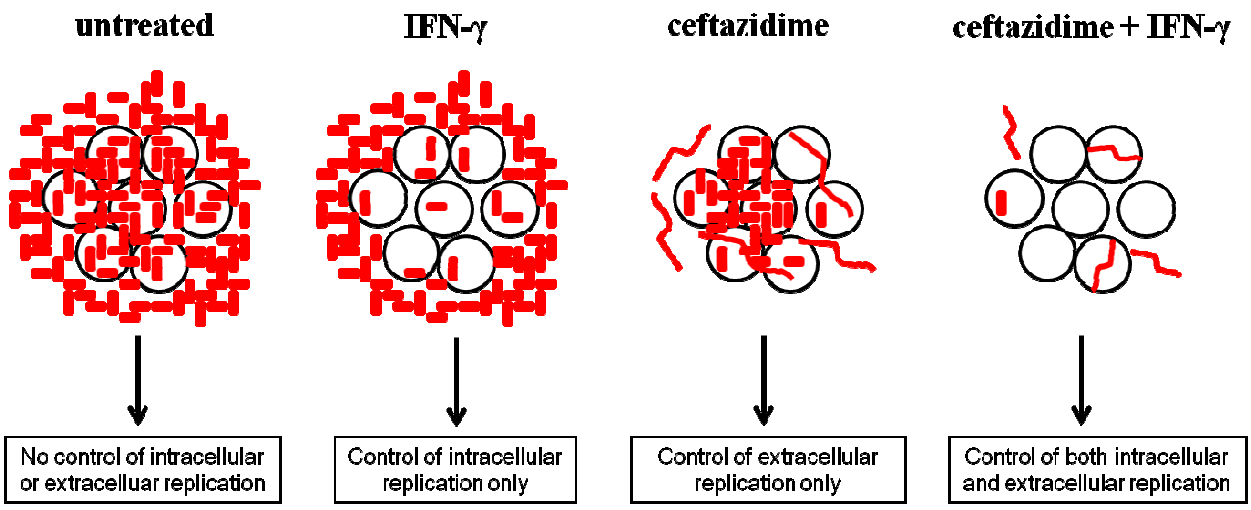

Figure 5.7: Compartmentalized killing describes the mechanism of synergy between IFN-γ and ceftazidime. During the macrophage infection assay there is a constant exchange between bacteria in the intracellular and extracellular compartments through invasion *into* cells and eventual rupture *out*. Therefore it is only with IFN-γ control of intracellular spread and replication, combined with ceftazidime control of extracellular bacterial burden, that synergy is achieved with low bacterial burden in the system as a whole. Filamentous bacteria are shown in ceftazidime and ceftazidime + IFN-γ treatment groups as seen in our actual macrophage infection assay. Although filamentous bacteria account for a significant proportion of remaining bacteria in the combination therapy treated macrophages, their role is undetermined as of now. Further experimentation will be required to determine their role in our macrophage infection assay (see Chapter 6 for suggested future experiments).

We believe our data suggest that there is no interaction between IFN-γ induced ROS and ceftazidime in the same compartment and instead, compartmentalized killing can completely explain the observed synergism. Ceftazidime would have to be taken up into the cell for a drug interaction to occur in the intracellular compartment. We had previously determined intracellular concentrations of ceftazidime to be around 50 fold lower than the MIC. To confirm that low levels of ceftazidime didn't have a role in enhancing IFN-γ mediated killing, we showed that any ceftazidime that *was* taken up during the 18 hour pre-treatment of macrophages was not sufficient to control intracellular bacteria on its own or enhance the IFN-γ effect (Figure 5.3B). It is unlikely that IFN-γ induction of ROS responses could be enhancing the ceftazidime killing

of extracellular bacteria during the macrophage infection since H_2O_2 is typically degraded before it can significantly accumulate across a membrane (37). But to confirm this theory, we showed that IFN-γ had no direct role in extracellular killing (Figure 5.2B) and supernatants from IFN-γ activated macrophages were unable to interact with ceftazidime to reduce bacteria (Figure A9).

In chapter 4 we had shown a strong role for IFN-γ induced ROS in the synergistic control of intracellular bacterial burden between IFN-γ and ceftazidime. It may seem a contradiction then, that in this chapter we show that IFN-γ pre-activated macrophages kill intracellular bacteria and yet we only show a minor role for ROS in the mechanism of this killing. We believe differences in timing between infection and IFN-γ activation may account for the observed difference in the contribution of ROS. For example, when resting macrophages are stimulated with both *Burkholderia* and treatments around the same time we see that IFN-γ induced ROS are critical for synergy owing to complete reversal of intracellular control of bacterial burden with addition of antioxidants. In contrast, when we pre-activate macrophages first, with 18 hours of IFN-γ stimulation, and subsequently infect with *Burkholderia*, we see only a small reversal of the IFN-γ killing with antioxidants, suggesting only a small role for ROS as the mechanism of killing.

One explanation for the observed deficiency of ROS mediated killing in the pre-activation model may be that IFN-γ activation in the absence of bacterial stimulation elicits a different degree of ROS response than simultaneous co-activation. This explanation is supported by other studies which have similarly shown differences in the types or degrees of macrophage responses between macrophages pre-activated with cytokines alone versus macrophages simultaneously activated with cytokines and pathogens (38-40). Furthermore, in our pre-activation studies, we imagine that any NAC and GSH taken up during the 3 hour incubation is

likely used immediately to scavenge ROS or serve other antioxidant roles. We predict that a more robust ROS response *is* elicited after bacterial infection of the pre-activated macrophages and that the ROS *does* significantly contribute to the observed time-dependent killing of intracellular *Burkholderia*, however there are no longer sufficient antioxidants available to reverse the killing and show the strong role for ROS. Another likely explanation for the discrepancy between the role of ROS between the two models of infection, is that in the first model, GSH addition to the combination therapy probably reversed some of the ceftazidime mediated extracellular killing. This would allow the extracellular pool of bacteria to replicate unchecked and infect more healthy cells, which could help explain the apparently high role of ROS.

In this chapter we showed that GSH completely reversed ceftazidime-mediated killing in a macrophage-free bacteria killing assay. One explanation for this effect is that GSH interfered with the common mechanism of antibiotic killing involving ROS generation in bacteria (41-45). However, several recent studies show strong evidence against a ROS-dependent mechanism of antibiotic killing (46-48). Additionally, one study specifically showed that exogenous glutathione could protect *E. coli* against bactericidal antibiotics as well as bacteriostatic antibiotics which do not induce oxidative stress, suggesting that the protection afforded by GSH extends past a purely ROS-scavenging role (49). Studies show that other antioxidants such as ascorbic acid are also capable of protecting against antibiotic killing, suggesting a broader protective effect (50, 51). Taken together these results suggest that it is unlikely that GSH, in our study, interfered with a ROS-mediated killing mechanism of ceftazidime.

One possible explanation for the GSH effect of inhibiting antibiotic killing is that GSH has in some way blocked antibiotic activity, either through direct reaction and inactivation or

through conjugation. Perhaps the best way to show whether GSH blocks antibiotic activity would be to pre-treat bacteria with high doses of GSH first, wash cells, and then add antibiotics. In this way, bacteria would be pre-loaded with the antioxidant, and ceftazidime would be unable to directly interact with it. One study has already conducted a similar study in *E. coli* and has shown that pre-treatment of *E. coli* with GSH or ascorbic acid did not protect bacteria against subsequent treatment with streptomycin, suggesting that GSH must be present with the antibiotic to exert its protective effect (50). This result strongly suggests that in our experiments, GSH and directly blocked ceftazidime activity or inactivated the antibiotic.

In mammalian cells, protection from electrophiles and xenobiotic compounds has been shown to occur through conjugation of these compounds to GSH, a reaction that is catalyzed by glutathione-*S* transferases (GST) followed by secretion from the cell (52). Bacteria also possess GSTs and it is speculated that bacteria may be able to similarly use GSH conjugation to reduce or eliminate the threat of antibiotics, although no studies have shown this to be true at this time (50, 53). It is possible that in our experiments *Burkholderia* uses GSTs to conjugate GSH to antibiotics and eliminate their threat. However, if we were to find that antioxidants besides GSH also protect *Burkholderia* against antibiotics, then GSTs would not be implicated in the protection, since conjugation specifically relies on a source of GSH and not just any antioxidant. Although we have not conducted experiments with other antioxidants, studies by Goswami et. al. have shown a role of other antioxidants such as ascorbic acid to protect bacteria from deadly antibiotics (50, 54). Therefore we believe it is improbable that GSTs are involved with antioxidant protection of *Burkholderia* from ceftazidime, and instead, direct reaction and inactivation of antibiotics by antioxidants may be more likely.

Our results also suggest against the use of the standard kanamycin protection assay to define specific and individual IFN-γ effects. The kanamycin protection assay, usually used as a tool to study the cellular response to IFN-γ, is a type of macrophage infection in which macrophages are treated with extracellular antibiotics during the entire experiment. The purpose of the addition of extracellular antibiotics is to enable the exclusive study of intracellular effects. Instead, we propose that in most macrophage infection models any addition of extracellular antibiotics is likely enhancing the overall bacterial killing in the system, which may artificially enhance the observed effect of the IFN-γ alone. Antibiotic killing in the extracellular compartment limits the number of viable bacteria that can infect healthy cells. In this way, the intracellular bacterial burden is likely to be much lower than in these cells than in cells only treated with IFN-γ. Furthermore, in studies that monitor cell viability, even a minor decrease in macrophage viability could be due to rupture of macrophages and release of hundreds or thousands of bacteria back into the extracellular space. If it weren't for the antibiotics in the extracellular compartment, these bacteria would likely re-infect nearby healthy cells. Both of these scenarios warn that scientists may be inadvertently documenting results as an effect of IFN-γ alone, when in fact, it is more probably an example of immuno-antimicrobial synergy, similar to our IFN-γ plus ceftazidime treated macrophages. Therefore, we caution against the kanamycin protection assay as a model to describe a single intracellular treatment effect.

In conclusion, we have shown that the major mechanism of immuno-antimicrobial synergy is due to separate and compartmentalized killing of IFN-γ and ceftazidime. We provided evidence that IFN-γ alone kills intracellular bacteria and we also showed a role for ROS responses as a mechanism of this killing. Ceftazidime alone was shown to kill extracellular bacteria and killing was completely reversed by GSH. Future studies are required to determine

the exact mechanism by which GSH protects against antibiotics, but regardless, we show important and relevant evidence that the antioxidant GSH effectively eliminates the killing capacity of ceftazidime. This result may have implications for avoidance of antioxidant supplements during infection, as they may inactivate antibiotics. Taken together, our results suggest that the classical macrophage infection model is a dynamic system of intracellular and extracellular bacteria. We further conclude that control of bacterial burden in each compartment can lead to strong synergistic reduction of bacteria from the entire system. Knowing the role of compartmentalized killing in immuno-antimicrobial therapy opens avenues to explore other therapies using any number of drug combinations which can reduce at least one compartment's bacteria load.

REFERENCES

1. **Limmathurotsakul D, Wongratanacheewin S, Teerawattanasook N, Wongsuvan G, Chaisuksant S, Chetchotisakd P, Chaowagul W, Day NP, Peacock SJ.** 2010. Increasing incidence of human melioidosis in Northeast Thailand. Am J Trop Med Hyg **82:**1113-1117.

2. **Wiersinga WJ, Currie BJ, Peacock SJ.** 2012. Melioidosis. N Engl J Med **367:**1035-1044.

3. **Dance DA.** 1991. Melioidosis: the tip of the iceberg? Clin Microbiol Rev **4:**52-60.

4. **Wiersinga WJ, van der Poll T, White NJ, Day NP, Peacock SJ.** 2006. Melioidosis: insights into the pathogenicity of *Burkholderia pseudomallei*. Nat Rev Microbiol **4:**272-282.

5. **Wuthiekanun V, Peacock SJ.** 2006. Management of melioidosis. Expert Rev Anti Infect Ther **4:**445-455.

6. **Schweizer HP.** 2012. Mechanisms of antibiotic resistance in *Burkholderia pseudomallei*: implications for treatment of melioidosis. Future Microbiol **7:**1389-1399.

7. **Jones AL, Beveridge TJ, Woods DE.** 1996. Intracellular survival of *Burkholderia pseudomallei*. Infect Immun **64:**782-790.

8. **Tandhavanant S, Thanwisai A, Limmathurotsakul D, Korbsrisate S, Day NP, Peacock SJ, Chantratita N.** 2010. Effect of colony morphology variation of *Burkholderia pseudomallei* on intracellular survival and resistance to antimicrobial environments in human macrophages in vitro. BMC Microbiol **10:**303.

9. **Jabbar Z, Currie BJ.** 2013. Melioidosis and the kidney. Nephrology (Carlton) **18:**169-175.

10. **Maharjan B, Chantratita N, Vesaratchavest M, Cheng A, Wuthiekanun V, Chierakul W, Chaowagul W, Day NP, Peacock SJ.** 2005. Recurrent melioidosis in patients in northeast Thailand is frequently due to reinfection rather than relapse. J Clin Microbiol **43:**6032-6034.

11. **Currie BJ, Fisher DA, Anstey NM, Jacups SP.** 2000. Melioidosis: acute and chronic disease, relapse and re-activation. Trans R Soc Trop Med Hyg **94:**301-304.

12. **Chaowagul W, Suputtamongkol Y, Dance DA, Rajchanuvong A, Pattara-arechachai J, White NJ.** 1993. Relapse in melioidosis: incidence and risk factors. J Infect Dis **168:**1181-1185.

13. **Kespichayawattana W, Rattanachetkul S, Wanun T, Utaisincharoen P, Sirisinha S.** 2000. *Burkholderia pseudomallei* induces cell fusion and actin-associated membrane protrusion: a possible mechanism for cell-to-cell spreading. Infect Immun **68:**5377-5384.

14. **Stevens MP, Galyov EE.** 2004. Exploitation of host cells by *Burkholderia pseudomallei*. Int J Med Microbiol **293:**549-555.

15. **Puthucheary SD, Nathan SA.** 2006. Comparison by electron microscopy of intracellular events and survival of *Burkholderia pseudomallei* in monocytes from normal subjects and patients with melioidosis. Singapore Med J **47:**697-703.

16. **Sun GW, Lu J, Pervaiz S, Cao WP, Gan YH.** 2005. Caspase-1 dependent macrophage death induced by *Burkholderia pseudomallei*. Cell Microbiol **7:**1447-1458.

17. **French CT, Toesca IJ, Wu TH, Teslaa T, Beaty SM, Wong W, Liu M, Schroder I, Chiou PY, Teitell MA, Miller JF.** 2011. Dissection of the *Burkholderia* intracellular life cycle using a photothermal nanoblade. Proc Natl Acad Sci U S A **108:**12095-12100.

18. **Hoppe I, Brenneke B, Rohde M, Kreft A, Haussler S, Reganzerowski A, Steinmetz I.** 1999. Characterization of a murine model of melioidosis: comparison of different strains of mice. Infect Immun **67:**2891-2900.

19. **Chieng S, Carreto L, Nathan S.** 2012. *Burkholderia pseudomallei* transcriptional adaptation in macrophages. BMC Genomics **13:**328.

20. **Haque A, Easton A, Smith D, O'Garra A, Van Rooijen N, Lertmemongkolchai G, Titball RW, Bancroft GJ.** 2006. Role of T cells in innate and adaptive immunity against murine *Burkholderia pseudomallei* infection. J Infect Dis **193:**370-379.

21. **Santanirand P, Harley VS, Dance DA, Drasar BS, Bancroft GJ.** 1999. Obligatory role of gamma interferon for host survival in a murine model of infection with *Burkholderia pseudomallei*. Infect Immun **67:**3593-3600.

22. **Breitbach K, Klocke S, Tschernig T, van Rooijen N, Baumann U, Steinmetz I.** 2006. Role of inducible nitric oxide synthase and NADPH oxidase in early control of *Burkholderia pseudomallei* infection in mice. Infect Immun **74:**6300-6309.

23. **Easton A, Haque A, Chu K, Lukaszewski R, Bancroft GJ.** 2007. A critical role for neutrophils in resistance to experimental infection with *Burkholderia pseudomallei*. J Infect Dis **195:**99-107.

24. **Charoensap J, Utaisincharoen P, Engering A, Sirisinha S.** 2009. Differential intracellular fate of *Burkholderia pseudomallei* 844 and *Burkholderia thailandensis* UE5 in human monocyte-derived dendritic cells and macrophages. BMC Immunol **10:**20.

25. **Breitbach K, Sun GW, Kohler J, Eske K, Wongprompitak P, Tan G, Liu Y, Gan YH, Steinmetz I.** 2009. Caspase-1 mediates resistance in murine melioidosis. Infect Immun **77:**1589-1595.

26. **Utaisincharoen P, Tangthawornchaikul N, Kespichayawattana W, Chaisuriya P, Sirisinha S.** 2001. *Burkholderia pseudomallei* interferes with inducible nitric oxide synthase (iNOS) production: a possible mechanism of evading macrophage killing. Microbiol Immunol **45:**307-313.

27. **Utaisincharoen P, Anuntagool N, Arjcharoen S, Limposuwan K, Chaisuriya P, Sirisinha S.** 2004. Induction of iNOS expression and antimicrobial activity by interferon (IFN)-beta is distinct from IFN-gamma in *Burkholderia pseudomallei*-infected mouse macrophages. Clin Exp Immunol **136:**277-283.

28. **Propst KL, Troyer RM, Kellihan LM, Schweizer HP, Dow SW.** 2010. Immunotherapy markedly increases the effectiveness of antimicrobial therapy for treatment of *Burkholderia pseudomallei* infection. Antimicrob Agents Chemother **54:**1785-1792.

29. **Brett PJ, Deshazer D, Woods DE.** 1997. Characterization of *Burkholderia pseudomallei* and *Burkholderia pseudomallei*-like strains. Epidemiol Infect **118:**137-148.

30. **Wand ME, Muller CM, Titball RW, Michell SL.** 2011. Macrophage and *Galleria mellonella* infection models reflect the virulence of naturally occurring isolates of *B. pseudomallei*, *B. thailandensis* and *B. oklahomensis*. BMC Microbiol **11:**11.

31. **Yi H, Cho KH, Cho YS, Kim K, Nierman WC, Kim HS.** 2012. Twelve positions in a beta-lactamase that can expand its substrate spectrum with a single amino acid substitution. PLoS One **7:**e37585.

32. **Bosio CM, Dow SW.** 2005. *Francisella tularensis* induces aberrant activation of pulmonary dendritic cells. J Immunol **175:**6792-6801.

33. **Slinker BK.** 1998. The statistics of synergism. J Mol Cell Cardiol **30:**723-731.

34. **Hseu YC, Sung JC, Shieh BS, Chen SC.** 2013. *Burkholderia pseudomallei* infection induces the expression of apoptosis-related genes and proteins in mouse macrophages. J Microbiol Immunol Infect.

35. **Brett PJ, Burtnick MN, Su H, Nair V, Gherardini FC.** 2008. iNOS activity is critical for the clearance of *Burkholderia mallei* from infected RAW 264.7 murine macrophages. Cell Microbiol **10:**487-498.

36. **Korichneva I, Hammerling U.** 1999. F-actin as a functional target for retro-retinoids: a potential role in anhydroretinol-triggered cell death. J Cell Sci **112 (Pt 15):**2521-2528.

37. **Imlay JA.** 2008. Cellular defenses against superoxide and hydrogen peroxide. Annu Rev Biochem **77:**755-776.

38. **Tangsudjai S, Pudla M, Limposuwan K, Woods DE, Sirisinha S, Utaisincharoen P.** 2010. Involvement of the MyD88-independent pathway in controlling the intracellular

fate of *Burkholderia pseudomallei* infection in the mouse macrophage cell line RAW 264.7. Microbiol Immunol **54:**282-290.

39. **Utaisincharoen P, Anuntagool N, Limposuwan K, Chaisuriya P, Sirisinha S.** 2003. Involvement of beta interferon in enhancing inducible nitric oxide synthase production and antimicrobial activity of *Burkholderia pseudomallei*-infected macrophages. Infect Immun **71:**3053-3057.

40. **Kamijo R, Harada H, Matsuyama T, Bosland M, Gerecitano J, Shapiro D, Le J, Koh SI, Kimura T, Green SJ, et al.** 1994. Requirement for transcription factor IRF-1 in NO synthase induction in macrophages. Science **263:**1612-1615.

41. **Dwyer DJ, Kohanski MA, Collins JJ.** 2009. Role of reactive oxygen species in antibiotic action and resistance. Curr Opin Microbiol **12:**482-489.

42. **Belenky P, Collins JJ.** 2011. Microbiology. Antioxidant strategies to tolerate antibiotics. Science **334:**915-916.

43. **Foti JJ, Devadoss B, Winkler JA, Collins JJ, Walker GC.** 2012. Oxidation of the guanine nucleotide pool underlies cell death by bactericidal antibiotics. Science **336:**315-319.

44. **Kohanski MA, Dwyer DJ, Hayete B, Lawrence CA, Collins JJ.** 2007. A common mechanism of cellular death induced by bactericidal antibiotics. Cell **130:**797-810.

45. **Wright GD.** 2007. On the road to bacterial cell death. Cell **130:**781-783.

46. **Keren I, Wu Y, Inocencio J, Mulcahy LR, Lewis K.** 2013. Killing by bactericidal antibiotics does not depend on reactive oxygen species. Science **339:**1213-1216.

47. **Liu Y, Imlay JA.** 2013. Cell death from antibiotics without the involvement of reactive oxygen species. Science **339:**1210-1213.

48. **Ezraty B, Vergnes A, Banzhaf M, Duverger Y, Huguenot A, Brochado AR, Su SY, Espinosa L, Loiseau L, Py B, Typas A, Barras F.** 2013. Fe-S cluster biosynthesis controls uptake of aminoglycosides in a ROS-less death pathway. Science **340:**1583-1587.

49. **Dhamdhere G, Krishnamoorthy G, Zgurskaya HI.** 2010. Interplay between drug efflux and antioxidants in *Escherichia coli* resistance to antibiotics. Antimicrob Agents Chemother **54:**5366-5368.

50. **Goswami M, Mangoli SH, Jawali N.** 2007. Effects of glutathione and ascorbic acid on streptomycin sensitivity of *Escherichia coli*. Antimicrob Agents Chemother **51:**1119-1122.

51. **Goswami M, Mangoli SH, Jawali N.** 2006. Involvement of reactive oxygen species in the action of ciprofloxacin against *Escherichia coli*. Antimicrob Agents Chemother **50:**949-954.

52. **Forman HJ, Zhang H, Rinna A.** 2009. Glutathione: overview of its protective roles, measurement, and biosynthesis. Mol Aspects Med **30:**1-12.

53. **Vuilleumier S.** 1997. Bacterial glutathione S-transferases: what are they good for? J Bacteriol **179:**1431-1441.

54. **Goswami M, Jawali N.** 2010. N-acetylcysteine-mediated modulation of bacterial antibiotic susceptibility. Antimicrob Agents Chemother **54:**3529-3530.

CHAPTER 6: OVERALL SIGNIFICANCE AND FUTURE DIRECTIONS OF SPECIFIC AIMS

RESEARCH SUMMARY AND SIGNIFICANCE

The main goal of the research presented in this dissertation was to determine the mechanism by which IFN-γ interacts with ceftazidime to synergistically eliminate intracellular bacterial burden inside infected macrophages. In chapter 3 we explored several potential mediators of immuno-antimicrobial synergy. While most of our results in chapter 3 showed evidence against our targets as major mediators of the synergistic effect, we maintain that these negative data may help future scientists, especially those which pursue a similar topic. In chapter 4 we identified an interaction between IFN-γ induced ROS responses and ceftazidime to synergistically reduce intracellular *Burkholderia*. Furthermore we demonstrated a role for IFN-γ induced ROS to prevent vacuolar escape which led to a lack of actin polymerization and reduced intracellular replication. In chapter 5 our results provided evidential support for a new model to describe the dynamics of the classical macrophage infection model. We also determined the separate independent roles for IFN-γ and ceftazidime. IFN-γ controlled intracellular replication and spread of infection, due in part to ROS responses, while ceftazidime alone killed extracellular bacteria.

We believe that our new understanding of the role of compartmentalized killing in immuno-antimicrobial therapy creates new possibilities for drug combinations for enhanced treatment of not only *B. pseudomallei* infection, but potentially other Gram negative intracellular pathogens, too. Just as we have already shown that other bactericidal antibiotics are capable of

synergizing with IFN-γ, we also propose that other compounds or drugs which enhance macrophage killing capacity or interfere with the intracellular lifestyle intracellular pathogens, may synergize with ceftazidime therapy. The best candidates for such compounds would be agents that directly induce a strong, endogenous IFN-γ response or induce endogenous ROS production, a mediator of IFN-γ responses. We have already shown evidence of the efficacy of both of these approaches. We previously found that cationic liposome-DNA complex (CLDC) elicited a particularly strong IFN-γ response which could then interact with ceftazidime treatment to synergistically enhance survival rates of mice to lethal *B. pseudomallei* challenge (1, 2). We also have also already shown that other ROS-inducers, such as BSO, are capable of synergy with ceftazidime, which supports the use of other ROS stimulators as non-specific, antibiotic enhancing agents.

The effectiveness of the immuno-antimicrobial therapy suggests the possibility for decreasing the dose of ceftazidime given to patients clinically if IFN-γ, IFN-γ inducing drugs, or other ROS-inducing drugs are given alongside antibiotic treatment. Additionally, immuno-antimicrobial therapy could reduce the length of the suggested two-week intravenous ceftazidime treatment since the intravenous antibiotic phase of melioidosis treatment is the most expensive and invasive portion of treatment and is not practical where access to healthcare is limited (3-5). Our results with in vivo administration of BSO with sub-therapeutic doses of ceftazidime showed 100% survival of mice, suggesting that decreased doses of ceftazidime may still fully protect against melioidosis when administered with ROS-inducing drugs. Furthermore, the dose of BSO that was used in our study, 2 mmol/kg once daily for three days, was well below the suggested dose of 8 mmol/kg every 4 hours (6), suggesting that we have already found a lower dose of BSO to be successful as well.

In conclusion, we have discovered a novel platform for future studies on drug combinations to enhance pathogen elimination. We suggest that a drug which only targets intracellular killing may combine well with a drug that only targets extracellular killing to synergistically reduce the number of bacteria in the system as a whole, reduce spread of the infection, and maintain the health of host cells. Additionally, our results warn against the use of certain ROS-scavengers and antioxidants as nutritional supplements, because they may mitigate the potency of antibiotic treatment during acute infection through eliminating the beneficial host ROS response or through inactivation of antibiotics.

UNANSWERED QUESTIONS AND FUTURE DIRECTIONS OF SPECIFIC AIMS:

We have answered the major questions that we intended through our research into the mechanism of immuno-antimicrobial synergy, however our results have generated many more questions that now need to be answered in order to fully understand the synergy. We have outlined these questions below and suggest experiments towards finding their answers.

How does ROS prevent vacuolar escape?

We found that IFN-γ and BSO, another ROS inducing drug, prevented *Burkholderia* from escaping the phagolysosome. The significance of this result cannot be overstated. By preventing vacuolar escape, ROS can inhibit replication in the cytoplasm, actin-tail polymerization, and also cell-to-cell spread of the infection. Furthermore, this IFN-γ induced ROS effect has been confirmed for other intracellular pathogens (7-9). But how ROS prevents vacuolar escape is still

an unanswered question. One possibility is that increased ROS, due to IFN-γ activation, kills bacteria in the phagosome before they have a chance to escape. Increased ROS could kill bacteria directly through irreparable damage to DNA and protein, or ROS could interact with other phagolysosome components to increase killing. For example, some scientists speculate that ROS may gain better access to bacteria due to pores or holes formed by antimicrobial peptides (10).

Another alternative is that ROS responses in the phagosome down regulates gene expression or otherwise interferes with the T3SS-3 apparatus, which is necessary for rapid escape of the vacuole (11-13). Future studies should look at gene expression levels of *Burkholderia* trapped in the phagolysosome of IFN-γ treated macrophages, to determine if components of their T3SS-3 apparatus and/or protein effectors are down-regulated compared to bacteria in untreated macrophages. However, we foresee that differences in gene expression may simply arise from imprecise timing of the collection of control bacteria. Therefore a more straight-forward solution would be to infect macrophages with mutant bacteria lacking a functional T3SS-3 and then either treat with IFN-γ or leave macrophages untreated. Mutant bacteria will be unable to escape the phagolysosome regardless of treatment, however, if the increase in ROS, due to IFN-γ, is directly microbicidal, we would expect greater intracellular killing in the IFN-γ treated macrophages. This result would suggest that IFN-γ, through induction of ROS, creates a phagolysosome which is more toxic to bacteria.

Does increased time in phagolysosome equate to increased killing?

If increased ROS due to IFN-γ or BSO isn't found to directly kill *Burkholderia* in the phagolysosome, and instead, ROS is suspected to interfere with T3SS-3 function, then we could

ask the question does prevention of vacuolar escape actually lead to increased killing? We would hope that increased exposure of *Burkholderia* to phagosome contents such as AMPs, lysozyme, and proteases would lead to increased killing (10), however studies show that *B. pseudomallei* is resistant to many host-derived antimicrobial defenses (14, 15). Therefore, it is important to determine whether *Burkholderia* that fail to escape the phagosome due to IFN-γ induced ROS, are eventually killed or instead regain the ability to escape, exhibit delayed escape, or perhaps remain inside the phagolysosome for an extended period of time. We could easily test these ideas using confocal microscopy to take short-interval time-lapse images of a particular IFN-γ treated macrophage with intracellular *Burkholderia*. This experiment would more definitively show whether preventing vacuolar escape has the degree of impact that we suspect.

Would immuno-antimicrobial therapy be an effective treatment for chronic melioidosis?

All of our studies on immuno-antimicrobial therapy have focused on treatment of acute melioidosis both in vitro and in vivo. However, we are curious if IFN-γ and ceftazidime might be effective treatment for chronic melioidosis, in which an infection has already been established for quite some time. C57BL/6 mice are good models for chronic melioidosis as they can carry heavy bacteria loads in liver and spleen for several weeks before succumbing to death (16). Future studies will investigate the effectiveness of IFN-γ or BSO combination with ceftazidime in a chronic melioidosis mouse model in the hope that immuno-antimicrobial therapy will be equally effective at later points of infection. However, some studies suggest that IFN-γ is not helpful, and instead is detrimental, in some models of established infections (17). There is a correlation between increased serum IFN-γ and increased severity of disease and prognosis in BALB/c mice as well as human patients with melioidosis (17, 18). Furthermore, a possible

explanation for the high susceptibility of BALB/c to *B. pseudomallei* has been its high, but slightly delayed, IFN-γ response (17, 19). However these studies were conducted with acute melioidosis. We still believe that in a chronic model IFN-γ would be beneficial and enhance the efficacy of ceftazidime treatment.

Are mitochondrial ROS and NADPH phagocyte oxidase-generated ROS equally important for the IFN-γ effect?

It is well known that IFN-γ increases expression of ROS in macrophages as well NADPH phagocyte oxidase subunit expression (20, 21). In our system, we have not evaluated whether IFN-γ substantially increases mitochondrial ROS production, although activation of NADPH oxidase has been shown to increase mitochondrial ROS production (22), and it is conceivable that mitochondrial ROS contributes to some threshold of total cellular ROS required for the IFN-γ effect. GSH is known to have similar distribution within the cytoplasm, mitochondria, and nucleus, though we are unaware of any studies that have identified the GSH concentration or localization in vacuoles such as the phagosome (23). Precursors to GSH, such as NAC, have been shown to eliminate mitochondrial ROS as well as reduce the respiratory burst from polymorphonuclear cells (24, 25). Therefore we should determine whether addition of GSH to our system has specifically scavenged NADPH oxidase-generated ROS, which we assume to be the main source of increased ROS due to IFN-γ stimulation, or mitochondrial ROS.

We propose future experiments to first test whether mitochondrial ROS actually plays a role in the IFN-γ effects. First we would detect an increase in total intracellular ROS due to IFN-γ using carboxy-H2DCFDA and flow cytometry. We would compare this increase in total ROS to any increase in mitochondrial ROS using mitoSOX red, a dye that detects superoxide

specifically from mitochondria. This experiment would indicate whether mitochondrial ROS is a component of IFN-γ induced ROS, though if it were not, we could not exclude the possibility that mitochondrial ROS still contributes to the overall threshold of intracellular ROS which may be important for IFN-γ killing and prevention of vacuolar escape. We could therefore use a specific mitochondrial antioxidant, such as mitoTEMPO (26) or SS peptides (27), to determine the necessity of mitochondrial ROS to IFN-γ mediated killing and prevention of vacuolar escape. We could similarly use an NADPH oxidase inhibitor, such as apocynin (22) to determine the relative importance of NADPH oxidase to IFN-γ mediated killing or vacuolar escape, though a more definitive result would come from measuring the killing efficiency of bone marrow macrophages from phox $^{-/-}$ mice pre-activated with IFN-γ and compared to a wild-type control.

Can other roles of GSH and NAC explain the reversal of immuno-antimicrobial synergy?

In chapter 4 we showed that NAC and GSH similarly reversed IFN-γ and ceftazidime immuno-antimicrobial synergy and provided evidence that this effect was due to their antioxidant properties. In our macrophage infection model, GSH and NAC have only shown a measurable effect, namely the reversal of synergy, when ROS is known to be increased. Although this result is consistent with a ROS-scavenging role, we cannot exclude the possibility that GSH and NAC may function in a different, non-antioxidant role to reverse the immuno-antimicrobial synergy, especially because we have never thought to test the ability of GSH and NAC to reverse ROS-independent killing before now.

NAC has also been shown to delay cell death and inhibit apoptosis through down-regulation of caspase-8 protein and mRNA expression, as well as inhibition of caspase-3 and caspase-7 proteolytic processing (28-30). Therefore it is a possibility that NAC, rather than

scavenging IFN-γ induced ROS, interfered with programmed cell death, which is thought to be a mechanism of macrophages to eliminate the intracellular niche for intracellular pathogen replication (31, 32). To test this, we propose future experiments with fluorescent microscopy of macrophage infections and simultaneous treatment with IFN-γ and NAC. If NAC serves an antioxidant and ROS-scavenging role, we should see bacterial actin tail formation and replication in cytoplasm inside macrophages treated with IFN-γ + NAC combined treatment, signifying escape from phagolysosomes. On the other hand, if NAC functions through inhibition of programmed cell death, we will likely see prevention of vacuolar escape similar to IFN-γ. Similar studies could be conducted with GSH.

Finally, GSH has been shown to inhibit *B. cenocepacia* adherence to and uptake into respiratory epithelial cells due to alteration of redox status of surface proteins (33). Therefore, GSH could have inhibited uptake of *B. thailandensis* in our macrophage infections. However we do not believe this is the case since inhibiting uptake would hypothetically lead to lower intracellular numbers instead of higher ones as we have regularly seen with GSH treatment in our experiments.

Does infection of pre-activated macrophages eventually induce a robust ROS response?

We have speculated in chapter 5 that pre-activation of macrophages with overnight incubation with IFN-γ likely elicits a different degree of ROS response compared to macrophages simultaneously stimulated with IFN-γ and *Burkholderia*. However we suspect that pre-activation with IFN-γ followed by infection with *Burkholderia*, would likely elicit a similar response to co-stimulation, if given the same amount of time. This is an important point, since

we argue that ROS responses probably play a larger role in IFN-γ mediated killing, than our assay allows for us to determine. In order to determine if infection of pre-activated macrophages eventually induces a robust ROS response, we would measure intracellular ROS production in these macrophages over time starting just before infection and sampling at various time points until 18 hours post infection. We would then compare the maximal ROS response to the ROS responses of macrophages co-stimulated with IFN-γ and bacteria for 18 hours. These experiments would determine the relative degrees of ROS responses with pre-activation versus co-stimulation.

Do bactericidal antibiotics kill *B. pseudomallei* through a ROS-dependent mechanism?

In the discussion section of chapter 5 we raised the question of how GSH protects bacteria from antibiotic killing. One explanation is that GSH may function as an antioxidant to scavenge deadly ROS generated in bacteria by the common mechanism of antibiotic-mediated death (34-38). However many recent studies provide evidence that antibiotics do not kill through ROS-mediated pathways (39-41). To more definitively determine if *B. pseudomallei* is killed by antibiotics in a ROS-dependent manner, we could treat a *katG* mutant strain, lacking catalase and peroxidase activity, with antibiotics and compare its susceptibility to a wild-type strain. Antioxidant and ROS-scavenging mutant bacteria have similarly been used to determine the role of ROS in antibiotic killing (40, 42, 43). If antibiotics kill through ROS-dependent mechanisms, a mutant incapable of degrading the toxic ROS generated by antibiotics, would be more susceptible to antibiotic killing, lowering the MIC for a particular antibiotic compared to a wild-type strain control. We do not suspect a ROS-mediated mechanism for ceftazidime lethality, therefore we would not expect a *katG* mutant to be more susceptible to ceftazidime.

How do GSH and other antioxidants protect bacteria from ceftazidime?

If GSH and other antioxidants don't protect against antibiotics by scavenging antibiotic induced ROS, then what is the mechanism of antioxidant protection? In chapter 5 we discussed evidence that suggests that antioxidants play a role in either blocking or inactivating antibiotics (44-46). Evidence for antioxidant inactivation or blocking of antibiotics comes from studies that show that exogenous but not endogenous GSH is protective (44) and GSH must be present at the time of antibiotic treatment to exert its protective effects (45). Additionally, GSH may not be protective for Gram positive bacteria suggesting a Gram negative specific component to the protective effect (47). We suggest an initial experiment to determine whether, in our system, ceftazidime is inactivated through direct reaction with GSH or conjugation to GSH. If other antioxidants besides GSH protect *Burkholderia* against different classes of antibiotics, then GSTs are not likely involved in the GSH protection against antibiotics since GSTs only use GSH for conjugation and not just any antioxidant. Further studies would need to be conducted to understand any direct reaction or inactivation of ceftazidime with antioxidants.

What role do filamentous bacteria play in our macrophage infection model?

We have seen through microscopy that filamented *Burkholderia* often make up a large proportion of the remaining intracellular and extracellular bacteria in the macrophages treated with the combination therapy (Figure 5.1). We are curious about the role of filamentous bacteria in our macrophage infection system, especially since studies show them to have decreased virulence compared to nonfilamentous *Burkholderia* (48). Chen found that filamentous bacteria reverted back to a nonfilamentous form after antibiotics were removed, but these bacteria were

resistant to antibiotics. Similarly, our preliminary experiments suggest that filamentous bacteria may be resistant to high doses of antibiotics (Figure A10). If filamentous bacteria show more antibiotic resistance, are these bacteria responsible for infection relapse? Why are there more filamentous bacteria in macrophages treated with the combination therapy? Future investigations should investigate these still unanswered questions.

Future directions summary

As illustrated in this chapter, there are several new directions in which we could take this project. We believe that one of the most pressing questions is whether both NADPH phagocyte oxidase generated ROS and mitochondrial generated ROS are both important for the IFN-γ effects seen in immuno-antimicrobial synergy. Another important question to address is how ROS can prevent vacuolar escape of bacteria in the phagolysosome. Future studies will certainly address these questions and the others suggested in this chapter. It is our hope that we can better understand the mechanism of immuno-antimicrobial synergy and use our understanding to suggest therapy enhancements for treatment of melioidosis.

REFERENCES

1. **Goodyear A, Kellihan L, Bielefeldt-Ohmann H, Troyer R, Propst K, Dow S.** 2009. Protection from pneumonic infection with *Burkholderia* species by inhalational immunotherapy. Infect Immun **77:**1579-1588.

2. **Propst KL, Troyer RM, Kellihan LM, Schweizer HP, Dow SW.** 2010. Immunotherapy markedly increases the effectiveness of antimicrobial therapy for treatment of *Burkholderia pseudomallei* infection. Antimicrob Agents Chemother **54:**1785-1792.

3. **Jabbar Z, Currie BJ.** 2013. Melioidosis and the kidney. Nephrology (Carlton) **18:**169-175.

4. **Wiersinga WJ, van der Poll T, White NJ, Day NP, Peacock SJ.** 2006. Melioidosis: insights into the pathogenicity of *Burkholderia pseudomallei*. Nat Rev Microbiol **4:**272-282.

5. **Schweizer HP.** 2012. Mechanisms of antibiotic resistance in *Burkholderia pseudomallei*: implications for treatment of melioidosis. Future Microbiol **7:**1389-1399.

6. **Griffith OW.** 1981. Depletion of glutathione by inhibition of biosynthesis. Methods Enzymol **77:**59-63.

7. **Portnoy DA, Schreiber RD, Connelly P, Tilney LG.** 1989. Gamma interferon limits access of *Listeria monocytogenes* to the macrophage cytoplasm. J Exp Med **170:**2141-2146.

8. **Lindgren H, Golovliov I, Baranov V, Ernst RK, Telepnev M, Sjostedt A.** 2004. Factors affecting the escape of *Francisella tularensis* from the phagolysosome. J Med Microbiol **53:**953-958.

9. **Myers JT, Tsang AW, Swanson JA.** 2003. Localized reactive oxygen and nitrogen intermediates inhibit escape of *Listeria monocytogenes* from vacuoles in activated macrophages. J Immunol **171:**5447-5453.

10. **Slauch JM.** 2011. How does the oxidative burst of macrophages kill bacteria? Still an open question. Mol Microbiol **80:**580-583.

11. **Stevens MP, Wood MW, Taylor LA, Monaghan P, Hawes P, Jones PW, Wallis TS, Galyov EE.** 2002. An Inv/Mxi-Spa-like type III protein secretion system in *Burkholderia pseudomallei* modulates intracellular behaviour of the pathogen. Mol Microbiol **46:**649-659.

12. **French CT, Toesca IJ, Wu TH, Teslaa T, Beaty SM, Wong W, Liu M, Schroder I, Chiou PY, Teitell MA, Miller JF.** 2011. Dissection of the *Burkholderia* intracellular life cycle using a photothermal nanoblade. Proc Natl Acad Sci U S A **108:**12095-12100.

13. **Burtnick MN, Brett PJ, Nair V, Warawa JM, Woods DE, Gherardini FC.** 2008. *Burkholderia pseudomallei* type III secretion system mutants exhibit delayed vacuolar escape phenotypes in RAW 264.7 murine macrophages. Infect Immun **76:**2991-3000.

14. **Tandhavanant S, Thanwisai A, Limmathurotsakul D, Korbsrisate S, Day NP, Peacock SJ, Chantratita N.** 2010. Effect of colony morphology variation of *Burkholderia pseudomallei* on intracellular survival and resistance to antimicrobial environments in human macrophages in vitro. BMC Microbiol **10:**303.

15. **Jones AL, Beveridge TJ, Woods DE.** 1996. Intracellular survival of *Burkholderia pseudomallei*. Infect Immun **64:**782-790.

16. **Leakey AK, Ulett GC, Hirst RG.** 1998. BALB/c and C57Bl/6 mice infected with virulent *Burkholderia pseudomallei* provide contrasting animal models for the acute and chronic forms of human melioidosis. Microb Pathog **24:**269-275.

17. **Liu B, Koo GC, Yap EH, Chua KL, Gan YH.** 2002. Model of differential susceptibility to mucosal *Burkholderia pseudomallei* infection. Infect Immun **70:**504-511.

18. **Lauw FN, Simpson AJ, Prins JM, Smith MD, Kurimoto M, van Deventer SJ, Speelman P, Chaowagul W, White NJ, van der Poll T.** 1999. Elevated plasma concentrations of interferon (IFN)-gamma and the IFN-gamma-inducing cytokines interleukin (IL)-18, IL-12, and IL-15 in severe melioidosis. J Infect Dis **180:**1878-1885.

19. **Koo GC, Gan YH.** 2006. The innate interferon gamma response of BALB/c and C57BL/6 mice to in vitro *Burkholderia pseudomallei* infection. BMC Immunol **7:**19.

20. **Mraheil MA, Billion A, Mohamed W, Rawool D, Hain T, Chakraborty T.** 2011. Adaptation of *Listeria monocytogenes* to oxidative and nitrosative stress in IFN-gamma-activated macrophages. Int J Med Microbiol **301:**547-555.

21. **Fang FC.** 2004. Antimicrobial reactive oxygen and nitrogen species: concepts and controversies. Nat Rev Microbiol **2:**820-832.

22. **Doughan AK, Harrison DG, Dikalov SI.** 2008. Molecular mechanisms of angiotensin II-mediated mitochondrial dysfunction: linking mitochondrial oxidative damage and vascular endothelial dysfunction. Circ Res **102:**488-496.

23. **Ault JG, Lawrence DA.** 2003. Glutathione distribution in normal and oxidatively stressed cells. Exp Cell Res **285:**9-14.

24. **Kalghatgi S, Spina CS, Costello JC, Liesa M, Morones-Ramirez JR, Slomovic S, Molina A, Shirihai OS, Collins JJ.** 2013. Bactericidal antibiotics induce mitochondrial dysfunction and oxidative damage in Mammalian cells. Sci Transl Med **5:**192ra185.

25. **Heller AR, Groth G, Heller SC, Breitkreutz R, Nebe T, Quintel M, Koch T.** 2001. N-acetylcysteine reduces respiratory burst but augments neutrophil phagocytosis in intensive care unit patients. Crit Care Med **29:**272-276.

26. **Dikalova AE, Bikineyeva AT, Budzyn K, Nazarewicz RR, McCann L, Lewis W, Harrison DG, Dikalov SI.** 2010. Therapeutic targeting of mitochondrial superoxide in hypertension. Circ Res **107:**106-116.

27. **Szeto HH.** 2006. Cell-permeable, mitochondrial-targeted, peptide antioxidants. AAPS J **8:**E277-283.

28. **Aggarwal A, Misro MM, Maheshwari A, Sehgal N, Nandan D.** 2010. N-acetylcysteine counteracts oxidative stress and prevents hCG-induced apoptosis in rat Leydig cells through down regulation of caspase-8 and JNK. Mol Reprod Dev **77:**900-909.

29. **Rosati E, Sabatini R, Ayroldi E, Tabilio A, Bartoli A, Bruscoli S, Simoncelli C, Rossi R, Marconi P.** 2004. Apoptosis of human primary B lymphocytes is inhibited by N-acetyl-L-cysteine. J Leukoc Biol **76:**152-161.

30. **Wu YJ, Muldoon LL, Neuwelt EA.** 2005. The chemoprotective agent N-acetylcysteine blocks cisplatin-induced apoptosis through caspase signaling pathway. J Pharmacol Exp Ther **312:**424-431.

31. **Miao EA, Leaf IA, Treuting PM, Mao DP, Dors M, Sarkar A, Warren SE, Wewers MD, Aderem A.** 2010. Caspase-1-induced pyroptosis is an innate immune effector mechanism against intracellular bacteria. Nat Immunol **11:**1136-1142.

32. **Breitbach K, Sun GW, Kohler J, Eske K, Wongprompitak P, Tan G, Liu Y, Gan YH, Steinmetz I.** 2009. Caspase-1 mediates resistance in murine melioidosis. Infect Immun **77:**1589-1595.

33. **D'Orazio M, Pacello F, Battistoni A.** 2012. Extracellular glutathione decreases the ability of *Burkholderia cenocepacia* to penetrate into epithelial cells and to induce an inflammatory response. PLoS One **7:**e47550.

34. **Dwyer DJ, Kohanski MA, Collins JJ.** 2009. Role of reactive oxygen species in antibiotic action and resistance. Curr Opin Microbiol **12:**482-489.

35. **Belenky P, Collins JJ.** 2011. Microbiology. Antioxidant strategies to tolerate antibiotics. Science **334:**915-916.

36. **Foti JJ, Devadoss B, Winkler JA, Collins JJ, Walker GC.** 2012. Oxidation of the guanine nucleotide pool underlies cell death by bactericidal antibiotics. Science **336:**315-319.

37. **Kohanski MA, Dwyer DJ, Hayete B, Lawrence CA, Collins JJ.** 2007. A common mechanism of cellular death induced by bactericidal antibiotics. Cell **130:**797-810.

38. **Wright GD.** 2007. On the road to bacterial cell death. Cell **130:**781-783.

39. **Keren I, Wu Y, Inocencio J, Mulcahy LR, Lewis K.** 2013. Killing by bactericidal antibiotics does not depend on reactive oxygen species. Science **339:**1213-1216.

40. **Liu Y, Imlay JA.** 2013. Cell death from antibiotics without the involvement of reactive oxygen species. Science **339:**1210-1213.

41. **Ezraty B, Vergnes A, Banzhaf M, Duverger Y, Huguenot A, Brochado AR, Su SY, Espinosa L, Loiseau L, Py B, Typas A, Barras F.** 2013. Fe-S cluster biosynthesis controls uptake of aminoglycosides in a ROS-less death pathway. Science **340:**1583-1587.

42. **Wang X, Zhao X.** 2009. Contribution of oxidative damage to antimicrobial lethality. Antimicrob Agents Chemother **53:**1395-1402.

43. **Goswami M, Mangoli SH, Jawali N.** 2006. Involvement of reactive oxygen species in the action of ciprofloxacin against *Escherichia coli*. Antimicrob Agents Chemother **50:**949-954.

44. **Dhamdhere G, Krishnamoorthy G, Zgurskaya HI.** 2010. Interplay between drug efflux and antioxidants in *Escherichia coli* resistance to antibiotics. Antimicrob Agents Chemother **54:**5366-5368.

45. **Goswami M, Mangoli SH, Jawali N.** 2007. Effects of glutathione and ascorbic acid on streptomycin sensitivity of *Escherichia coli*. Antimicrob Agents Chemother **51:**1119-1122.

46. **Vuilleumier S.** 1997. Bacterial glutathione S-transferases: what are they good for? J Bacteriol **179:**1431-1441.

47. **Paez PL, Becerra MC, Albesa I.** 2010. Effect of the association of reduced glutathione and ciprofloxacin on the antimicrobial activity in *Staphylococcus aureus*. FEMS Microbiol Lett **303:**101-105.

48. **Chen K, Sun GW, Chua KL, Gan YH.** 2005. Modified virulence of antibiotic-induced *Burkholderia pseudomallei* filaments. Antimicrob Agents Chemother **49:**1002-1009.

APPENDIX I: SUPPLEMENTAL FIGURES

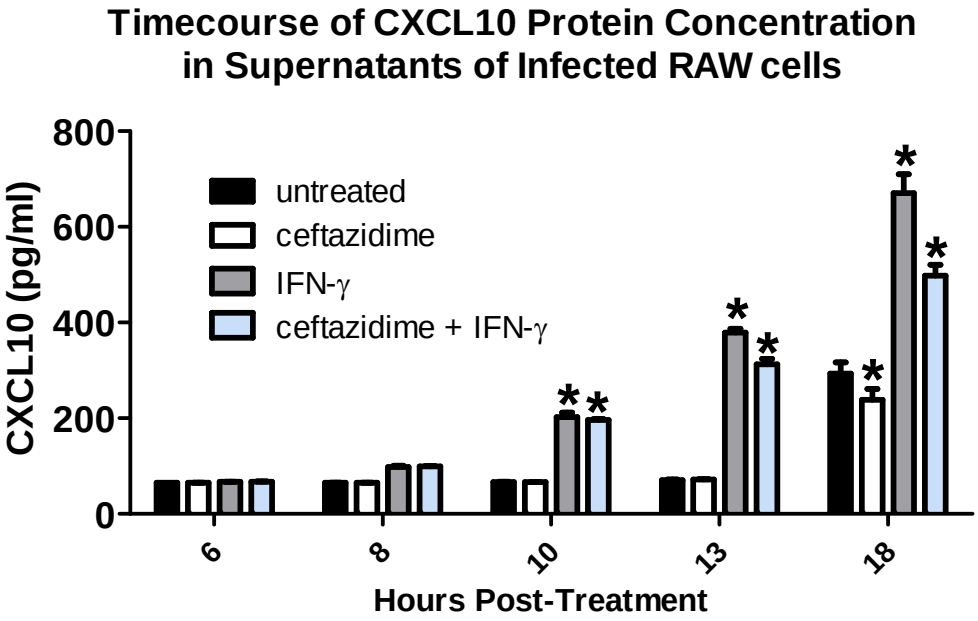

Figure A1: Timecourse of CXCL10 protein concentration in supernatants during macrophage infection. RAW 264.7 macrophages were infected with *B. thailandensis* and treated with either ceftazidime (10 µg/ml), IFN-γ (10 ng/ml), or the combination of ceftazidime and IFN-γ. At 6, 8, 10, 13, and 18 hours after treatment a sample of supernatant was taken from wells and assessed for CXCL10 protein concentration by ELISA. Statistical differences compared to the untreated control were assessed for each time point by repeated measures two-way ANOVA, *$P < 0.05$. Data is representative of one experiment with treatment groups run in triplicate.

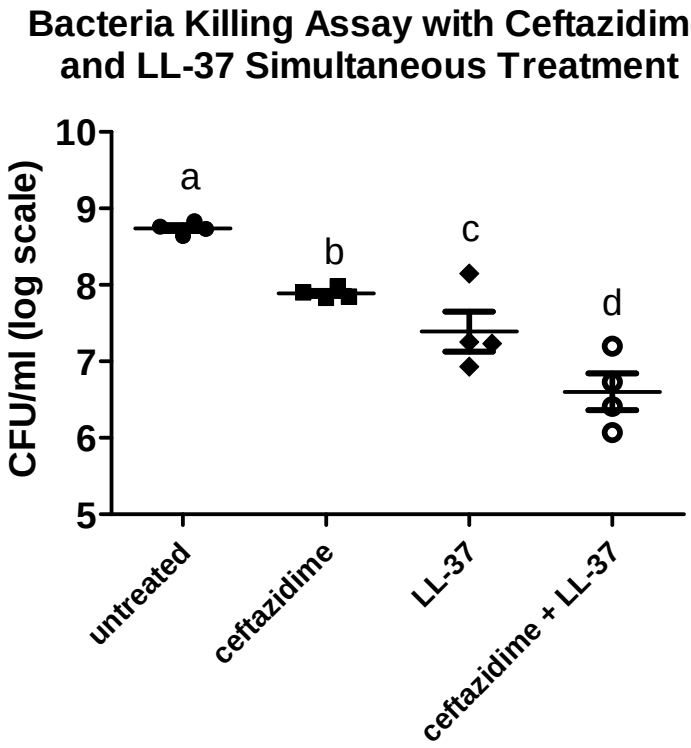

Figure A2: Additive inhibition effects of LL-37 and ceftazidime when simultaneously added to *E. coli*. *E. coli* was grown to mid-log phase and subsequently treated simultaneously with ceftazidime (50 ng/ml), LL-37 (15 µg/ml), or ceftazidime and LL-37 for 6 hours on a rotary shaker (200 rpm). Surviving bacteria were enumerated by plating serial dilutions of remaining bacteria on LB agar followed by colony counts 24-48 hours later. Statistical differences were assessed by one-way ANOVA and Tukey's post-test, $a > b > c > d$, $P < 0.05$. Data is representative of one experiment with treatment groups run in quadruplicate.

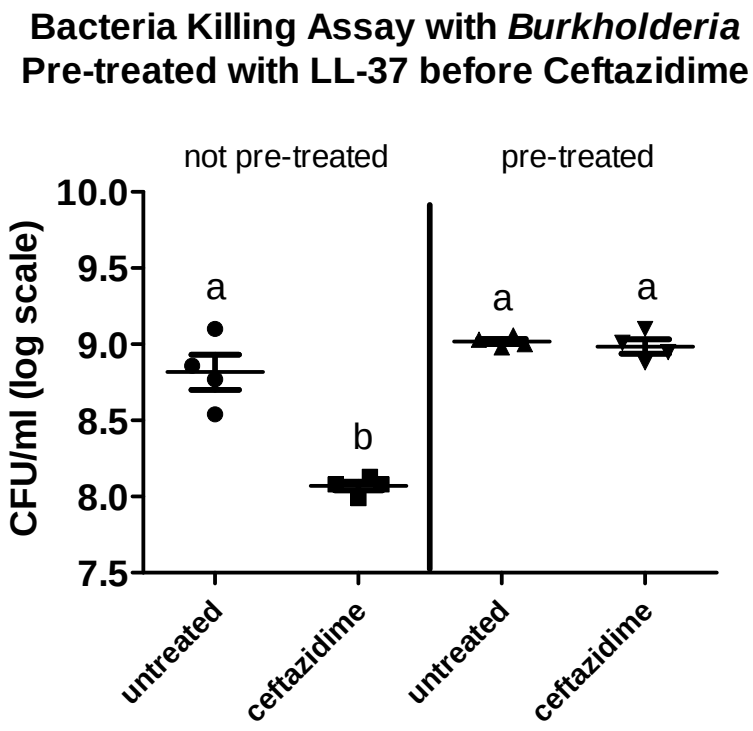

Figure A3: LL-37 treated bacteria are more resistant to growth inhibition by ceftazidime. *E. coli* was treated with LL-37 (15 µg/ml) for one hour and subsequently treated with ceftazidime (50 ng/ml) for an additional 6 hours in 96-well plates. Surviving bacteria were enumerated by plating serial dilutions of remaining bacteria on LB agar followed by colony counts 24-48 hours later. Statistical differences were assessed by one-way ANOVA and Tukey's post-tests, $a > b$, $P < 0.05$. Data is representative of one experiment with treatment groups run in quadruplicate.

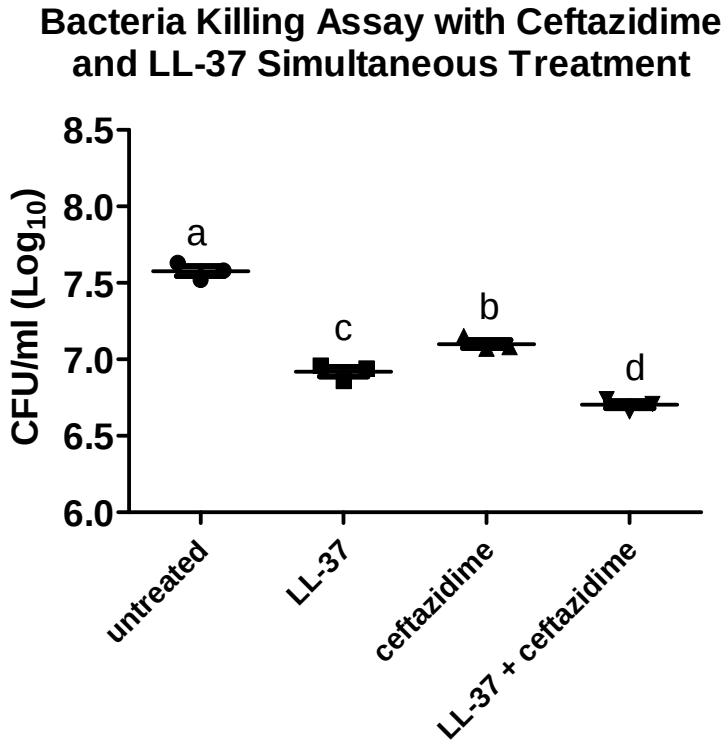

Figure A4: Synergistic growth inhibition of *Burkholderia* with ceftazidime and LL-37 combination. *B. thailandensis* was grown to mid-log phase, diluted in 1 mM potassium phosphate buffer, and added to 96-well plates at a density of $1x10^6$ CFU/ml. Bacteria was initially incubated with LL-37 (30 µg/ml) for 1 hour. After 1 hour, a TSB solution was added to the wells so that the final concentration was 1x. Ceftazidime was added to the wells and plates were incubated an additional 5 hours to make the total treatment time 6 hours. Surviving bacteria were enumerated by plating serial dilutions of wells on LB and counting colonies 24-48 hours later. Statistically significant differences were assessed by one-way ANOVA and Tukey's post-test, $a > b > c > d$, $P < 0.05$. Data is representative of one experiment with treatment groups run in triplicate.

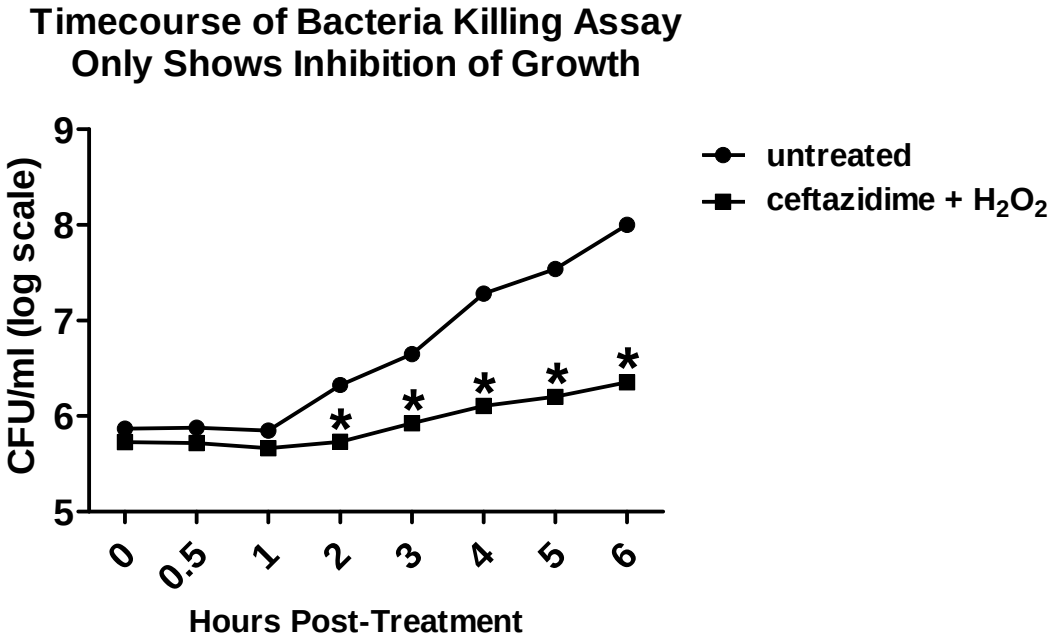

Figure A5: Ceftazidime and H_2O_2 only inhibit growth during bacteria killing assay. *B. thailandensis* was grown to mid-log phase and then plated into a 96-well plate with ceftazidime (750 ng/ml) and H_2O_2 (20 µM) with a total well volume of 200 µl. Plates were incubated for 6 hours and at various time points bacteria were plated from wells to determine increasing bacterial burden. Statistical differences between treated and untreated group were assessed at each time point by two-way ANOVA, $P < 0.05$. Data is representative of one experiment with treatment groups run in triplicate for each time point.

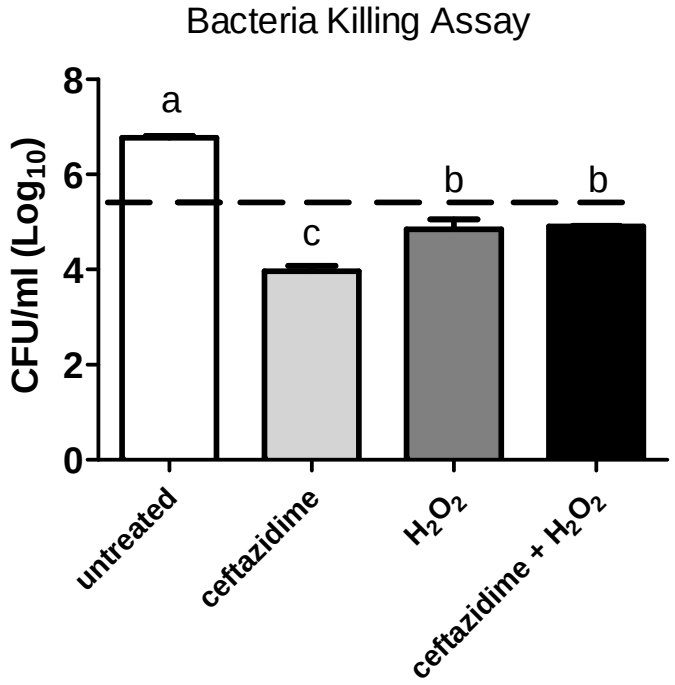

Figure A6: Ceftazidime and H_2O_2 do not interact to synergistically kill *Burkholderia*. *B. thailandensis* was grown to mid-log phase, and then plated into 96-well plates (starting density shown as dashed line) with either ceftazidime (10 µg/ml), H_2O_2 (80 µM), or the combination of both treatments for 3 hours at 37°C. Surviving bacteria were enumerated by plating serial dilutions of remaining bacteria in wells after 3 hours. Data is representative of one experiment with treatment groups run in duplicate.

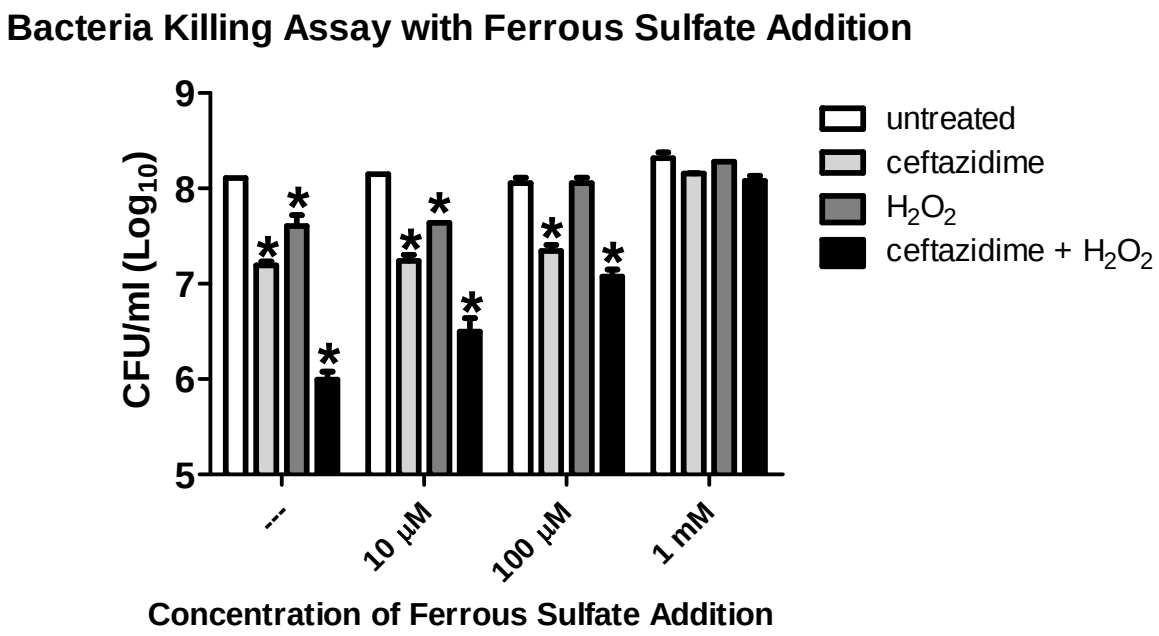

Figure A7: Ferrous sulfate prevents growth inhibition due to ceftazidime or H2O2. *B. thailandensis* was grown to mid-log phase and then plated into a 96-well plate at an initial density of $1x10^6$ CFU/ml. Ceftazidime (750 ng/ml), H_2O_2 (20 µM), and/or ferrous sulfate were added to bacteria resulting in a total well volume of 200 µl. Plates were incubated for 6 hours at 37°C. Remaining bacterial burden was assessed by plating serial dilutions of wells onto LB agar after 6 hour treatment. Statistical differences between treated groups and untreated control were assessed for each concentration of ferrous sulfate addition by two-way ANOVA, *$P < 0.05$. Data is representative of one experiment with treatment groups run in duplicate.

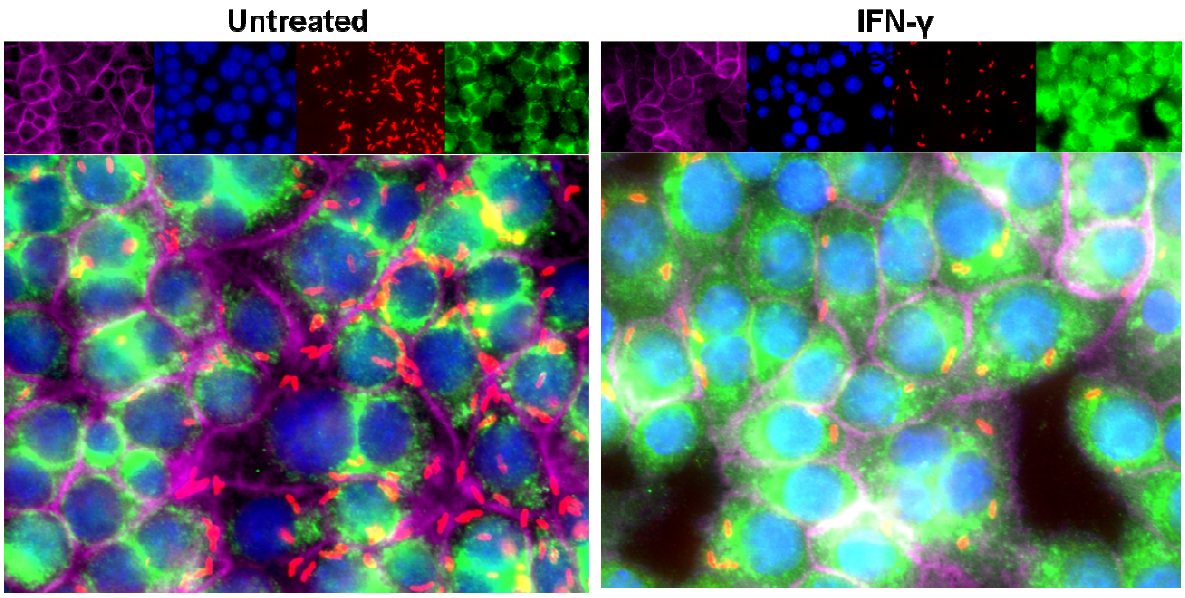

Figure A8: Higher proportion of LAMP-1 colocalization with *Burkholderia* in IFN-γ treated macrophages. RAW 264.7 macrophages were infected with *B. thailandensis* and treated for 10-12 hours with IFN-γ (10 ng/ml). After treatment, cells were prepared for fluorescent microscopy (see Materials and Methods). Above images show untreated (left) and IFN-γ treated (right) single color images (top) and overlays (bottom) of macrophages stained for CD11b (purple), nuclei (blue), *Burkholderia* (red), and LAMP-1 (green). Data are representative of 10 fields of view for 2 independent experiments.

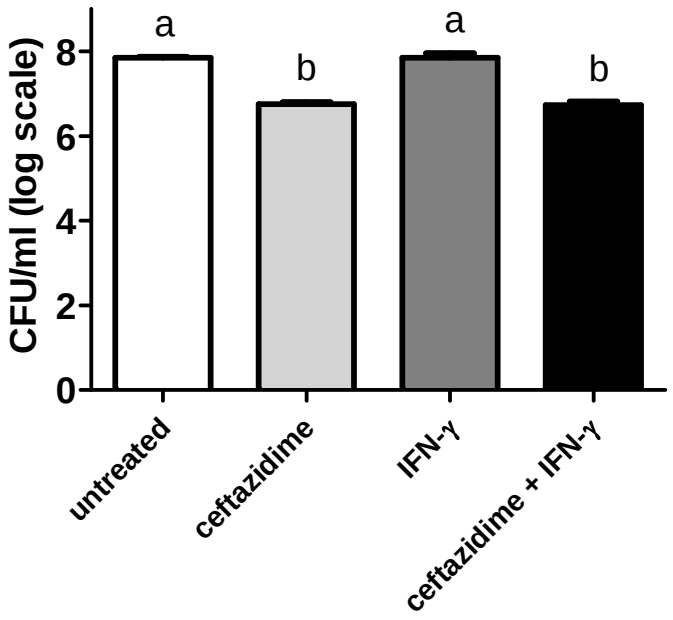

Figure A9: Supernatants from IFN-γ activated macrophages do not interact with ceftazidime to synergistically kill *B. thailandensis*. RAW 264.7 macrophages were stimulated with IFN-γ (10 ng/ml) for 18 hours. Then supernatants were combined with ceftazidime (10 µg/ml) and incubated with *B. thailandensis* in 96 well plates for 6 hours before plating serial dilutions of well contents to enumerate surviving bacteria. Statistical differences were assessed by one-way ANOVA, a > b, $P < 0.05$. Data is representative one experiment with treatment groups run in quadruplicate.

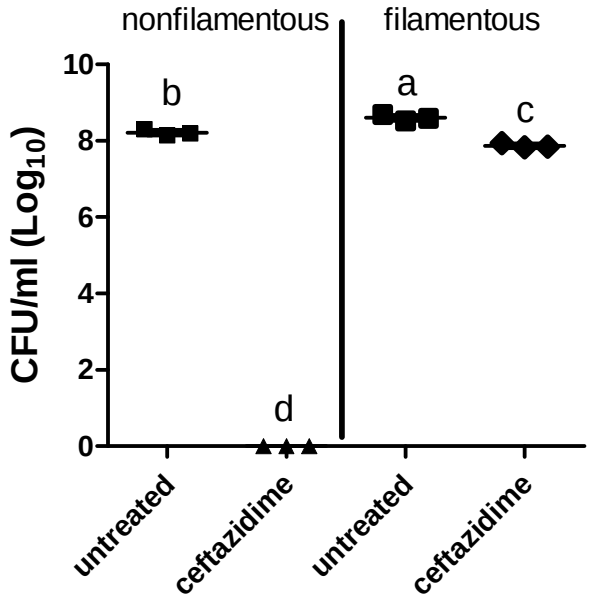

Figure A10: Filamentous bacteria are resistant to high doses of ceftazidime. *Escherichia coli* were incubated overnight with sub-lethal concentrations of ceftazidime to induce filamentation. Filamentous and non-filamentous bacteria were then inoculated into 96-well plates at the same initial density (as determined by plating) and incubated with 10 µg/ml ceftazidime for an additional 18 hours. Surviving *E. coli* were plated and enumerated. Statistical differences were determined by one-way ANOVA a > b > c > d, $P < 0.05$. Data represents one experiment with treatment groups run in triplicate.